Instituto Nacional de Matemática Pura e Aplicada

Post-Blowup Dynamics for the Nonlinear Schrödinger Equation

by

José Manuel Escorcia Tafur

Rio de Janeiro-RJ

December 2021

Instituto Nacional de Matemática Pura e Aplicada

Post-Blowup Dynamics for the Nonlinear Schrödinger Equation

by

José Manuel Escorcia Tafur [†]

under the supervision of Prof. Alexei A. Mailybaev

Thesis presented to the Postgraduate Program in Mathematics at Instituto Nacional de Matemática Pura e Aplicada-IMPA as partial fulfillment of the requirements for the degree of Doctor of Mathematics.

Rio de Janeiro-RJ

December 2021

[†]This work had financial support from CNPq

Aos meus pais Trinidad e Damaso por serem o motor da minha vida.

Abstract

In this work we present a systematic numerical study of the post-blowup dynamics of singular solutions of the 1D focusing critical NLS equation in the framework of a nonlinear damped perturbation. The first part of this study shows that initially the post-blowup is well described by the adiabatic approximation, in which the collapsing core approaches an universal profile and the solution width is governed by a system of ODEs (reduced system). After that, a non-adiabatic regime is observed soon after the maximum of the solution, in which our direct numerical simulations show a clear deviation from the dynamics based on the reduced system. Our study suggests that such non-adiabatic regime is caused by the increasing influx of mass into the collapsing core of the solution, which is not considered in the derivation of the reduced system. Also, adiabatic theoretical predictions related to the wave-maximum and wave-dissipation are compared with our numerical simulations.

The second part of this work corresponds to the non-adiabatic dynamics. Here, numerical simulations reveal a dominant linear regime, caused by the rapid defocusing process. A fact observed in this linear regime is the numerical verification that the collapsing core approaches the universal profile, after removing some oscillations resulting from the interference with the tail. Finally, our numerical study indicates that in the limit of vanishing dissipation, and in a free-space domain, the critical mass is radiated to infinity instantly at the collapse time.

Keywords: Nonlinear Schrödinger equation (NLS), singular solutions, nonlinear damping perturbation, adiabatic approximation.

Resumo

Neste trabalho, apresentamos um estudo numérico sistemático da dinâmica pós-explosão de soluções singulares da equação unidimensional crítica não linear de Schrödinger com focalização no caso de uma perturbação amortecida não linear. A primeira parte deste estudo mostra que, inicialmente, a pós-explosão é bem descrita por uma aproximação adiabática, na qual o núcleo colapsante se aproxima de um perfil universal, e a espessura de solução é governada por um sistema de equações diferenciais ordinárias (sistema reduzido). Em seguida, um regime não adiabático é observado logo após o máximo da solução, para o qual nossas simulações numéricas diretas mostram um claro desvio em relação à dinâmica proveniente do sistema reduzido. Nosso estudo sugere que tal regime não adiabático é causado pelo crescente influxo de massa no núcleo colapsante da solução, o qual não é considerado na derivação do sistema reduzido. Adicionalmente, previsões teóricas adiabáticas relacionadas ao máximo da onda e à dissipação da onda são comparadas com as nossas simulações numéricas.

A segunda parte deste trabalho corresponde à dinâmica não adiabática. Nela, simulações numéricas revelam um regime linear dominante, causado pelo rápido processo de desfocalização. Um fato observado neste regime linear é a verificação numérica de que o núcleo colapsante se aproxima de um perfil universal, após a remoção de algumas oscilações decorrentes da interferência com a cauda. Finalmente, nosso estudo numérico indica que no limite de dissipação zero, e em espaço aberto como domínio, a massa crítica é irradiada para o infinito instantaneamente no momento de colapso.

Palavras-chave: Equação de Schrödinger não linear (NLS), soluções singulares, perturbação de amortecimento não linear, aproximação adiabática.

Acknowledgments

I thank God for giving me strength enough to believe in me in the moments that I felt faint.

To my parents, Trinidad Tafur and Damaso Escorcia, who even in the distance gave me their love and support to finish this project.

I also want to express my sincere gratitude to my thesis supervisor Alexei A. Mailybaev, for allowing me to be part of his research and for all the support and patience received throughout this process. Without his invaluable guidance, this project would never have been successfully completed.

To my friends Júlia Domingues, Hugo Saraiva, Ciro Campolina, and Marlon Lopez for making the instance in Brazil an unforgettable experience.

To CNPq for their financial support, and to all the others who somehow contributed to this achievement.

Agradecimentos

Agradeço a Deus por me dar força para acreditar em mim mesmo quando senti que não conseguiria.

Aos meus pais, Trinidad Tafur e Damaso Escorcia, que mesmo à distância me deram seu amor e apoio para finalizar este projeto.

Também quero expressar meus sinceros agradecimentos ao meu orientador de tese, Alexei A. Mailybaev, por me permitir fazer parte de sua pesquisa e por todo o apoio e paciência ao longo deste processo. Sem a sua orientação inestimável, este projeto nunca teria sido concluído com êxito.

Aos amigos Júlia Domingues, Hugo Saraiva, Ciro Campolina e Marlon Lopez por tornarem a estadia no Brasil uma experiência inesquecível.

Ao CNPq pelo apoio financeiro, e a todos os demais que de alguma forma contribuíram para essa conquista.

Contents

Chapter 1

Introduction

The focusing nonlinear Schrödinger (NLS) equation

$$i\psi_t + \Delta\psi + |\psi|^{2\sigma}\psi = 0, \tag{1.1}$$

appears as fundamental model in different branches of physics, e.g., Bose-Einstein condensate [28], fluid dynamics [60] and nonlinear optics [17]. Here ψ is a complex-valued function depending of the time t and the space variable $\boldsymbol{x}$. We denote by Δ the Laplacian operator in dimension $d \geq 1$ and $\sigma > 0$ represents the nonlinearity-power. It is well known that in the *sub-critical* case ($\sigma d < 2$), solutions of the equation (1.1) are global in time for every initial condition in the Sobolev space $H^1(\mathbb{R}^d)$. In contrast, both the *critical* ($\sigma d = 2$) and *super-critical* ($\sigma d > 2$) cases admit singular (blowup) solutions, i.e., solutions that collapse in finite time (blowup time). Singular solutions are characterized by an unbounded growth of $\nabla\psi$ close to the blowup time. A necessary condition for collapse in the critical case is that L^2 norm of initial conditions in $H^1(\mathbb{R}^d)$ must be equal or greater than a certain critical value M_c (depending on the dimension). In this thesis our interest is the blowup solutions in the critical case.

1.1 History of the problem

The history of the singular solutions, at least in the context of nonlinear optics, begins in 1965 with the celebrated paper of Kelley titled *Self-focusing of optical beams* [33]. In optics, the NLS equation (1.1) with $d = 2$ and $\sigma = 1$, is the leading-order model for paraxial propagation of intense laser beams in a homogeneous Kerr medium.

The function ψ represents the slowly-varying amplitude of the electric field, t is the direction of propagation, and $\boldsymbol{x} = (x, y)$ are the coordinates in the transverse plane. In [33], Kelley shows by using an informal dimensional argument that the two-dimensional NLS equation admits solutions that become singular at a finite (distance) T_c. Also, the first numerical simulation of blowup solutions was done by Kelley in that same paper. In the numerical simulation carried out by Kelley, the intensity of the laser beam, $|\psi|^2$, only increased by a factor of 10. It is important to point out that even this level of focusing was a numerical challenge at the time.

The first analysis of the self-focusing dynamics was done in 1966 by Akhmanov et al. [1] using the *aberrationless approximation method*. The main idea of that method is based on the assumption that in the blowup dynamics solutions maintain a self-similar Gaussian profile. Therefore, the substitution of the Gaussian ansatz in the NLS equation allowed to obtain a system of ordinary differential equations independent of the transverse variables (reduced equations) and equivalent to the original NLS equation. The use of the aberrationless method contributed successfully in the analytical approximation of the beam width and the blowup time (distance). Soon it became clear that some predictions based on the aberrationless approximation can be incorrect [2, 12, 44]. Accordingly, appears the so-called *variational approach* in which the Gaussian ansatz is replaced with super-Gaussian or sech profile [12]. However, also this new approach led to some incorrect results [24].

During the 1980s and early 1990s, numerical simulations of singular NLS solutions with initial mass slightly above M_c showed that close the singularity solutions can be decomposed into two components [27, 36, 37, 38, 43]. One of them, is the collapsing core, which approaches the universal profile

$$|\psi_{R^{(0)}}|^2 = \frac{1}{L^d(t)} \left(R^{(0)} \left(\frac{r}{L(t)} \right) \right)^2, \tag{1.2}$$

regardless of the initial condition. Here $R^{(0)}(\boldsymbol{x})$ is the function describing the ground state solution of the equation (2.17) given below, and $L(t) \to 0$ at the singularity. The other component is the tail or outer part of the solution, which does not participate in the collapse. This fact was crucial in deriving a new reduced equations in order to describe the NLS equation. These equations were first derived in 1985 by Fraiman [27] from a linear-stability analysis of perturbations around the universal profile. The

same equations were rederived in 1988 by Papanicolaou and coworkers [36, 38] from a solvability condition. Malkin [43] derived the reduced equations in 1993 by considering the evolution of the mass (L^2 norm) of the collapsing core. All these derivations were fundamentally based on numerical and physical arguments. A rigorous derivation of the reduced equations turned out to be a hard problem. Indeed, the first rigorous derivation was done in 2001 by Perelman for $d = 1$ and certain initial conditions [58]. Merle and Raphael in a series of papers published between 2003 and 2006 proved that fact for initial conditions whose L^2 norm is slightly above the critical constant M_c and dimensions $1 \leq d \leq 5$ [47, 48, 49, 50, 51, 52].

As we mentioned before, the NLS equation (1.1) models the propagation of intense laser beams in a Kerr medium. Since the laser beams continue to propagate forward all the time, it is important to continue the singular solutions after the singularity time. Therefore, when NLS solutions collapse, this indicates that some of the terms neglected in the derivation become important near the singularity. Different mechanisms for continue singular NLS solutions have been proposed in the literature: nonlinear saturation, nonlinear damping, nonparaxiality and normal dispersion, see e.g., [17] and references therein. In these terms, and motivated by the vanishing- viscosity solutions of hyperbolic conservation laws is natural to ask if one of these mechanisms play the role of "viscosity" in the NLS, but the existing theory is quite limited. Although it has been known that NLS model breaks down when the input mass is sufficiently high since 1965, an equivalent theory to continue solutions after the singularity for the NLS has yet to be developed.

The existing theory to study any perturbation of the NLS equation is called *modulation theory*, and it was developed by Fibich and Papanicolaou in 1998-1999 [25, 26]. This theory is based on the adiabatic approximation. Such adiabatic approach assumes that after the singularity the collapsing core remains close to the universal profile $\psi_{R^{(0)}}$, by neglecting any interaction (mass transfer) between the collapsing core and the tail.

1.2 Problem studied in the thesis and overview of the results

In this thesis we will focus on the 1D critical damped NLS equation

$$i\psi_t + \psi_{xx} + (1 + i\delta)|\psi|^4\psi = 0, \tag{1.3}$$

where $\delta \geq 0$ is a small parameter. The nonlinear dissipation in the previous equation, $i\delta|\psi|^4\psi$, corresponds to three-photon absorption in nonlinear optics [7] or four-body collisions which cause loss of atoms from the Bose-Einstein condensate [14], and in the context of the complex quintic Ginzburg-Landau equation [11, 23]. Newly, this kind of equations has been proposed as a mechanism for turbulent dissipation [10, 31, 42]. For example, in [10, 42] were considered turbulence based on collapses in the 1D and 2D NLS respectively, and there is attenuation after collapse due to the dissipation. In these studies also a forcing term was considered in the NLS models. The aim of this thesis is to present a systematic numerical study of the post-collapse dynamics of singular NLS solutions in the framework of the equation (1.3).

Equation (1.3) is solved by using the fourth-order split step method, and with a periodic initial condition whose mass is approximately 45.76% above the critical mass $M_c = \frac{\sqrt{3}\pi}{2}$. We notice that, in the numerical simulations carried out for the equation (1.3) in order to verify the adiabatic approach, the initial mass was $2.5\% - 10.25\%$ above the critical one, see e.g., [21, 22]. In these terms, the initial condition used in our simulations is not close to the universal profile $\psi_{R^{(0)}}$.

The first main objective of the present thesis is to see how well is described the post-blowup dynamics for the reduced system (adiabatic approximation), taking into account the not closeness of our initial condition with the $\psi_{R^{(0)}}$ profile. Therefore, theoretical predictions concerning to the wave-maximum and wave-dissipation (two-dimensional prediction) are compared with our direct numerical simulations. Our findings are in qualitative agreement with the exponential growth of the wave-maximum, but differing with the estimated power of δ. In two dimension the adiabatic approach predicts the dissipation of a finite amount of mass in the limit of δ going to zero [16], in contrast, in one dimension our measurements suggest a different behavior, in which no mass is dissipated in the limit of vanishing damping.

Our numerical simulations evidenced the breakdown of the adiabatic approach soon after the maximum of the solution, as was also reported in [21, 22]. As a new contribution, we highlight that our analysis offers another plausible explanation of the invalidity of the adiabatic approximation. In fact, we argue that this invalidity could be caused by the increasing influx of mass into the collapsing core, since this effect is neglected in the adiabatic approach.

Due to the lack of validity of the reduced system (adiabatic approach), the second goal of this thesis is to describe the non-adiabatic stage. In such non-adiabatic stage, a quasi-linear regime is observed as a consequence of the rapid defocusing process. Surprisingly, and apart from some oscillations due to the interference with the tail, in this linear regime the closedness of the solution to the universal profile $\psi_{R^{(0)}}$ is verified.

As a consequence of the dominant linear regime in the post-collapse, the outward radiation of mass through the formation of high frequencies is observed. Therefore, the numerical simulations suggest that in a free-space domain and in the limit of vanishing damping, the collapsed critical mass M_c is instantly radiated to infinity at the collapsing time. In consequence, one can expect that turbulent behavior depends dramatically on boundary conditions: periodic vs infinite or absorbing boundaries.

1.3 Thesis organization

This thesis is organized as follows:

- In Chapter 2 we present the well known $H^1(\mathbb{R}^d)$ theory of the general NLS equation (1.1). Here general properties as: conservation laws, symmetries, H^1 singularity and solitary wave solutions are introduced. Concerning to the critical case, $\sigma d = 2$, crucial concepts as: lens transformation, explicit solutions and blowup rate among others are presented. Likewise, the main result in the singular critical NLS theory concerning the universality of the profile of generic blowup solutions is established (Theorem 2.6). All the subsequent chapters are devoted to the critical NLS, i.e., $\sigma d = 2$.

- In Chapter 3 the main steps of the derivation of the reduced system (equations) for the critical NLS equation (1.1) is shown (Proposition 3.1). Reduced system

comes from taking into account the quasi self-similar dynamics of the collapse, and the rate of change of the mass of the collapsing core. The fundamental fact in the derivation of such system of equations is the universality of the profile of the solution close to the singularity time. Indeed, such universality allows to approximate the nonlinear equation (1.1) by the time-independent linear Schrödinger equation, and in this way by using the well known WKB method the rate of change of the mass of the collapsing core is computed. Although the derivation presented here is not rigorous, it has the advantage to provide a physical interpretation of the reduced system.

- In Chapter 4 we introduce the $d-$dimensional critical nonlinear damped NLS. Firstly, it is established that under this perturbation singular solutions become regular and global in time (Theorem 4.1). In this same chapter the existing theory to treat any perturbation, and in particular the one here considered, of the critical NLS (modulation theory) is presented. Therefore, in terms of the modulation theory assumptions (adiabatic dynamics) a corresponding reduced system is derived (Proposition 4.1). We point out that adiabatic approximation is not rigorous, and it is based on informal arguments and numerical simulations.

- In Chapter 5 we expose the existing continuation results for the explicit and generic solutions established in the framework of the damped NLS equation (Propositions 5.1 and 5.2). Since such results are based on the adiabatic approximation, they are not rigorous. Also, theoretical predictions of the adiabatic approach related to the wave-maximum and wave-dissipation (only in the case $d = 2$) are described.

- In Chapter 6 we will focus in describing the numerical method used in our numerical simulations. Numerical simulations were carried out by the fourth-order split step method. The main idea of the mehod is to split the NLS into its linear and nonlinear parts, and in this form the approximation of the solution is obtained by solving iteratively each of these problems. In order to monitor the consistency of the method, we checked the conservation laws in the absence of dissipation and the mass balance equation for the damped NLS. The accuracy of the method was maintained by using Fourier interpolation, in such a way that the error was kept

at the level of round-off noise. Also, the initial condition and its properties are described in this chapter.

- In Chapter 7 the intention is to verify that the collapsing core of the solution of the NLS equation (1.3) with $\delta = 0$ approaches the universal $\psi_{R^{(0)}}$ profile for times close to the singularity. In this chapter we verified the validity of the corresponding reduced system as well. Also, our numerical simulation shows a reasonable verification of the power laws predicted for the solution tail.

- In Chapter 8 we present the first part of our new results related to the damped NLS (1.3). Here the main goal is to see how well the post-collapse dynamics is described by the adiabatic approach. The damped NLS (1.3) was solved by using different values of δ, which verified numerically the convergence to the non-dissipative case as long as δ decreases to zero. Similarly, the approach of the collapsing core toward $\psi_{R^{(0)}}$ is verified for the damped NLS. To carry out the main objective of the chapter, we compared the soluion of the reduced system with our direct numerical simulations. In these terms, predictions of the adiabatic approach with respect to the wave-maximum and wave-dissipation (two dimension) are compared to ones obtained by numerical simulations. Our results show a qualitative agreement with the theoretical exponential growth of the maximum of the solution, but the predicted power of δ was different. Adiabatic approximation forecasts, at least in two dimension, that in the limit of δ going to zero a finite amount of mass is dissipated in a single collapse, in contrast, in our one-dimensional problem we have observed the opposite, no mass is dissipated in the collapse event. Finally, the numerical simulations show the breakdown of the adiabatic approximation shortly after the peak of the solution. Then, our result coincides with [21, 22]. We hypothesize that such invalidity of the reduced system comes from of the influx of mass into the inner core observed in the numerical simulations.

- In Chapter 9 the goal is to describe the post-adiabatic dynamics. In this stage our numerical simulations reveal a quasi linear regime, verified by the direct comparison of the terms $|\psi_{xx}|$ and $|\psi|^5$. Also, the verification of the universal profile

$\psi_{R^{(0)}}$ in such linear phase is presented. This was an expected result since $\psi_{R^{(0)}}$ almost balances dispersion and nonlinearity. Ultimately, simulations indicate that in the zero-dissipation limit the collapsed mass M_c is instantly outward radiated at the collapsing instant. Consequently, for a better numerical description of the post-collapse dynamics a type of absorbing boundary conditions are required.

- In Chapter 10 we provide some conclusions and perspectives.
- In Appendix A we provide the perturbation analysis for $U = R^{(0)} + \epsilon h$ required in the derivations of the reduced system for the damped/undamped NLS.
- In Appendix B we provide the details of the derivation of the reduced system given in the Chapter 3.
- In Appendix C we provide the details of the derivation of the reduced system given in the Chapter 4.

Chapter 2

Nonlinear Schrödinger Equation

In this chapter the reader will be introduced to the focusing nonlinear Schrödinger equation (NLS) in the context of the Sobolev space $H^1(\mathbb{R}^d)$. In this order of ideas, some known properties and basic results concerning the NLS and its H^1 singular solutions are presented.

2.1 General $H^1(\mathbb{R}^d)$ theory

The focusing nonlinear Schrödinger (NLS) equation of the form

$$i\psi_t + \Delta\psi + |\psi|^{2\sigma}\psi = 0, \tag{2.1}$$

is a canonical physical equation used in the study of water waves [57], Bose-Einstein condensation [28] and nonlinear optics [17]. The wavefunction ψ is complex-valued function depending of the time $t \in \mathbb{R}$ and the space variable $\boldsymbol{x} \in \mathbb{R}^d$. Here we denote by Δ the Laplacian operator in dimension $d \geq 1$ and $\sigma > 0$ represents the nonlinearity-power. Throughout this thesis we will consider the NLS in the Sobolev space H^1 context, and the parameter σ is always assumed in the so-called H^1-*subcritical regime*,

$$\begin{cases} 0 < \sigma < \infty, & \text{for } d \leq 2, \\ 0 < \sigma < \frac{2}{d-2}, & \text{for } d > 2. \end{cases} \tag{2.2}$$

We begin defining the Sobolev space $H^1(\mathbb{R}^d)$:

Definition 2.1 ($H^1(\mathbb{R}^d)$ space)**.** *We define the Sobolev $H^1(\mathbb{R}^d)$ space as*

$$H^1(\mathbb{R}^d) := \{f(\boldsymbol{x}) \in L^2(\mathbb{R}^d) : \nabla f(\textit{in the distribution sense}) \in L^2(\mathbb{R}^d)\}.$$

This space is endowed with the norm $\|f\|^2_{H^1(\mathbb{R}^d)} := \|f\|_2^2 + \|\nabla f\|_2^2$.

For more information about distributions and Sobolev spaces, see e.g., [40, 61]. NLS equation (2.1) with the initial condition $\psi(\boldsymbol{x}, 0) = \psi_0(\boldsymbol{x})$ is conveniently replaced by its integral form (Duhamel's formula):

$$\psi(\boldsymbol{x}, t) = U(t)\psi_0(\boldsymbol{x}) + i\int_0^t U(t-s)|\psi(s)|^{2\sigma}\psi(s)ds, \tag{2.3}$$

where U is the free Schrödinger operator defined as

$$U(t)f(\boldsymbol{x}) := \left(\frac{1}{4\pi i t}\right)^{d/2} \int e^{i\frac{|\boldsymbol{x}-\boldsymbol{x}'|^2}{4t}} f(\boldsymbol{x}')d\boldsymbol{x}'. \tag{2.4}$$

For further details, see e.g., [8, 9, 40, 62]. Existence theorems are proved in this new formulation. Indeed, we have the following result [29, 30, 32, 39, 65, 69]:

Theorem 2.1 (H^1 solutions)**.** *Let σ be in the H^1-subcritical regime (2.2). Then, for any initial condition $\psi_0 \in H^1(\mathbb{R}^d)$, there exists, locally in time, a unique maximal solution of (2.3) in $C([0,T), H^1(\mathbb{R}^d))$, where the maximal means that if $T < \infty$, then*

$$\|\psi(t)\|_{H^1(\mathbb{R}^d)} \to \infty, \quad \text{as } t \to T. \tag{2.5}$$

In addition, ψ conserves the following finite quantities:

$$M(t) := \int |\psi|^2 d\boldsymbol{x} \equiv M(0), \quad (\textit{Mass} - L^2 \textit{ norm}), \tag{2.6}$$

$$H(t) := \int |\nabla\psi|^2 \, d\boldsymbol{x} - \frac{1}{\sigma+1}\int |\psi|^{2\sigma+2} d\boldsymbol{x} \equiv H(0), \quad (\textit{Hamiltonian}), \tag{2.7}$$

$$P(t) := i\int (\psi\nabla\psi^* - \psi^*\nabla\psi)\, d\boldsymbol{x} \equiv P(0), \quad (\textit{Linear momentum}). \tag{2.8}$$

The quantity $M(t)$ has the meaning of either the number of particles in a Bose-Einstein condensate [28], or the optical power in optics [1, 2]; it is also called the mass in other applications [64]. In this thesis, we will refer to it as mass. In order to motive the name of the quantity $H(t)$, we can observe that

$$H = \int \mathcal{H} d\boldsymbol{x}, \quad \mathcal{H} = |\nabla\psi|^2 - \frac{1}{\sigma+1}|\psi|^{2\sigma+2}. \tag{2.9}$$

Then, the variational derivative of H with respect to ψ^* satisfies

$$\frac{\delta H}{\delta \psi^*} = \frac{\partial \mathcal{H}}{\partial \psi^*} - \nabla \cdot \frac{\partial \mathcal{H}}{\partial \nabla \psi^*} \tag{2.10}$$

$$= -|\psi|^{2\sigma}\psi - \nabla \cdot \nabla \psi \tag{2.11}$$

$$= -|\psi|^{2\sigma}\psi - \Delta \psi. \tag{2.12}$$

In these terms, NLS equation (2.1) can be rewritten as

$$i\psi_t = \frac{\delta H}{\delta \psi^*}, \tag{2.13}$$

and then it is a Hamiltonian equation, see e.g., [62]. In most applications, the Hamiltonian corresponds to energy, but through this thesis we will refer to it just as Hamiltonian.

Remark 2.1. *Throughout this thesis we will understand NLS solutions in the context of the Theorem 2.1.*

The aim of this thesis is the singular solutions, then, in terms of the Theorem 2.1 we adopt the following definition:

Definition 2.2 (H^1 Singular solution)**.** *A solution of the NLS (2.1) becomes singular at T_c, where $0 < T_c < \infty$, if $\psi(t) \in H^1(\mathbb{R}^d)$ for $0 \leq t < T_c$, and*

$$\lim_{t \to T_c} \|\psi(t)\|_{H^1(\mathbb{R}^d)} = \infty. \tag{2.14}$$

In other words, ψ is a singular solution if it ceases to be in the space $H^1(\mathbb{R}^d)$ at certain finite time. Singularity is also called *collapse* or *blowup*. In this thesis we will use any of them indistinctly. Due to the conservation laws previously described in Theorem 2.1, one can state an equivalent definition of singularity. Indeed, as a consequence of the mass conservation follows

Corollary 2.1. *ψ becomes singular at T_c if and only if $\lim_{t \to T_c} \|\nabla \psi(t)\|_2 = \infty$.*

Similarly, by Hamiltonian conservation one has

Corollary 2.2. *ψ becomes singular at T_c if and only if $\lim_{t \to T_c} \|\psi(t)\|_{2\sigma+2} = \infty$.*

Therefore, $\|\nabla \psi\|_2$ and $\|\psi\|_{2\sigma+2}$ become infinity at the singularity. The next corollary indicates that also the L^∞ norm of ψ (the maximal amplitude) becomes infinity at the singularity.

Lemma 2.1. *If ψ becomes singular at T_c, then* $\lim_{t\to T_c} \|\psi(t)\|_\infty = \infty$.

Proof. We will reasoning by negation, assuming that $\limsup_{t\to T_c} \|\psi\|_\infty = A < \infty$. Then, by applying the interpolation inequality $\|f\|_{2\sigma+2} \leq \|f\|_\infty^{\frac{\sigma}{\sigma+1}} \|f\|_2^{\frac{1}{\sigma+1}}$, and mass conservation, we have

$$\lim_{t\to T_c} \|\psi\|_{2\sigma+2}^{2\sigma+2} \leq A^{2\sigma} \lim_{t\to T_c} \|\psi\|_2^2 = A^{2\sigma}\|\psi_0\|_2^2 < \infty, \tag{2.15}$$

but this fact contradicts Corollary 2.2. □

NLS singularity is typically a local phenomenon, i.e., the solutions collapse at a point $\boldsymbol{x}_c \in \mathbb{R}^d$.

Definition 2.3 (Singularity point)**.** *Let ψ be a solution of the NLS (2.1) that becomes singular in $H^1(\mathbb{R}^d)$ at $t = T_c$. We say that ψ becomes singular at $\boldsymbol{x} = \boldsymbol{x}_c \in \mathbb{R}^d$, if for any $\epsilon > 0$, at least one the following conditions hold*

$$\lim_{t\to T_c} \|\psi\|_{H^1(|\boldsymbol{x}-\boldsymbol{x}_c|<\epsilon)} = \infty \quad \textit{or} \quad \lim_{t\to T_c} \|\psi\|_{L^{2\sigma+2}(|\boldsymbol{x}-\boldsymbol{x}_c|<\epsilon)} = \infty. \tag{2.16}$$

Definition 2.4 (subcritical, critical and supercritical NLS)**.** *The NLS (2.1) is called subcritical if $0 < \sigma d < 2$, critical if $\sigma d = 2$, and supercritical if $\sigma d > 2$.*

In the *subcritical* case ($\sigma d < 2$), solutions of the equation (2.1) are globally regular in time for every initial condition in the Sobolev space $H^1(\mathbb{R}^d)$ [66]. In contrast, in the *critical* ($\sigma d = 2$) and *supercritical* ($\sigma d > 2$) cases, solutions may develop a singularity in finite time (blowup). For example, for $\sigma d \geq 2$, a negative value of Hamiltonian is sufficient for collapse [65]. In the critical case, we will see that there exits a critical mass M_c (depending of the dimension d), such that the solution may collapse in finite time.

2.1.1 Wave-guide solutions

The NLS equation (2.1) admits the waveguide solutions $\psi(\boldsymbol{x}, t) = \exp(it)R(\boldsymbol{x})$, with the function R satisfying the stationary equation

$$\Delta R(\boldsymbol{x}) - R + |R|^{2\sigma} R = 0, \qquad R'(0) = 0, \qquad R(\infty) = 0. \tag{2.17}$$

It is well known, when $d = 1$ the equation (2.17) has the unique solution

$$R(x) = \pm(1+\sigma)^{1/2\sigma} \cosh^{-1/\sigma}(\sigma x). \tag{2.18}$$

In contrast, for $d \geq 2$, equation (2.17) admits an infinite countable number of solutions. The solution with the minimal mass (L^2 norm), which we denote by $R^{(0)}$, is unique and is called the *ground state*.

Many properties of the solutions of the equation (2.17) are described for example in [17]. In this thesis we will focus just in some of them, which will be useful in the singular NLS theory. The next two results establish that in the critical case the mass of the ground state $R^{(0)}$ is the minimal mass (critical mass) for collapse.

Theorem 2.2 ([6, 66])**.** *A sufficient condition for global existence in the critical NLS is*

$$\|\psi_0\|_2^2 < \|R^{(0)}\|_2^2, \tag{2.19}$$

where $R^{(0)}$ is the ground state of (2.17).

Therefore, a necessary condition for collapse in the critical NLS is that the solution mass be at least that of the ground state.

Corollary 2.3. *The minimal (critical) mass of a collapsing solution of the critical NLS is given by $M_c = \|R^{(0)}\|_2^2$, where $R^{(0)}$ is the ground state of (2.17).*

Since the waveguide solutions of the critical NLS propagate without changing their profile, diffraction (Laplacian) and nonlinearity are exactly balanced. We know that a negative Hamiltonian is a sufficient condition for solution blowup, and the mass of the ground state is the minimal mass for collapse. We will show that $R^{(0)}$ is the borderline case of these conditions.

Lemma 2.2 ([59])**.** *Let $R(\boldsymbol{x})$ be a solution of (2.17) with $R \in H^1(\mathbb{R}^d)$. Then,*

$$H(R) = \frac{\sigma d - 2}{2 - \sigma(d-2)} \|R\|_2^2. \tag{2.20}$$

Therefore, Lemma 2.2 implies that in the critical case, $\sigma d = 2$, the Hamiltonian of R vanishes, i.e., $H(R) = 0$. In other words, in the critical case, the ground state $R^{(0)}$ satisfies the *dual borderline properties:* $\|R^{(0)}\|_2^2 = M_c$ and $H(R^{(0)}) = 0$. The next result shows that in fact it is the unique profile with the dual borderline properties, see e.g., [17] for the proof.

Lemma 2.3. *Let $\sigma d = 2$ (critical NLS). Then $\|f\|_2^2 = M_c$ and $H(f) = 0$ if and only if $f = e^{i\alpha}\lambda^{d/2}R^{(0)}(\lambda|\boldsymbol{x} - \boldsymbol{x}_0|)$ for some $\alpha \in \mathbb{R}$, $\lambda > 0$, and $\boldsymbol{x}_0 \in \mathbb{R}^d$.*

This important characteristic of $R^{(0)}$ is crucial in the study of singular solutions for the NLS equation in the critical regime. It will be clear in the next section. Finally, we close this section calculating the asymptotic behavior of $R(\boldsymbol{x})$ for large $|\boldsymbol{x}|$,

Lemma 2.4 ([17])**.** *Let $R(\boldsymbol{x})$ be a nontrivial solution of (2.17) in $H^1(\mathbb{R}^d)$. Then,*

$$\lim_{r\to\infty} \frac{R(r)}{r^{-\frac{d-1}{2}}e^{-r}} = A_R, \qquad r = |\boldsymbol{x}|, \tag{2.21}$$

where A_R is a constant. Therefore, we will denote this fact by

$$R(\boldsymbol{x}) \sim A_R r^{-\frac{d-1}{2}} e^{-r}, \qquad r \gg 1. \tag{2.22}$$

Since in dimension $d \geq 2$ equation (2.17) has an countable number of solutions, the value of the constant A_R can depend of it.

2.1.2 Whole and partial collapse

In this section we will address the question of what is the amount of mass collapsing into the singularity. The importance of knowing this fact is crucial in applications in which one wants to control the amount of mass at the target.

Definition 2.5 (Amount of mass that collapses into the singularity)**.** *Let ψ be an NLS solution that collapses at $\boldsymbol{x} = \boldsymbol{x}_c$ as $t \to T_c$, and let*

$$M_\epsilon := \liminf_{t\to T_c} \int_{|\boldsymbol{x}-\boldsymbol{x}_c|<\epsilon} |\psi|^2 d\boldsymbol{x}. \tag{2.23}$$

Then, the amount of mass that collapses into the singularity is

$$M_{collapse} := \lim_{\epsilon\to 0^+} M_\epsilon. \tag{2.24}$$

Definition 2.6 (Whole collapse)**.** *A solution undergoes a whole collapse, if it collapses into the singularity point $\boldsymbol{x}_c$ as a delta function that contains all the mass, i.e., if*

$$\lim_{t\to T_c} |\psi|^2 = \|\psi_0\|_2^2 \delta(\boldsymbol{x} - \boldsymbol{x}_c), \tag{2.25}$$

where the limit is in the sense of distributions.

Definition 2.7 (Partial collapse). *A solution undergoes a partial collapse, if it collapses into the singularity point $\boldsymbol{x}_c$ as a delta function that contains a positive fraction of the mass, i.e., if*

$$\lim_{t\to T_c} |\psi|^2 = M_{partial}\delta(\boldsymbol{x}-\boldsymbol{x}_c) + |\phi(x)|^2, \tag{2.26}$$

where $0 < M_{partial} < \|\psi_0\|_2^2$, $0 \neq \phi \in L^2$ is the limit of the non-collapsing tail, and the limit is in the sense of distributions.

Therefore, in the whole collapse $M_{\text{collapse}} = \|\psi_0\|_2^2$, and $M_{\text{collapse}} = M_{\text{partial}}$ in partial collapse.

Definition 2.8 (Strong collapse). *A solution undergoes a strong collapse, if the amount of mass that collapses into the singularity is positive, i.e., $M_{collapse} > 0$.*

Definition 2.9 (Weak collapse). *A solution undergoes a weak collapse, if the amount of mass that collapses into the singularity is zero, i.e., $M_{collapse} = 0$.*

In these terms, one has that both whole and partial collapses are strong collapses. In particular, in the critical case, any singular solution of the NLS undergoes a strong collapse where the amount of mass concentrates into the singularity is at least M_c. It is shown in the following theorem.

Theorem 2.3 (Mass concentration [53, 55, 67]). *Let ψ be a solution of the critical NLS (2.1) which becomes singular at T_c. Then there exists a continuous function $\boldsymbol{x}_0(t)$, such that for all $\epsilon > 0$,*

$$\liminf_{t\to T_c} \|\psi\|^2_{L^2(|\boldsymbol{x}-\boldsymbol{x}_0(t)|<\epsilon)} \geq M_c. \tag{2.27}$$

Then, as a consequence we have the following corollary.

Corollary 2.4. *All singular solutions of the critical NLS (2.1) undergo a strong collapse with $M_{collapse} \geq M_c$.*

Next, we will define the concept of variance which is closely related to the whole collapse in the NLS.

Definition 2.10 (Variance). *Let ψ be a NLS solution. Then, the variance around $\boldsymbol{x}_0$ of ψ is defined as*

$$Var(t;\boldsymbol{x}_0) = \int |\boldsymbol{x}-\boldsymbol{x}_0|^2 |\psi(\boldsymbol{x},t)|^2 d\boldsymbol{x}. \tag{2.28}$$

Now, one can see that the vanishing of the variance is a sufficient condition for the whole collapse in the NLS.

Lemma 2.5 ([54]). *Let ψ be a solution of the NLS that collapses at $\boldsymbol{x}_c$ as $t \to T_c$. If the variance vanishes at the singularity, i.e., if*

$$\lim_{t\to T_c} Var(t;\boldsymbol{x}_c) = \lim_{t\to T_c} \int |\boldsymbol{x}-\boldsymbol{x}_c|^2 |\psi(\boldsymbol{x},t)|^2 d\boldsymbol{x} = 0, \tag{2.29}$$

then the solution undergoes a whole collapse.

Proof. Let $\epsilon > 0$, then we have

$$\int_{|\boldsymbol{x}-\boldsymbol{x}_c|>\epsilon} |\psi|^2 d\boldsymbol{x} \le \frac{1}{\epsilon^2} \int_{|\boldsymbol{x}-\boldsymbol{x}_c|>\epsilon} |\boldsymbol{x}-\boldsymbol{x}_c|^2 |\psi|^2 d\boldsymbol{x} \le \frac{1}{\epsilon^2} \int_{\mathbb{R}^d} |\boldsymbol{x}-\boldsymbol{x}_c|^2 |\psi|^2 d\boldsymbol{x}. \tag{2.30}$$

Therefore, by the assumption

$$\lim_{t\to T_c} \int_{|\boldsymbol{x}-\boldsymbol{x}_c|>\epsilon} |\psi|^2 d\boldsymbol{x} = 0. \tag{2.31}$$

Conservation of mass implies

$$\lim_{t\to T_c} \int_{|\boldsymbol{x}-\boldsymbol{x}_c|<\epsilon} |\psi|^2 d\boldsymbol{x} = \|\psi_0\|_2^2. \tag{2.32}$$

□

2.1.3 NLS symmetries

Equation (2.1) possesses the following symmetries, which map a solution $\psi(\boldsymbol{x},t)$ into a new solution of the form

a) Space, time and phase shifts: $e^{i\theta}\psi(\boldsymbol{x}+\boldsymbol{x}_0, t+t_0)$, $\quad t_0, \theta \in \mathbb{R}$, $\boldsymbol{x}_0 \in \mathbb{R}^d$;

b) Dilations: $\mu^{1/\sigma}\psi(\mu\boldsymbol{x}, \mu^2 t)$, $\quad \mu > 0$;

c) Galilean transformations: $\exp\left(\dfrac{i\boldsymbol{c}\cdot\boldsymbol{x}}{2} - \dfrac{i|\boldsymbol{c}|^2 t}{4}\right)\psi(\boldsymbol{x}-\boldsymbol{c}t, t)$, $\quad \boldsymbol{c} \in \mathbb{R}^d$.

In the critical case, $\sigma d = 2$, NLS equation (2.1) admits the additional symmetry, which was discovered in 1970 by Talanov [63]:

Lemma 2.6 (Lens transformation [34, 63])**.** *Let*

$$\tilde{\psi}(\boldsymbol{x},t) := \frac{1}{L^{d/2}(t)} \exp\left(i\frac{L_t}{L}\frac{|\boldsymbol{x}|^2}{4}\right)\psi(\boldsymbol{\xi},\tau), \tag{2.33}$$

where

$$\xi = \frac{\boldsymbol{x}}{L(t)}, \quad \tau = \int_0^t \frac{ds}{L^2(s)}, \tag{2.34}$$

and $L(t) = \alpha(T_c - t)$ is a linear function with an arbitrary scaling constant $\alpha > 0$ and time shift $T_c \in \mathbb{R}$. Then, $\psi(\boldsymbol{x},t)$ is a solution of the critical NLS if and only if $\tilde{\psi}(\boldsymbol{x},t)$ is a solution of the critical NLS.

Remark 2.2. *If we take $L(t) \equiv 1/\mu$, with μ a positive constant, the lens transformation reduces to the dilation transformations.*

Remark 2.3. *The relevance of the lens transformation in the singular NLS theory is based on the fact that it determines the structure of the singular solutions close to the collapse (with $L(t)$ a nonlinear function), as it will be seen in the next section.*

2.2 Critical NLS

From now on and until the end of the thesis it is assumed that NLS is in the critical regime, i.e., $\sigma d = 2$. The aim in this section is: the construction of explicit singular solutions, the introduction of the blowup rate concept, and the presentation of the universality of singular solutions.

2.2.1 Explicit singular solutions

In the previous sections we have shown that NLS admits the waveguide solutions $\psi = e^{it}R(\boldsymbol{x})$, where $R(\boldsymbol{x})$ is a solution of the stationary equation (2.17). Therefore, applying the lens transformation to the waveguide solutions we obtain the explicit solution for the critical NLS (2.1):

$$\psi_R^{\text{explicit}}(\boldsymbol{x},t) = \frac{1}{L^{d/2}(t)} R\left(\frac{r}{L(t)}\right)\exp\left(i\tau + i\frac{L_t}{L}\frac{r^2}{4}\right), \tag{2.35}$$

with

$$L(t) = T_c - t \quad \text{and} \quad \tau = \int_0^t \frac{ds}{L^2(s)} = \frac{t}{T_c(T_c - t)}. \tag{2.36}$$

As it is expected, these kind of solutions blow up at time $t = T_c$ and singularity point $\boldsymbol{x}_c = 0$; as it is shown in the next results:

Lemma 2.7. *$\psi_R^{explicit}$ is an $H^1(\mathbb{R}^d)$ solution of the critical NLS (2.1) that becomes singular at T_c.*

Proof. Using the fact $R \in H^1(\mathbb{R}^d)$, we deduce that $\psi_R^{\text{explicit}} \in H^1(\mathbb{R}^d)$ for each $0 \leq t < T_c$. Moreover, by using the equations (2.35)-(2.36) one gets

$$\|\psi_R^{\text{explicit}}\|_{4/d+2}^{4/d+2} = \frac{1}{(T_c - t)^2}\|R\|_{4/d+2}^{4/d+2}. \tag{2.37}$$

Then, $\|\psi_R^{\text{explicit}}\|_{4/d+2}^{4/d+2} \to \infty$ as $t \to T_c$. Hence, by Corollary 2.2 with $\sigma d = 2$, the explicit solutions are singular at T_c. □

Lemma 2.8 ([17])**.** *$\psi_R^{explicit}$ becomes singular at $\boldsymbol{x}_c = 0$ as $t \to T_c$.*

In Figure 2.1 we have plotted the profile of $|\psi_R^{\text{explicit}}|^2$ close the collapse. Here the blowup time is $T_c = 1$ and dimension $d = 1$. We can observe, as it is expected, that the maximum of the solution increases as $t \to 1$.

Two important properties of the explicit solutions ψ_R^{explicit} is concerned to the mass and the variance. In fact, they satisfy

$$\|\psi_R^{\text{explicit}}\|_2^2 = \|R\|_2^2, \qquad Var(\psi_R^{\text{explicit}}) = (T_c - t)^2 Var(R). \tag{2.38}$$

Consequently, the variance of the explicit solutions vanishes at the singularity, and then by the Lemma 2.5 these solutions undergo a whole collapse with $M_{\text{collapse}} = \|R\|_2^2$. In addition, if $R = R^{(0)}$ then $\psi_{R^{(0)}}^{\text{explicit}}$ are examples of singular solutions with exactly the critical mass M_c.

The fact that $\psi_{R^{(0)}}^{\text{explicit}}$ has exactly the minimal mass for collapse, allows us to ask about the uniqueness of such solutions. A positive answer of this question was given by Merle in [45, 46], showing that these are the only minimal-mass solutions:

Theorem 2.4 ([45, 46])**.** *Let ψ be a solution of the critical NLS which blows up at $0 < T_c < \infty$, such that the initial condition satisfies the relation $\|\psi_0\|_2^2 = M_c$. Then there exist $\alpha, \theta \in \mathbb{R}$ and $\boldsymbol{x}_0, \boldsymbol{c} \in \mathbb{R}^d$, such that for $0 \leq t < T_c$,*

$$\psi(\boldsymbol{x}, t) = \frac{1}{[\alpha(T_c - t)]^{d/2}} R^{(0)}\left(\left|\frac{\boldsymbol{x} - \boldsymbol{x}_0 - t\boldsymbol{c}}{\alpha(T_c - t)}\right|\right) \exp\left(i\theta + \frac{i}{\alpha^2(Tc - t)} - \frac{i|\boldsymbol{x} - \boldsymbol{x}_0 - t\boldsymbol{c}|^2}{4(T_c - t)}\right) \times \exp\left(\frac{i\boldsymbol{c}\cdot(\boldsymbol{x} - \boldsymbol{x}_0)}{2} - \frac{i|\boldsymbol{c}|^2 t}{4}\right). \tag{2.39}$$

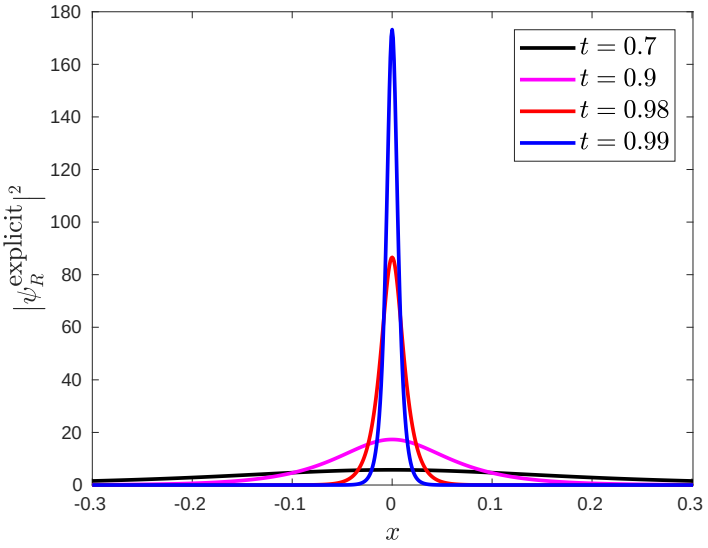

Figure 2.1: Profile of the explicit blowup solution ψ_R^{explicit} close the critical time $T_c = 1$ for an one-dimensional problem.

Notice that the solution (2.39) coincides with (2.35) up to symmetries, see Subsection 2.1.3.

2.2.2 Blowup rate

An important property of blowup solutions is their blowup rate. It is defined as follows:

Definition 2.11 (Blowup rate)**.** *Let ψ be an NLS solution that collapses at T_c. The blowup rate of ψ is the rate at which*

$$l(t) = \frac{1}{\|\nabla\psi(t)\|_2}, \tag{2.40}$$

goes to zero as $t \to T_c$.

By Hamiltonian conservation one has,

$$\lim_{t\to T_c} \frac{\|\nabla\psi\|_2^2}{\frac{d}{d+2}\|\psi\|_{4/d+2}^{4/d+2}} = 1. \tag{2.41}$$

Therefore, the blowup rate can be redefined in the convenient way

$$l(t) = \frac{1}{\|\nabla\psi(t)\|_2} = \left(\frac{1}{\frac{d}{d+2}\|\psi\|_{4/d+2}^{4/d+2}}\right)^{1/2} = \left(\frac{2/d+1}{\|\psi\|_{4/d+2}^{4/d+2}}\right)^{1/2}. \tag{2.42}$$

Under this new definition of blowup rate, it is possible to show that explicit solutions collapse with a linear blowup rate:

Lemma 2.9. *$\psi_R^{explicit}$ has a linear blowup rate, i.e.,*

$$l(t) \sim c(T_c - t), \quad \text{as } t \to T_c, \tag{2.43}$$

with c is a positive constant.

Proof. By the new definition of blowup rate, one has

$$l(t) = \left(\frac{2/d+1}{\|\psi_R^{\text{explicit}}\|_{4/d+2}^{4/d+2}} \right)^{1/2} = \frac{(2/d+1)^{1/2}}{\|R\|_{4/d+2}^{2/d+1}} (T_c - t). \tag{2.44}$$

□

Then, the blowup rate is linearly proportional to the dimensionless width $L(t)$, i.e., $l(t) \sim c_l L(t)$ for some positive constant c_l. We will see later that this fact holds for a more general solutions of the critical NLS equation for times close the blowup time (see equation (2.49) below).

In 1990 Cazenave and Weissler proved in [9] that the blowup rate of singular solutions is at least a square root. It is established in the following results.

Theorem 2.5 ([9])**.** *Let ψ be a solution of the critical NLS (2.1) that becomes singular at T_c. Then there exists a positive constant $K = K(\|\psi_0\|_2)$ such that*

$$\|\nabla\psi\|_2 \geq \frac{K}{\sqrt{T_c - t}}, \quad 0 \leq t < T_c. \tag{2.45}$$

Corollary 2.5. *The blowup rate of singular solutions of the critical NLS is at least square root, i.e.,*

$$l(t) \leq M_K (T_c - t)^{1/2}, \quad 0 \leq t < T_c, \tag{2.46}$$

where M_K is a positive constant that depends only on $\|\psi_0\|_2$.

2.2.3 Universal blowup profile

In 1965, Kelley in [33] shows by using an informal dimensional argument that the two-dimensional NLS equation admits solutions that become singular at a finite time

T_c. Also, the first numerical simulation of blowup solutions was done by Kelley in that same paper.

The first analysis of the self-focusing dynamics was done in 1966 by Akhmanov et al. [1] using the *aberrationless approximation method*. In that method the blowup dynamics of the solutions were assumed self-similar with a Gaussian profile. Therefore, the substitution of the Gaussian ansatz in the NLS equation allowed to obtain a system of ordinary differential equations independent of the spatial variables and equivalent to the original NLS equation. This method contributed successfully in the analytical approximation of the beam width and the blowup time (distance). Soon after, it becomes clear that some predictions based on the aberrationless approximation can be incorrect [2, 12, 44]. Accordingly, appears the called *variational approach* in which the Gaussian ansatz is replaced with super-Gaussian or sech profile [12]. However, also this new approach led to some incorrect results [24]. Indeed, both approaches in some sense are equivalent: they assumed that in the blowup dynamics solutions maintain a self-similar profile. Therefore, some of the wrong conclusions obtained by these methods were: The variance vanishes at the blowup point, the whole collapse of the singular solutions (see Lemma 2.5) and the over-estimates of the critical mass M_c, see, e.g., [17] for full details.

Many numerical simulations carried out during the 1980s and early 1990s [27, 36, 37, 38, 43], suggested that solutions, whose initial mass is slightly above the critical mass M_c, split into two components. One of them, the collapsing core, blows up following the universal profile modulated by the ground state $R^{(0)}$, i.e.,

$$|\psi_{R^{(0)}}|^2 = \frac{1}{L^d(t)}\left(R^{(0)}\left(\frac{r}{L(t)}\right)\right)^2, \tag{2.47}$$

with $L(t) \to 0$ as $t \to T_c$. The second one, the tail or outer part, does not participate in the collapse. This universality has been observed also in numerical simulations accomplished late 1990s and until 2005 [18, 20, 24]. For instance, in 2000 Fibich and Ilan [24] observed the convergence to the $\psi_{R^{(0)}}$ profile for the two-dimensional cubic NLS with an elliptic initial condition. Also, in 2001, they observed this universal profile in simulations with a noisy high-mass Gaussian initial condition with mass $15M_c$ and 10% complex-valued noise [20]. In 2005, Fibich et al. in [18] considered as an initial condition a Gaussian function with the high total mass $M \approx 38M_c$. Those simulations

showed that the collapsing core convergences toward $\psi_{R^{(0)}}$ profile as well.

The convergence to this universal profile, was first rigorously proved by Perelman in 2001 for the one-dimensional NLS with a certain class of initial conditions close to the ground state [58]. Later, in a series of papers published between 2003 and 2006, Merle and Raphael treated rigorously the general case. The results are summarized in the following theorem:

Theorem 2.6 ([47, 48, 49, 50, 51, 52])**.** *Let $d \leq 5$, and let ψ be a solution of the critical NLS with the initial condition $\psi(\boldsymbol{x}, 0) = \psi_0(\boldsymbol{x})$ that becomes singular at T_c. Then, there exists a universal constant $m^* > 0$, which depends only on the dimension, such that for any $\psi_0 \in H^1(\mathbb{R}^d)$ such that*

$$M_c < \|\psi_0\|_2^2 < M_c + m^*, \quad H(\psi_0) < \left(\frac{Im \int \psi_0^* \nabla \psi_0}{\|\psi_0\|_2} \right)^2,$$

the following hold:

a) There exist parameters $(\tau(t), \boldsymbol{x}_0(t), L(t)) \in \mathbb{R} \times \mathbb{R}^d \times \mathbb{R}^+$, and a function $0 \neq \phi \in L^2$, such that

$$\psi(\boldsymbol{x}, t) - \psi_{R^{(0)}}(\boldsymbol{x} - \boldsymbol{x}_0(t), t) \xrightarrow{L^2} \phi(\boldsymbol{x}), \quad as \quad t \to T_c,$$

where

$$\psi_{R^{(0)}}(\boldsymbol{x}, t) = \frac{1}{L^{d/2}(t)} R^{(0)} \left(\frac{r}{L(t)} \right) \exp \left(i\tau(t) + i \frac{L_t}{L} \frac{r^2}{4} \right).$$

Moreover, the blowup point is finite, i.e., $\boldsymbol{x}_c := \lim_{t \to T_c} \boldsymbol{x}_0(t)$.

b) As $t \to T_c$,

$$L(t) \sim \sqrt{2\pi} \left(\frac{T_c - t}{\log |\log(T_c - t)|} \right)^{1/2} \quad (\textbf{\textit{Loglog law}}).$$

Theorem 2.6 establishes that close the blow time, the core of the singular solutions approaches the quasi self-similar profile $\psi_{R^{(0)}}$ for certain initial conditions. By item (a), the wave-function ψ can be splitted as

$$\psi = \begin{cases} \psi_{\text{collapse}}, & |\boldsymbol{x} - \boldsymbol{x}_0(t)| = \mathcal{O}(L(t)), \\ \psi_{\text{tail}}, & |\boldsymbol{x} - \boldsymbol{x}_0(t)| \gg L(t), \end{cases} \tag{2.48}$$

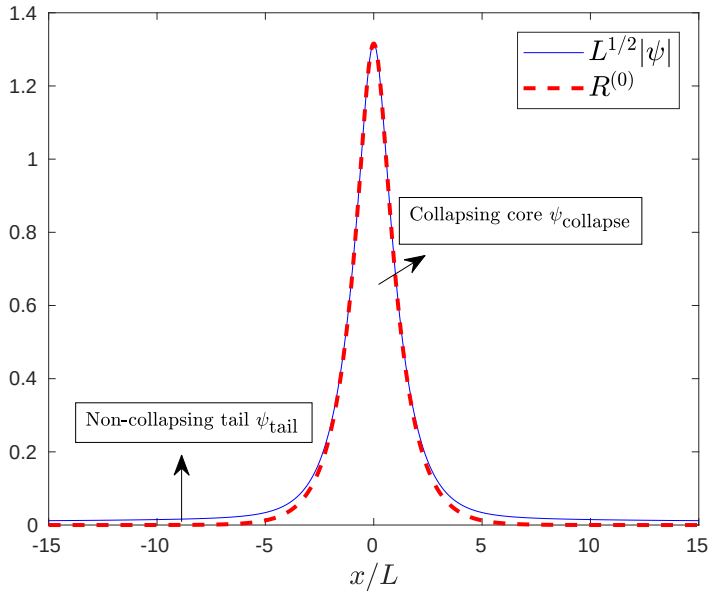

Figure 2.2: Illustration of the blowup dynamics established in Theorem 2.6 for an one-dimensional problem.

where $\psi_{\text{collapse}} \approx \psi_{R^{(0)}}$, $\psi_{\text{tail}} \approx \phi$ as $t \to T_c$, see Figure 2.2 for an illustration of Theorem 2.6. Also, the blowup rate is given by

$$l(t) = \left(\frac{2/d+1}{\|\psi\|_{4/d+2}^{4/d+2}} \right)^{1/2} = \frac{(2/d+1)^{1/2}}{\|R^{(0)}\|_{4/d+2}^{2/d+1}} L(t). \tag{2.49}$$

Consequently, unlike the explicit solutions, item (b) implies that the blowup rate of general solutions have a slow loglog correction (Loglog law). In addition, the mass conservation and the fact that the mass of $\psi_{R^{(0)}}$ is equal to M_c, imply that the amount of mass that collapses into the singularity is exactly M_c (partial collapse). In other words,

Lemma 2.10 ([49])**.** *Under the conditions of the Theorem 2.6,*

$$|\psi|^2 \longrightarrow M_c \delta(\boldsymbol{x} - \boldsymbol{x}_c) + |\phi|^2, \quad \text{as} \quad t \to T_c,$$

where $\|\phi\|_2^2 = \|\psi_0\|_2^2 - M_c$, *and the convergence is in the sense of distributions. In particular, the amount of mass that collapses into the singularity is* $M_{collapse} = M_c$.

Remark 2.4. *The exact value of the constant* $m^* = m^*(d)$ *does not follow from the proof of Theorem 2.6. Some estimates yield* $m^* \leq M_c$, *see e.g., [17]. In this way, the proof of the previous result is just valid for initial conditions with mass less than* $2M_c$.

Remark 2.5. *During the 1990s, Malkin and Fibich [15, 43] showed that the loglog law is only valid at extremely large focusing leves (well above* 10^{50}*). The physical validity of the NLS equation, however, breaks down after focusing by* $10^2 - 10^3$*. Therefore, in [15, 43] the reduced system was solved in the domain of physical interest (moderate focusing levels) in which the solution with approaches a squared root law. Recently in 2013, Lushnikov et al. in [41] modified the previous reduced system in order to cover domain of phisical interest.*

Remark 2.6. *In Lemma 2.3 was shown that the ground state* $R^{(0)}$ *is the unique profile (up to scaling) satisfying the dual borderline properties, i.e.,* $\|R^{(0)}\|_2^2 = M_c$ *and* $H(R^{(0)}) = 0$*. Therefore, any reduction of the mass or Hamiltonian by a small perturbation, can led to a global and singular solution respectively. These important properties explain in some sense, why the self-similar Gaussian/Sech profiles used in the first analysis of self-focusing (aberrationless approximation/variational methods) led to wrong conclusions [2, 12, 24, 44]. Any other profile, even if it is so close to* $R^{(0)}$*, can not satisfies both conditions needed in the dual borderline properties.*

Although Theorem 2.6 does not hold for all initial conditions, all numerical simulations carried out until 2005 [18, 20, 24] supported that blowup solutions of the critical NLS collapse with the $\psi_{R^{(0)}}$ profile at a blowup rate slightly faster than a square root (Loglog law), as we mentioned before. Further simulations performed by Fibich et al. in 2005-2007 [18, 19], suggested that there may exist H^1 singular solutions of the critical NLS that collapse with a self-similar ring profile which is different from $\psi_{R^{(0)}}$, and at a square root blowup rate without a loglog correction. These new solutions have a local minimum at $r = 0$ and its global maximum is attained at certain $0 < r_{\max} < \infty$. Up to now, it is not clear whether they maintain the self-similar ring profile all the way up to the singularity. Since in this thesis we only focus on H^1 singular solutions collapsing with the universal profile $\psi_{R^{(0)}}$, we will not profound on these new solutions.

2.3 Concluding remarks

As we have seen, there are several relevant aspects that differ the explicit blowup solutions from the generic blowup solutions of the critical NLS:

1. Generically NLS blowup solutions undergo a partial collapse, while ψ_R^{explicit} undergoes a whole collapse.

2. In the critical NLS the blowup rate of singular solutions is a square root with a loglog correction for solutions that collapse with the $\psi_{R^{(0)}}$ profile. In comparison, the blowup rate of explicit solutions are linear.

3. The explicit solutions ψ_R^{explicit} collapse with the self-similar R profile. In contrast, generic blowup solutions collapse asymptotically with the $\psi_{R^{(0)}}$ profile, i.e., the collapse is quasi self-similar.

Chapter 3

Derivation of Reduced System

In Chapter 2, we saw that generically, critical NLS solutions collapse with the $\psi_{R^{(0)}}$ profile at a square root blowup rate with a loglog correction, see Theorem 2.6. This universality of the collapsing core, enabled to approximate collapsing NLS solutions by a system of ODEs called *reduced equations* (see Proposition 3.1), governing the dynamics of $L(t)$, which are independent of $\boldsymbol{x}$.

In the present chapter, we show the main steps of the derivation of such reduced equations for the blowup dynamics following [17]. Further details of the derivation can be found in Appendix B. Likewise of [17], we will consider radial NLS solutions with singularity point $\boldsymbol{x}_c = 0$ to simplify the presentation. However, reduced system is also valid in the nonradial case. We point out that the derivation presented here is not rigorous, and it uses several assumptions which were originally based on numerical simulations [17, 43, 25]. Some advantages of this derivation is that it is much shorter than the given by Merle and Raphael [47, 48, 49, 50, 51, 52], and it provides a physical interpretation to the reduced equations.

3.1 Quasi self-similar collapse

So far, we have seen that independent of the initial condition (radial and non-radial), collapsing core becomes radial about the singularity point and approaching the universal profile $\psi_{R^{(0)}}$. Therefore, in order to simplify the presentation we will assume that the solution is radial and $\boldsymbol{x}_c = 0$, i.e., $\psi(\boldsymbol{x}, t) = \psi(r, t)$ with $r = |\boldsymbol{x}|$. In these

terms, the NLS equation

$$i\psi_t(\boldsymbol{x},t)+\Delta\psi+|\psi|^{\frac{4}{d}}\psi=0, \tag{3.1}$$

can be replaced by its radial version (by using $\Delta\psi=\psi_{rr}+\frac{d-1}{r}\psi_r$)

$$i\psi_t(r,t)+\psi_{rr}+\frac{d-1}{r}\psi_r+|\psi|^{\frac{4}{d}}\psi=0. \tag{3.2}$$

Therefore, through this chapter we will work with the radial NLS equation (3.2).

In the previous chapter, we saw that in light of Theorem 2.6, singular NLS solutions can be decomposed as

$$\psi=\begin{cases}\psi_{\text{collapse}}, & 0\le r\le \xi_c L(t),\\ \psi_{\text{tail}}, & r\ge \xi_c L(t),\end{cases} \tag{3.3}$$

where $\xi_c=\mathcal{O}(1)$, $\xi_c\gg 1$ and

$$\psi_{\text{collapse}}\approx\psi_{R^{(0)}}(r,t)=\frac{1}{L^{d/2}(t)}R^{(0)}(\xi)\exp\left(i\tau(t)+i\frac{L_t}{L}\frac{r^2}{4}\right), \qquad \text{as} \quad t\to T_c, \tag{3.4}$$

where

$$\xi=\frac{r}{L(t)}, \qquad \frac{d\tau}{dt}=\frac{1}{L^2(t)}, \tag{3.5}$$

and $R^{(0)}$ is the ground state of

$$R''(\xi)+\frac{d-1}{\xi}R'-R+|R|^{\frac{4}{d}}R=0, \qquad R'(0)=0, \qquad R(\infty)=0. \tag{3.6}$$

The non-collapsing tail, as time approaches the blowup, convergences to the non-universal frozen state

$$\psi_{\text{tail}}\approx\phi(r)\in L^2, \qquad \text{as} \quad t\to T_c. \tag{3.7}$$

The objective of this chapter is derive the reduced equations given in the following result:

Proposition 3.1 ([27, 36, 38]). *Let $\psi(r,t)$ be a solution of the critical NLS (3.2) that collapses with the $\psi_{R^{(0)}}$ profile. Then as $t\to T_c$, the dynamics of $L(t)$ is governed, to leading order, by the* ***reduced equations (system)***

$$L_{tt}(t)=-\frac{\beta}{L^3}, \quad \beta_t(t)=-\frac{\nu(\beta)}{L^2}, \tag{3.8}$$

where $0 < \beta \ll 1$,

$$\nu(\beta) = c_\beta e^{-\pi/\sqrt{\beta}}, \qquad c_\beta = \frac{2A_R^2}{N^{radial}}, \tag{3.9}$$

$$A_R = \lim_{r\to\infty} e^r r^{\frac{d-1}{2}} R^{(0)}(r), \qquad N^{radial} = \frac{1}{4}\int_0^\infty r^2 |R^{(0)}|^2 r^{d-1} dr. \tag{3.10}$$

The first equation in the reduced system, $L_{tt} = -\beta/L^3$, is obtained by taking into account that close the singularity NLS solution is quasi self-similar. On the other hand, second equation in reduced system, $\beta_t = -\nu(\beta)/L^2$, comes for example by considering the tunneling effect by computing the evolution of the mass of the collapsing core. The derivation of (3.8)-(3.10) was one of the hardest challenges in the NLS research during the 1980s. These equations were first derived by Fraiman [27] in 1985 from a linear-stability analysis of perturbations around the profile $\psi_{R^{(0)}}$. In 1988 these equations were rederived by Papanicolaou and coworkers [36, 38] from a solvability condition. Malkin in [43] derived the same equations in 1993 by considering the mass evolution of the collapsing core.

The first rigorous derivation of (3.8)-(3.10) was done by Perelman [58] in 2001 for the one-dimensional NLS and certain class of initial conditions. A rigorous derivation for initial conditions whose mass is somewhat above M_c in dimensions $1 \leq d \leq 5$ was given by Merle and Raphael in 2003-2006 (Theorem 2.6). The derivation given here follows [17]. It is basically a combination of the derivations found in [43, 26]. As we mentioned before, this derivation is not rigorous and it is based on the original assumptions observed in numerical simulations and asymptotic analysis. A point in favor of this derivation is that it provides a physical interpretation of the reduced system.

A fundamental tool in the derivation of the reduced system is the well known *WKB method or quasi-classical limit* in quantum mechanics:

Lemma 3.1 ([3, 35])**.** *Let* $\Psi(x)$ *be a solution of*

$$\Psi''(x) + \frac{d-1}{x}\Psi' + \frac{1}{\epsilon^2}Q(x)\Psi = 0, \tag{3.11}$$

such that $Q(x) \neq 0$. *Then,* $\Psi \approx \Psi^{WKB}(x)$ *as* $\epsilon \to 0$, *where*

$$\Psi^{WKB}(x) = \frac{1}{x^{\frac{d-1}{2}} Q^{\frac{1}{4}}(x)} \left(a_1 e^{-\frac{i}{\epsilon}\int^x \sqrt{Q}} + a_2 e^{\frac{i}{\epsilon}\int^x \sqrt{Q}} \right). \tag{3.12}$$

Proof. We look a solution of the form $\Psi = e^{\frac{1}{\epsilon}h_0(x)+h_1(x)+\epsilon h_2(x)+\cdots}$, where $\frac{1}{\epsilon}h_0(x) \gg h_1(x) \gg \epsilon h_2(x) \gg \cdots$ as $\epsilon \to 0$. Substituting that expression into equation (3.11) one obtains

$$\left(\frac{1}{\epsilon}h_0'' + h_1'' + \cdots\right) + \left(\frac{1}{\epsilon}h_0' + h_1' + \cdots\right)^2 + \frac{d-1}{x}\left(\frac{1}{\epsilon}h_0' + h_1' + \cdots\right) + \frac{Q}{\epsilon^2} = 0. \quad (3.13)$$

Balancing the leading $\mathcal{O}(\epsilon^{-2})$ terms we have

$$(h_0')^2 + Q = 0. \quad (3.14)$$

Then,

$$h_0' = \pm i\sqrt{Q}, \qquad h_0 = \pm i\int^x \sqrt{Q}. \quad (3.15)$$

Now balancing the $\mathcal{O}(\epsilon^{-1})$ terms gives

$$h_0'' + 2h_0'h_1' + \frac{d-1}{x}h_0' = 0. \quad (3.16)$$

Thus,

$$h_1' = -\frac{d-1}{2x} - \frac{h_0''}{2h_0'}, \qquad h_1 = -\frac{d-1}{2}\log x - \frac{1}{2}\log h_0'. \quad (3.17)$$

It can be verified that $\epsilon h_2(x) = o(1)$. Therefore, the result follows. □

It can be shown that when $Q(x_0) = 0$ and $Q'(x_0) \neq 0$, the WKB approximation is valid if $|x - x_0| \gg \epsilon^{\frac{2}{3}}$, see e.g., [3].

In order to facilitate the derivation of the reduced system, we provide in the next Subsection 3.1.1 the main steps involved in such derivation; and in the Appendix B, details of each step are shown.

3.1.1 Proof of Proposition 3.1: Main steps

The main steps in the derivation of reduced equations (3.8)-(3.10) are:

1. We introduce the *generalized lens transformation*

$$\psi(r,t) = \frac{1}{L^{d/2}(t)}\Psi(\xi,\tau)\exp\left(i\tau(t) + i\frac{L_t}{L}\frac{r^2}{4}\right), \quad (3.18)$$

where ξ and τ are given by (3.5), and Ψ satisfying the equation

$$i\Psi_\tau(\xi,\tau) + \Psi_{\xi\xi} + \frac{d-1}{\xi}\Psi_\xi - \Psi + |\Psi|^{\frac{4}{d}}\Psi + \frac{1}{4}\beta(t)\xi^2\Psi = 0, \quad (3.19)$$

with $\beta(t) = -L^3L_{tt}$. Then, we have derived the first equation of the reduced system: $L_{tt} = -\beta(t)/L^3$.

2. Expanding Ψ as

$$\Psi = \Psi_0 + \Psi_1 + \Psi_2 + \cdots, \qquad \Psi_0 \gg \Psi_1 \gg \Psi_2 \cdots, \tag{3.20}$$

one expects that $\Psi(\xi,\tau) \approx \Psi_0(\xi,\tau) \approx R^{(0)}(\xi)$ for $0 \le \xi \le \xi_c$. Hence, the leading-order equation for Ψ_0 is given by

$$\Psi_{0,\xi\xi} + \frac{d-1}{\xi}\Psi_{0,\xi} - \Psi_0 + |\Psi_0|^{\frac{4}{d}}\Psi_0 + \frac{1}{4}\beta\xi^2\Psi_0 = 0, \qquad 0 \le \xi \le \xi_c, \tag{3.21}$$

with the radial condition $\Psi_0'(0) = 0$.

3. Now since β is small, we expand the function Ψ_0 in terms of it:

$$\Psi_0(\xi;\beta) = R^{(0)}(\xi) + \beta g(\xi) + \mathcal{O}(\beta^2), \qquad g = \Psi_{0,\beta}(\xi;0). \tag{3.22}$$

In these terms, we have the following result whose proof can be found in Appendix B (see Lemma B.1):

Lemma 3.2 ([43]). *Let $M_{collapse}^{radial}$ denote the radial mass of the collapsing core, i.e.,*

$$M_{collapse}^{radial} = \int_0^{\xi_c L(t)} |\psi|^2 r^{d-1} dr. \tag{3.23}$$

Then,

$$M_{collapse}^{radial} = M_c^{radial} + \beta N^{radial} + \mathcal{O}(\beta^2), \qquad 0 < \beta \ll 1, \tag{3.24}$$

where

$$M_c^{radial} = \int_0^{\infty} |R^{(0)}|^2 r^{d-1} dr, \qquad N^{radial} = \frac{1}{4}\int_0^{\infty} r^2 |R^{(0)}|^2 r^{d-1} dr. \tag{3.25}$$

Corollary 3.1. *β is proportional to the excess mass above M_c of the collapsing core, i.e.,*

$$\beta \approx \frac{M_{collapse}^{radial} - M_c^{radial}}{N^{radial}} = \frac{M_{collapse} - M_c}{N}, \tag{3.26}$$

with

$$M_{collapse} = \int_{|\boldsymbol{x}| \le \xi_c L(t)} |\psi|^2 d\boldsymbol{x}, \qquad M_c = \int |R^{(0)}|^2 d\boldsymbol{x}, \tag{3.27}$$

and

$$N = \frac{1}{4}\int |\boldsymbol{x}|^2 |R^{(0)}|^2 d\boldsymbol{x}. \tag{3.28}$$

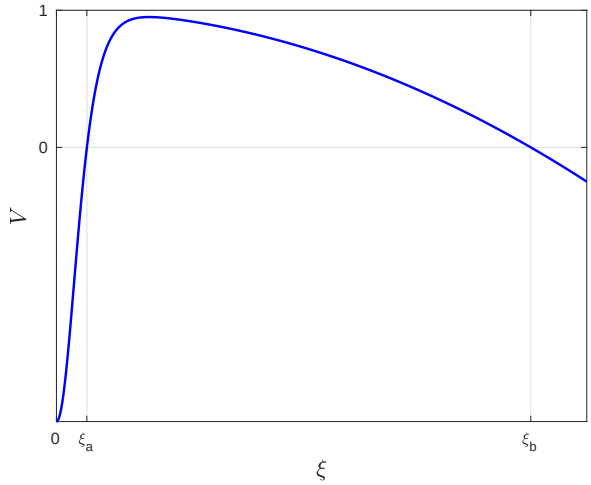

Figure 3.1: Illustration of the potential $V(\xi)$ in (3.31).

By Lemma 3.2 we get

$$\frac{d}{dt}M_{\text{collapse}}^{\text{radial}} \approx \beta_t N^{\text{radial}}. \tag{3.29}$$

4. Note that by using the transformation (3.18), the rate of change of the mass of the collapsing core is also given by

$$\frac{d}{dt}M_{\text{collapse}}^{\text{radial}} = \frac{1}{L^2}\left[i\xi^{d-1}\Psi^*\Psi_\xi + c.c.\right]_{\xi=\xi_c}, \tag{3.30}$$

where c.c. stands for complex conjugate, see Lemma B.2 in Appendix B. Then, in the next steps the idea is to approximate the right-hand side of equation (3.30), by using $\Psi \approx \Psi_0$ and WKB approximation, and compare the result with (3.29).

5. The equation for Ψ_0 (3.21) can be written as

$$\Psi_{0,\xi\xi} + \frac{d-1}{\xi}\Psi_{0,\xi} - V(\xi)\Psi_0 = 0, \qquad V(\xi) = 1 - |\Psi_0|^{\frac{4}{d}} - \frac{1}{4}\beta\xi^2. \tag{3.31}$$

Since $\Psi_0 \approx R^{(0)}$, equation for Ψ_0 is linear and the potential $V(\xi)$ has two turning points: $\xi_a = \mathcal{O}(1)$ where $R^{(0)} \approx 1$ and $\xi_b \approx 2\beta^{-1/2}$, see Figure 3.1. Then, in the classical-inaccessible region $1 \ll \xi < \xi_b$ where $V > 0$, Ψ_0 is exponentially decreasing, and then we can approximate Ψ_0 short after the second turning point. We will approximate solutions of (3.31) by using the WKB method, however, it breaks down at and near the turning point ξ_b. Therefore, we will obtain two WKB approximations: one valid to the right of ξ_b, denoted by $\Psi_0^{\text{WKB,right}}$, and another

valid to the left of ξ_b, denoted by $\Psi_0^{\text{WKB,left}}$. Each of these WKB approximations has two undetermined coefficients; those of $\Psi_0^{\text{WKB,right}}$ will be denoted by a_1 and a_2, and those of $\Psi_0^{\text{WKB,left}}$ by b_1 and b_2. From the frozen state condition it will follow that $a_1 = 0$, see Lemma B.3. To find the value of a_2, we will use the connection formula past the turning point to express b_1 and b_2 in terms of a_1 and a_2. Finally, the value of b_1, hence of a_2, will be determined by matching $\Psi_0^{\text{WKB,left}}$ with the approximation $\Psi_0 \approx R^{(0)}$, see Lemma B.4. At the end of the process one obtains

$$\frac{1}{L^2}\left[i\xi^{d-1}\Psi^*\Psi_\xi + c.c.\right]_{\xi=\xi_c} \approx -\frac{2A_R^2}{L^2}e^{-\frac{\pi}{\sqrt{\beta}}}. \tag{3.32}$$

6. Finally, by equations (3.29) and (3.32) we derive the second equation in the reduced system:

$$\beta_t = -\frac{2A_R^2}{N^{\text{radial}}L^2}e^{-\frac{\pi}{\sqrt{\beta}}}. \tag{3.33}$$

3.2 Numerical values of M_c, N, A_R and c_β

In this section, we will provide the numerical values of different constants used in the chapter. Indeed, we establish the numerical values of the following constants

$$M_c = \int |R^{(0)}(\boldsymbol{x})|^2 d\boldsymbol{x}, \qquad N = \frac{1}{4}\int |\boldsymbol{x}|^2 |R^{(0)}(\boldsymbol{x})|^2 d\boldsymbol{x}, \tag{3.34}$$

$$M_c^{\text{radial}} = \int_0^\infty |R^{(0)}(r)|^2 r^{d-1} dr, \qquad N^{\text{radial}} = \frac{1}{4}\int_0^\infty r^2 |R^{(0)}(r)|^2 r^{d-1} dr, \tag{3.35}$$

and

$$A_R = \lim_{r\to\infty} e^r r^{\frac{d-1}{2}} R^{(0)}(r), \qquad c_\beta = \frac{2A_R^2}{N^{\text{radial}}}, \tag{3.36}$$

for dimensions $d = 1, 2$ [17]. Clearly, $M_c = w_d M_c^{\text{radial}}$ and $N = w_d N^{\text{radial}}$, where w_d is the surface area of the unit sphere in d dimensions.

3.2.1 Case $d = 1$

In this case, we have an explicit formula for the ground state $R^{(0)}(x) = 3^{1/4}\,\text{sech}^{1/2}(2x)$. Then,

$$M_c = \frac{\sqrt{3}\pi}{2} \approx 2.7207, \qquad M_c^{\text{radial}} = \frac{\sqrt{3}\pi}{4} \approx 1.3603. \tag{3.37}$$

In addition,

$$R^{(0)}(x) = 3^{1/4}\left(\frac{e^{2x}+e^{-2x}}{2}\right)^{-1/2} \sim 3^{1/4}2^{1/2}e^{-x}, \quad x \to \infty. \tag{3.38}$$

In this terms, we have that $A_R = \lim_{r\to\infty} e^r R^{(0)}(r) = 3^{1/4}2^{1/2} \approx 1.8612$. Lastly,

$$N = \frac{\sqrt{3}\pi^3}{128} \approx 0.4196, \qquad N^{\text{radial}} = \frac{\sqrt{3}\pi^3}{256} \approx 0.2098, \tag{3.39}$$

and $c_\beta = \dfrac{1024}{\pi^3} \approx 33.0256$.

3.2.2 Case $d = 2$

For $d = 2$, we have an countable number of solutions. There is not an explicit expression for the ground state $R^{(0)}$, so it should be calculated numerically, yielding

$$M_c \approx 11.701, \qquad M_c^{\text{radial}} \approx 1.8623. \tag{3.40}$$

$$N \approx 3.4740, \qquad N^{\text{radial}} \approx 0.5529, \tag{3.41}$$

and

$$A_R = \lim_{r\to\infty} e^r r^{1/2} R^{(0)}(r) \approx 3.52, \qquad c_\beta \approx 44.8. \tag{3.42}$$

3.3 Concluding remarks

In this chapter we have shown that generically singular solutions collapse with the $\psi_{R^{(0)}}$ profile where

$$\psi_{R^{(0)}}(r,t) = \frac{1}{L^{d/2}(t)} R^{(0)}(\xi) \exp\left(i\tau(t) + i\frac{L_t}{L}\frac{r^2}{4}\right), \tag{3.43}$$

with

$$\xi = \frac{r}{L(t)}, \qquad \frac{d\tau}{dt} = \frac{1}{L^2(t)}, \tag{3.44}$$

and $R^{(0)}$ is the ground state of

$$R''(\xi) + \frac{d-1}{\xi}R' - R + |R|^{\frac{4}{d}}R = 0, \qquad R'(0) = 0, \qquad R(\infty) = 0. \tag{3.45}$$

Here, the solution width L is a nonlinear function governed by the system of ODEs (reduced system)

$$L_{tt}(t) = -\frac{\beta}{L^3}, \quad \beta_t(t) = -\frac{\nu(\beta)}{L^2}, \tag{3.46}$$

where $0 < \beta \ll 1$,

$$\nu(\beta) = c_\beta e^{-\pi/\sqrt{\beta}}, \qquad c_\beta = \frac{2A_R^2}{N^{\text{radial}}}, \tag{3.47}$$

$$A_R = \lim_{r\to\infty} e^r r^{\frac{d-1}{2}} R^{(0)}(r), \qquad N^{\text{radial}} = \frac{1}{4}\int_0^\infty r^2 |R^{(0)}|^2 r^{d-1} dr. \tag{3.48}$$

Derivation of the reduced system provides some interpretations:

1. The function β is proportional to the excess mass above M_c of the collapsing core (Corollary 3.1). The observation that $\lim_{t\to T_c} \beta = 0$ implies that the amount of mass that collapses into the singularity is exactly M_c, which is in according to Lemma 2.10.

2. The exponentially-small term $\nu(\beta)$ in the reduced system accounts for mass transfer from ψ_{collapse} to ψ_{tail}. Since β is small near the collapse, the self-focusing process becomes adiabatic, i.e., the rate at which $L(t)$ goes to zero is exponentially faster than the rate at which the excess mass above M_c of the collapsing core goes to zero.

3. The reduced equations are derived by using the approximation given in Corollary 3.1 which has an $\mathcal{O}(\beta)$ accuracy. Then, reduced equations have an $\mathcal{O}(\beta)$ accuracy.

Chapter 4

Nonlinear Damping Perturbation

In Chapter 2 we showed that NLS solutions may develop a singularity in finite time. Since physical quantities are not singular, it implies that close the singularity some terms neglected in the derivation of the NLS are important. In order to avoid that issue, different mechanisms to continue the solution after the singularity have been proposed: nonlinear saturation, linear and nonlinear damping, nonparaxiality and normal dispersion, see e.g., [17, 25] and references therein. Since any perturbation is assumed small, we expect the dynamics of the perturbed NLS is close to the dynamics of the unperturbed NLS. Indeed, numerical simulations supported this assumption, and an asymptotic theory called *modulation theory* that approximates any perturbed critical NLS by reduced equations was developed in [17, 25, 26]. Modulation theory is based on the assumption that collapsing core asymptotically approaches the fundamental state $\psi_{R^{(0)}}$ after the singularity with an adiabatic defocusing process. This chapter is focused on the introduction of the modulation theory, and its application to the nonlinear damping perturbation. The derivation of the reduced system presented here follows [17, 25], and it is not rigorous.

4.1 Nonlinear Damped NLS

In this chapter we will consider the nonlinearly-damped critical NLS

$$i\psi_t(\boldsymbol{x},t) + \Delta\psi + (1+i\delta)|\psi|^{\frac{4}{d}}\psi = 0, \qquad 0 < \delta \ll 1. \tag{4.1}$$

The nonlinear dissipation in the perturbed NLS (4.1) corresponds to three-photon absorption in nonlinear optics [7] or four-body collisions which cause loss of atoms from the Bose-Einstein condensate [14], and in the context of the complex quintic Ginzburg-Landau equation [11]. Recently, these kind of damped NLS (4.1) has been proposed as a mechanism for turbulent dissipation [10, 31, 42].

The current chapter has two goals: show that equation (4.1) indeed cures the singularity and then allows us to continue the solution after the blowup time, and the introduction to the existing modulation theory that allows to derive a reduced equations governing the adiabatic dynamics of the NLS (4.1). As in the undamped NLS, equation (4.1) is conveniently replaced by its integral form

$$\psi(\boldsymbol{x},t) = U(t)\psi_0(\boldsymbol{x}) + (i-\delta)\int_0^t U(t-s)|\psi(s)|^{\frac{4}{d}}\psi(s)ds, \tag{4.2}$$

where U is the free Shrödinger operator defined in (2.4). Corresponding to the first goal of this chapter, the global existence, we follow [17]. We point out that such result is a direct consequence of the Theorem 4.7.1 established in [8].

Theorem 4.1 ([17])**.** *Let $\delta > 0$. Then for every initial condition $\psi_0 \in H^1(\mathbb{R}^d)$, there exists a unique global solution ψ of (4.2) in $C\left([0,\infty), H^1(\mathbb{R}^d)\right)$.*

Proof. Multiplying equation (4.1) by ψ^*, adding the complex conjugate equation, and integrating over $\boldsymbol{x}$ we get

$$\frac{d}{dt}\int |\psi|^2 d\boldsymbol{x} = -2\delta \int |\psi|^{\frac{4}{d}+2} d\boldsymbol{x}. \tag{4.3}$$

Hence, integrating in time

$$\int |\psi|^2 d\boldsymbol{x} + 2\delta \int_0^t \left(\int |\psi|^{\frac{4}{d}+2} d\boldsymbol{x}\right) dt = \int |\psi_0|^2 d\boldsymbol{x}. \tag{4.4}$$

In these terms, the Strichartz norm

$$\|\psi\|^{\frac{4}{d}+2}_{L^{\frac{4}{d}+2}\left((0,t);L^{\frac{4}{d}+2}(\mathbb{R}^d)\right)} := \int_0^t \left(\int |\psi|^{\frac{4}{d}+2} d\boldsymbol{x}\right) dt \tag{4.5}$$

is globally bounded for $0 \le t < \infty$. By [8, Theorem 4.7.1] with $\lambda = 1 + i\delta$ and $q = r = 4/d+2$, the solution of (4.2) blows up if and only if this Strichartz norm blows up. In these terms, the solution of (4.2), and therefore of (4.1), exists globally. □

Remark 4.1. *By Corollary 2.2, when $\delta = 0$ the $L^{4/d+2}$ norm of the solution becomes infinite. Therefore, equation (4.3) implies that for $0 < \delta \ll 1$, the mass losses become important only as ψ approaches the collapse time.*

The previous Theorem 4.1 establishes that for each $\delta > 0$, solutions of the nonlinear damping NLS (4.1) are global in time. Consequently, motivated by the vanishing-viscosity solutions of hyperbolic conservation laws is natural to ask if this mechanism play the role of "viscosity" in the NLS, but the existing theory is quite limited. Despite it has been known that NLS model breaks down when the input mass is sufficiently high since 1965, an equivalent theory for the NLS has yet to be developed.

The existing theory used to treat any perturbation of the critical NLS is called *modulation theory*, and was developed by Fibich and Papanicolaou [25, 26] in 1998. Such theory assumes that after the singularity solution continues in the fundamental state $\psi_{R^{(0)}}$, and the dynamics remains adiabatic. Likewise of in the unperturbed NLS, modulation theory approximates the pure NLS dynamics by a system of ODEs called reduced equations, which are independent of the space variable $\boldsymbol{x}$. In the next sections, we will introduce the modulation theory assumptions and the derivation of the corresponding reduced equations.

4.2 Modulation theory

In this section we will introduce the modulation theory. This theory is developed for singular solutions of the unperturbed NLS collapsing with the $\psi_{R^{(0)}}$ profile. As we saw, the perturbation in NLS (4.1), $i\delta|\psi|^{\frac{4}{d}}\psi$, regularizes the solution, see Theorem 4.1. In this terms, modulation theory assumes a dominant adiabatic stage, in which the damped NLS solution remains close to the universal profile $\psi_{R^{(0)}}$ provided that $0 < \delta \ll 1$.

More clearly, modulation theory is based on the following premises:

1. The collapsing core ψ_{collapse} is close to the $\psi_{R^{(0)}}$ profile, where

$$\psi_{R^{(0)}}(\boldsymbol{x}, t) = \frac{1}{L^{\frac{d}{2}}(t)} R^{(0)}(\boldsymbol{\xi}) e^{i\tau + i\frac{L_t}{4L}r^2}, \tag{4.6}$$

with

$$\boldsymbol{\xi} = \frac{\boldsymbol{x}}{L}, \qquad \tau = \int_0^t \frac{ds}{L^2(s)}, \tag{4.7}$$

$r = |\boldsymbol{x}|$ and $R^{(0)}$ is the ground state of

$$\Delta R(\boldsymbol{\xi}) - R + |R|^{\frac{4}{d}} R = 0, \quad R'(0) = 0, \quad R(\infty) = 0. \tag{4.8}$$

2. Let $\beta(t) := -L^3 L_{tt}$. Then, we assume $|\beta| \ll 1$. Note that contrary to the unperturbed case in which $\beta > 0$, in the perturbed case β is allowed to assume both positive and negative values.

Under the validity of the last two conditions we establish the main result of this chapter:

Proposition 4.1 ([25, 26])**.** *Let conditions 1-2 hold. Then, self-focusing in the perturbed critical NLS (4.1) is governed, to leading order, by the* ***reduced equations***

$$\beta_t + \frac{\nu(\beta)}{L^2} = -\frac{2\delta c_d}{NL^2}, \qquad \beta = -L^3 L_{tt}, \tag{4.9}$$

with $c_d = \|R^{(0)}\|_{\frac{4}{d}+2}^{\frac{4}{d}+2}$ *and*

$$\nu(\beta) := \begin{cases} c_\beta e^{-\pi/\sqrt{\beta}}, & \beta > 0, \\ 0, & \beta \leq 0, \end{cases} \tag{4.10}$$

$$c_\beta = \frac{2A_R^2}{N^{radial}}, \quad A_R = \lim_{r\to\infty} e^r r^{(d-1)/2} R^{(0)}(r), \quad N^{radial} = \frac{1}{4}\int_0^\infty r^2 (R^{(0)})^2 r^{d-1} dr, \tag{4.11}$$

and $N = w_d N^{radial}$ *with* w_d *is the surface area of the* d*-dimensional unit sphere.*

Remark 4.2. *The extra term in the reduced system (4.9)-(4.11),* $-\frac{2\delta c_d}{NL^2}$*, comes from taking into account dissipation effects. Also, note that in this new reduced system the weak coupling between* $\psi_{collapse}$ *and* ψ_{tail} *is neglected, i.e.,* $\nu(\beta) = 0$ *for* $\beta \leq 0$*.*

Next, we will derive reduced equations given in the Proposition 4.1. Similarly as we did in the previous chapter, we will stipulate the next subsection to the main steps of the derivation, and corresponding details of such derivation can be found in Appendix C.

4.2.1 Proof of Proposition 4.1: Main steps

The proof of Proposition 4.1 is similar to the unperturbed critical NLS, in which the reduced equations are derived from balance of mass. Indeed, the main steps are:

1. Under the assumption that the adiabatic stage in the perturbed NLS is the same of the adiabatic stage of the unperturbed NLS, the total mass can be decomposed as

$$\int |\psi|^2 d\boldsymbol{x} = M_{\text{collapse}} + M_{\text{tail}}, \tag{4.12}$$

where

$$M_{\text{collapse}} = \int_{|\boldsymbol{x}|<\xi_c L(t)} |\psi|^2 d\boldsymbol{x}, \qquad M_{\text{tail}} = \int_{|\boldsymbol{x}|>\xi_c L(t)} |\psi|^2 d\boldsymbol{x}, \tag{4.13}$$

and $\xi_c = \mathcal{O}(1)$ with $\xi_c \gg 1$. In theses terms, the rate of mass change (4.3) becomes

$$\frac{d}{dt} M_{\text{collapse}} + \frac{d}{dt} M_{\text{tail}} = -2\delta \int |\psi|^{\frac{4}{d}+2} d\boldsymbol{x}. \tag{4.14}$$

Therefore, the idea in the next steps is approximate the equation (4.14).

2. In order to approximate the first term in the left-hand side of (4.14), $\frac{d}{dt} M_{\text{collapse}}$, we introduce the generalized lens transformation

$$\psi(\boldsymbol{x}, t) = \frac{1}{L^{d/2}(t)} \Psi^\delta(\boldsymbol{\xi}, \tau) \exp\left(i\tau(t) + i \frac{L_t}{L} \frac{r^2}{4} \right), \tag{4.15}$$

where $\boldsymbol{\xi}$ and τ are given by (4.7), and Ψ^δ satisfies the equation

$$i\Psi^\delta_\tau + \Delta_{\boldsymbol{\xi}} \Psi^\delta - \Psi^\delta + (1 + i\delta) |\Psi^\delta|^{\frac{4}{d}} \Psi^\delta + \frac{1}{4} \beta(t) |\boldsymbol{\xi}|^2 \Psi^\delta = 0, \tag{4.16}$$

with $\beta(t) = -L^3 L_{tt}$.

3. We expand

$$\Psi^\delta = \Psi^\delta_0 + \Psi^\delta_1 + \Psi^\delta_2 + \cdots, \tag{4.17}$$

and we expect that Ψ^δ_0 satisfies the stationary equation

$$\Delta_{\boldsymbol{\xi}} \Psi^\delta_0 - \Psi^\delta_0 + |\Psi^\delta_0|^{\frac{4}{d}} \Psi^\delta_0 + \frac{1}{4} \beta |\boldsymbol{\xi}|^2 \Psi^\delta_0 = 0. \tag{4.18}$$

Here, we did not add the perturbation because we assume that, as in the unperturbed case, Ψ^δ_0 is essentially real for $\boldsymbol{\xi} = \mathcal{O}(1)$.

4. Since we are assuming $|\beta| \ll 1$ and $0 < \delta \ll 1$,

$$\Psi_0^\delta(\boldsymbol{\xi};\beta) = R^{(0)}(\boldsymbol{\xi}) + \beta g(\boldsymbol{\xi}) + \delta h(\boldsymbol{\xi},\tau) + \mathcal{O}(\beta^2, \beta\delta, \delta^2). \tag{4.19}$$

In these terms, we can stablish the following result whose proof can be found in Appendix C (see Lemma C.1):

Lemma 4.1. *Let conditions 1-2 hold. Then,*

$$M_{collapse} = M_c + N\beta(t) + \mathcal{O}(\beta^2, \beta\delta, \delta^2). \tag{4.20}$$

Corollary 4.1. *β is proportional to the excess mass above M_c of the collapsing core, i.e.,*

$$\beta \approx \frac{M_{collapse} - M_c}{N}. \tag{4.21}$$

This interpretation for β is not valid for general perturbations, see e.g., [25, 17]. By Lemma 4.1, one deduces that

$$\frac{d}{dt} M_{\text{collapse}} \approx N\beta_t. \tag{4.22}$$

5. Since the perturbation is small, we assume that mass radiation from the high-intensity core to the tail is still given by

$$\frac{d}{dt} M_{\text{tail}} \approx \frac{N\nu(\beta)}{L^2}, \tag{4.23}$$

and then by (4.22)

$$\frac{d}{dt}\int |\psi|^2 d\boldsymbol{x} = \frac{d}{dt} M_{\text{collapse}} + \frac{d}{dt} M_{\text{tail}} \tag{4.24}$$

$$\approx N\beta_t + \frac{N\nu(\beta)}{L^2}. \tag{4.25}$$

6. To approximate the right-hand side of (4.14), we use the transformation (4.15) and the fact $\Psi^\delta \approx R^{(0)}$, and we obtain

$$-2\delta \int |\psi|^{4/d+2} d\boldsymbol{x} \approx -\frac{2\delta c_d}{L^2}, \tag{4.26}$$

with $c_d = \|R^{(0)}\|_{\frac{4}{d}+2}^{\frac{4}{d}+2}$.

7. Therefore, the balance equation (4.14) becomes

$$\beta_t + \frac{\nu(\beta)}{L^2} = -\frac{2\delta c_d}{NL^2}. \tag{4.27}$$

4.3 Concluding remarks

We have presented an asymptotic theory (modulation theory) to describe the self-focusing dynamics of the damped NLS (4.1). In such theory, the collapsing core of the solution is assumed to be close to the $\psi_{R^{(0)}}$ profile, where

$$\psi_{R^{(0)}}(\boldsymbol{x},t)=\frac{1}{L^{\frac{d}{2}}(t)}R^{(0)}(\boldsymbol{\xi})e^{i\tau+i\frac{L_t}{4L}r^2}, \tag{4.28}$$

with

$$\boldsymbol{\xi}=\frac{\boldsymbol{x}}{L},\qquad \tau=\int_0^t\frac{ds}{L^2(s)}, \tag{4.29}$$

$r=|\boldsymbol{x}|$ and $R^{(0)}$ is the ground state of

$$\Delta R(\boldsymbol{\xi})-R+|R|^{\frac{4}{d}}R=0,\quad R'(0)=0,\quad R(\infty)=0. \tag{4.30}$$

Here $L(t)$ is a nonlinear function governed to leading order by the system of ODEs (reduced system):

$$\beta_t+\frac{\nu(\beta)}{L^2}=-\frac{2\delta c_d}{NL^2},\qquad \beta=-L^3L_{tt}, \tag{4.31}$$

with $c_d=\|R^{(0)}\|^{\frac{4}{d}+2}_{\frac{4}{d}+2}$ and

$$\nu(\beta):=\begin{cases} c_\beta e^{-\pi/\sqrt{\beta}}, & \beta>0,\\ 0, & \beta\le 0,\end{cases} \tag{4.32}$$

$$c_\beta=\frac{2A_R^2}{N^{\text{radial}}},\quad A_R=\lim_{r\to\infty}e^r r^{(d-1)/2}R^{(0)}(r),\quad N^{\text{radial}}=\frac{1}{4}\int_0^\infty r^2(R^{(0)})^2r^{d-1}dr, \tag{4.33}$$

From the derivation of the reduced system comes some interpretations:

1. Contrary to the unperturbed case, the function β can assume negative values.

2. Similarly to the unperturbed case, β is proportional to the excess mass above the critical mass M_c of the collapsing core of the solution (Corollary 4.1). Therefore, we see through (4.32) that modulation theory does not take into account the interaction between ψ_{collapse} and ψ_{tail}, after that the mass of ψ_{collapse} reaches the value M_c, i.e., only dissipative effects are considered for $\beta\le 0$.

3. By Lemma 4.1 we see that reduced equations have an $\mathcal{O}(\beta,\delta)$ accuracy.

Chapter 5

Continuation of the NLS Solutions

In Chapter 2 we saw that NLS solutions may develop a singularty in finite time when the initial mass is equal or greater than certain critical quantity M_c. It was shown that solutions with initial mass slightly above M_c collapse with the universal $\psi_{R^{(0)}}$ profile. Under this universality, in Chapter 3, the dynamics of the pure NLS equation was replaced by an $\boldsymbol{x}$-independent system of ODEs (reduced equations), governing the dynamics of the width solution $L(t)$. In the subsequent Chapter 4, we introduced the nonlinear damping perturbation for the NLS with the objective to regularize the solution after the singularity. Like in the unperturbed case, a corresponding reduced system was derived for the damped NLS within the framework of the modulation theory.

In the current chapter, we will present some well known results concerning the continuation of the singular NLS solutions through the damped perturbation [21, 22]. Each continuation presented here was accomplished by the analysis of the reduced equations. Therefore, these results are not rigorous and are based on numerical simulations.

5.1 Review of modulation theory

Consider the damped NLS equation

$$i\psi_t(\boldsymbol{x},t) + \Delta\psi + (1+i\delta)|\psi|^{\frac{4}{d}}\psi = 0, \tag{5.1}$$

with δ is postive small parameter. In the modulation theory, it is assumed that the collapsing core of solutions of (5.1) approaches the profile

$$\psi_{R^{(0)}}(\boldsymbol{x},t)=\frac{1}{L^{\frac{d}{2}}(t)}R^{(0)}(\boldsymbol{\xi})e^{i\tau+i\frac{L_t}{4L}r^2}, \tag{5.2}$$

with

$$\boldsymbol{\xi}=\frac{\boldsymbol{x}}{L},\qquad \tau=\int_0^t\frac{ds}{L^2(s)}, \tag{5.3}$$

$r=|\boldsymbol{x}|$ and $R^{(0)}$ is the ground state of

$$\Delta R(\boldsymbol{\xi})-R+|R|^{\frac{4}{d}}R=0,\quad R'(0)=0,\quad R(\infty)=0. \tag{5.4}$$

The function $L(t)$ is governed, to leading order, by the following system of ODEs:

$$\beta_t+\frac{\nu(\beta)}{L^2}=-\frac{2\delta c_d}{NL^2},\qquad \beta=-L^3L_{tt}, \tag{5.5}$$

with $c_d=\|R^{(0)}\|^{\frac{4}{d}+2}_{\frac{4}{d}+2}$ and

$$\nu(\beta):=\begin{cases} c_\beta e^{-\pi/\sqrt{\beta}}, & \beta>0,\\ 0, & \beta\le 0,\end{cases} \tag{5.6}$$

$$c_\beta=\frac{2A_R^2}{N^{\text{radial}}},\quad A_R=\lim_{r\to\infty}e^r r^{(d-1)/2}R^{(0)}(r),\quad N^{\text{radial}}=\frac{1}{4}\int_0^\infty r^2(R^{(0)})^2r^{d-1}dr, \tag{5.7}$$

Also, in Chapter 4 we have shown that for any $\delta>0$ solutions of (5.1) are global in time, see Theorem 4.1. Therefore, singular solutions can be continued after the singularity.

Throughout this chapter we will adopt the following definition of a continuation:

Definition 5.1 (Continuation beyond the singularity)**.** *Let $\psi(\boldsymbol{x},t)$ be an NLS solution of (5.1) for $\delta=0$ and initial condition ψ_0 that collapses at T_c. For $\delta>0$, let $\psi^\delta(\boldsymbol{x},t)$ be a solution of (5.1) with the same initial condition ψ_0, such that*

1. *For any $0<\delta\ll 1$, ψ^δ exists for $0\le t<\infty$.*
2. *$\lim_{\delta\to 0^+}\psi^\delta=\psi$ for $0\le t<T_c$. Then, the continuation of ψ beyond the singularity is defined as*

$$\psi^{continuation}:=\lim_{\delta\to 0^+}\psi^\delta,\quad T_c<t<\infty. \tag{5.8}$$

Remark 5.1. *As we mentioned before, the continuation results presented here are based on informal arguments and numerical simulations. Therefore, a priori the limit established in condition 2 has not a well-defined sense.*

The continuation results shown in this chapter correspond to the explicit solution and general solutions collapsing with the universal $\psi_{R^{(0)}}$ profile [21, 22].

5.2 Continuation of explicit solutions

The first continuation that we will show corresponds to the explicit singular solutions $\psi^{\text{explicit}}_{R^{(0)}}$. In Chapter 2, we saw that these solutions have the form

$$\psi^{\text{explicit}}_{R^{(0)}}(\boldsymbol{x},t) = \frac{1}{L^{d/2}(t)} R^{(0)}\left(\frac{r}{L(t)}\right) \exp\left(i\tau + i\frac{L_t}{L}\frac{r^2}{4}\right), \tag{5.9}$$

with

$$L(t) = T_c - t \quad \text{and} \quad \tau = \int_0^t \frac{ds}{L^2(s)} = \frac{t}{T_c(T_c-t)}, \tag{5.10}$$

and collapsing at $\boldsymbol{x}_c = 0$ and $t = T_c$. In 2011, Fibich and Klein [21] calculated the vanishing critical nonlinear damping continuation of $\psi^{\text{explicit}}_{R^{(0)}}$. Since our intention is show the role that play the reduced system in continuing singular NLS solutions, in what follows, we will present such continuation result and some ideas of the proof. Further details can be found in [21]. The result is the following:

Proposition 5.1 ([21])**.** *Let ψ^{δ} be the solution of the critical damped NLS (5.1) with initial condition $\psi_0(\boldsymbol{x}) = \psi^{explicit}_{R^{(0)}}(r,0)$. Then for any $\theta \in \mathbb{R}$, there exists a sequence $\delta_n \to 0^+$, depending on θ, such that*

$$\lim_{\delta_n \to 0^+} \psi^{\delta_n} = \begin{cases} \psi^{explicit}_{R^{(0)}}(r,t), & \text{if } 0 \le t < T_c, \\ \psi^{explicit*}_{R^{(0)},\kappa}(r, 2T_c - t)e^{i\theta}, & \text{if } t > T_c, \end{cases} \tag{5.11}$$

where $\psi^{explicit}_{R^{(0)},\kappa}$ is given by (5.9)-(5.10) with

$$L(t) = \kappa(T_c - t), \quad \tau = \frac{1}{\kappa^2}\frac{t}{T_c(T_c-t)}. \tag{5.12}$$

In particular, the width of ψ^{δ}, $L(t;\delta)$, satisfies

$$\lim_{\delta \to 0^+} L(t;\delta) = \begin{cases} T_c - t, & \text{if } 0 \le t < T_c, \\ \kappa(t - T_c), & \text{if } t > T_c. \end{cases} \tag{5.13}$$

The constant κ is given by

$$\kappa = \pi \left[Bi(0)Ai'(s') - Ai(0)Bi'(s') \right] \approx 1.614, \tag{5.14}$$

where Ai and Bi are the Airy and Bairy functions, respectively, and $s' \approx -2.6663$ is the first negative root of $G(s) = \sqrt{3}Ai(s) - Bi(s)$.

Remark 5.2. *According to the previous result, continuation of the explicit solution (5.9) by vanishing nonlinear damping, is again an explicit solution with a finite higher expanding velocity L_t, see equation (5.13). In addition, the post-collapse limit is only determined up to multiplication by e^{θ}. This phase-loss property follows from the fact that the phase of $\psi^{explicit}_{R^{(0)}}$ becomes infinite at T_c. Indeed, the accumulative phase at $\boldsymbol{x} = 0$, $\tau = \tau(t)$, satisfies $\tau(T_c) = \infty$, see equation (5.10).*

Proof. Firstly, note that from the explicit solution given in (5.9)-(5.10) one has

$$L(0) = T_c, \quad L_t(0) = -1, \quad L_{tt}(0) = 0. \tag{5.15}$$

Then, the idea is to solve the reduced system (5.5)-(5.7) by using the previous values, i.e., with the initial conditions

$$L(0) = T_c, \quad L_t(0) = -1, \quad \beta(0) = -L^3(0)L_{tt}(0) = 0. \tag{5.16}$$

By other hand, the expression for β_t in equation (5.5) implies that $\beta_t < 0$. Therefore, $\beta \leq 0$ and consequently $\nu(\beta) \equiv 0$. The fact $\nu(\beta) \equiv 0$ is expected because in this case the total mass is exactly M_c, i.e., there is not tail, and then no mass-transfer. In these terms, the reduced system (5.5)-(5.7) becomes

$$\beta = -L^3 L_{tt}, \qquad \beta_t = -\frac{\tilde{\delta}}{L^2}, \quad \tilde{\delta} = \frac{2c_d\delta}{N}, \tag{5.17}$$

with initial conditions (5.16).

The next step is solve this new reduced system (5.17). To do that, one observes that $\beta_\tau = -\tilde{\delta}$, and consequently $\beta(\tau) = -\tilde{\delta}\tau$. Now, to solve for $L = L(t;\delta)$ we introduce the function $A = 1/L$, and observe that it satisfies

$$A_{\tau\tau} = \beta A = -\tilde{\delta}\tau A, \qquad A(0) = \frac{1}{T_c}, \quad A_\tau(0) = 1. \tag{5.18}$$

The change of variable $s = -\tilde{\delta}^{\frac{1}{3}}\tau$ transforms this last equation into the Airy's equation

$$A_{ss} = sA, \qquad A(0) = \frac{1}{T_c}, \quad A_s(0) = -\tilde{\delta}^{-\frac{1}{3}}. \tag{5.19}$$

The solution of (5.19) is given by

$$A(s) = k_1 \mathrm{Ai}(s) + k_2 \mathrm{Bi}(s), \tag{5.20}$$

with

$$k_1 = \pi \left(\tilde{\delta}^{-\frac{1}{3}} \mathrm{Bi}(0) + \frac{\mathrm{Bi}'(0)}{T_c} \right), \quad k_2 = -\pi \left(\tilde{\delta}^{-\frac{1}{3}} \mathrm{Ai}(0) + \frac{\mathrm{Ai}'(0)}{T_c} \right). \tag{5.21}$$

A crucial fact is the following limit

$$\lim_{\tilde{\delta} \to 0^+} s(t;\delta) = \begin{cases} 0, & \text{if } 0 \leq t < T_c, \\ s', & \text{if } t > T_c, \end{cases} \tag{5.22}$$

where $s' \approx -2.6663$ is the first negative root of $G(s) = \sqrt{3}\mathrm{Ai}(s) - \mathrm{Bi}(s)$. This fact is supported by numerical integration in [21].

By using $L = A^{-1}$, equation (5.20), and definitions of τ and s, we get

$$L_t = -A^{-2} A_s \frac{ds}{dt} = \tilde{\delta}^{\frac{1}{3}} A_s = \tilde{\delta}^{\frac{1}{3}} \left[k_1 \mathrm{Ai}'(s) + k_2 \mathrm{Bi}'(s) \right]. \tag{5.23}$$

By the definition of the coefficients k_1 and k_2 in (5.21), one deduces the limits

$$\lim_{\tilde{\delta} \to 0^+} \tilde{\delta}^{\frac{1}{3}} k_1 = \pi \mathrm{Bi}(0), \qquad \lim_{\tilde{\delta} \to 0^+} \tilde{\delta}^{\frac{1}{3}} k_2 = -\pi \mathrm{Ai}(0). \tag{5.24}$$

Therefore, from equations (5.22)-(5.24) we have

$$\lim_{\tilde{\delta} \to 0^+} L_t = \lim_{\tilde{\delta} \to 0^+} \tilde{\delta}^{\frac{1}{3}} \left[k_1 \mathrm{Ai}'(s) + k_2 \mathrm{Bi}'(s) \right] \tag{5.25}$$

$$= \begin{cases} \pi \left[\mathrm{Bi}(0)\mathrm{Ai}'(0) - \mathrm{Ai}(0)\mathrm{Bi}'(0) \right], & \text{if } 0 \leq t < T_c, \\ \pi \left[\mathrm{Bi}(0)\mathrm{Ai}'(s') - \mathrm{Ai}(0)\mathrm{Bi}'(s') \right], & \text{if } t > T_c. \end{cases} \tag{5.26}$$

Since $\pi \left[\mathrm{Bi}(0)\mathrm{Ai}'(0) - \mathrm{Ai}(0)\mathrm{Bi}'(0) \right] = -1$, and by definition of the constant κ, follows

$$\lim_{\tilde{\delta} \to 0^+} L_t = \begin{cases} -1, & \text{if } 0 \leq t < T_c, \\ \kappa, & \text{if } t > T_c. \end{cases} \tag{5.27}$$

Finally, equation (5.13) follows from the facts $L(0;0) = T_c$ and $L(T_c;0) = 0$. The rest of the conclusions given in (5.11) were supported by numerical simulations, as can be observed in [21]. □

5.3 Continuation of loglog collapse

In this section we present the continuation for singular solutions collapsing with the $\psi_{R^{(0)}}$ profile, and satisfying the loglog law established in Theorem 2.6. In the continuation of explicit solutions, the explicit solvability of the reduced system was crucial in finding such continuation. In what follows, we establish the continuation result with some ideas used in the proof. Note that contrary to the explicit case, the treatment of the reduced system is based in asymptotic analyses and numerical simulations. The continuation result is the following:

Proposition 5.2 ([21, 22])**.** *Let ψ be a solution of the NLS (5.1) with $\delta = 0$ and initial condition ψ_0 that collapses with the $\psi_{R^{(0)}}$ profile (5.2) at the loglog law at time T_c. Let ψ^δ be the solution of the damped NLS ($\delta > 0$) with the same initial condition ψ_0. Then $\lim_{\delta\to 0^+} \psi^\delta = \psi$ for $0 \le t < T_c$. In addition, for any $0 < \delta \ll 1$, there exist $\theta(\delta) \in \mathbb{R}$ and $\phi \in L^2$ such that*

$$\lim_{\delta\to 0^+} \left[\psi^\delta - \psi^*_{R^{(0)}}(r, 2T_c - t; \delta)e^{i\theta(\delta)}\right] \xrightarrow{L^2} \phi(r), \quad as\ t \to T_c^+, \tag{5.28}$$

with some function $L(t;\delta)$, such that

$$\lim_{t\to T_c^+}\lim_{\delta\to 0^+} L(t;\delta) = 0, \quad \lim_{t\to T_c^+}\lim_{\delta\to 0^+} L_t(t;\delta) = \infty, \quad \lim_{\delta\to 0^+}\theta(\delta) = \infty. \tag{5.29}$$

Remark 5.3. *Proposition 5.2 establishes that similarly to the continuation of explicit solutions, this continuation has the phase-loss property. Unlike the continuation of $\psi^{explicit}_{R^{(0)}}$, however, the post-collapse velocity of the expanding core becomes infinite. According to the authors of [21, 22], this infinite velocity is a consequence of the infinite pre-collapse velocity of collapsing loglog solutions, see Theorem 2.6. Also, the authors suggested that due to the infinite velocity of the expanding core, it immediately interacts with the non-collapsing tail, implying the break down of the reduced system shortly after the collapse.*

Proof. Since in this case solutions approach the $\psi_{R^{(0)}}$ profile as $\delta \to 0^+$, the analysis of reduced system is asymptotic. We don't pretend to be exhaustive in the details, and only we will focus in some ideas that will be relevant in the subsequents chapters.

Let $\tilde{\delta}$ be as was defined in (5.17). Then, for fixed $\tilde{\delta}$, as $\beta \to 0^+$, the term $\nu(\beta)$ becomes negligible compared with $\tilde{\delta}$. Therefore, to leading order the reduced equations

become again

$$\beta = -L^3 L_{tt}, \qquad \beta_t = -\frac{\tilde{\delta}}{L^2}, \quad \tilde{\delta} = \frac{2c_d\delta}{N}, \tag{5.30}$$

with the general initial conditions

$$L(0) = L_0, \qquad L_t(0) = L_0', \qquad \beta(0) = \beta_0 > 0. \tag{5.31}$$

Note that β_0 is positive because initially the amount of mass in the collapsing core is greater to the critical one. Since $\beta_\tau = -\tilde{\delta}$, we have

$$\beta(\tau) = \beta_0 - \tilde{\delta}\tau, \quad \beta_0 = \beta(0) > 0. \tag{5.32}$$

Let introduce the function $A = \frac{1}{L}$, then A satisfies the equation

$$A_{\tau\tau} = (\beta_0 - \tilde{\delta}\tau)A. \tag{5.33}$$

The change of variable $s = \tilde{\delta}^{-\frac{2}{3}}\beta_0 - \tilde{\delta}^{\frac{1}{3}}\tau$ transforms the previous equation into Airy's equation

$$A_{ss} = sA, \qquad A(s_0) = A_0, \quad A_s(s_0) = -\tilde{\delta}^{-\frac{1}{3}}\frac{A_0'}{A_0^2}, \tag{5.34}$$

where $A_0 = 1/L_0$, $A_0' = -L_0'/L_0^2$ and $s_0 = \tilde{\delta}^{-\frac{2}{3}}\beta_0 \gg 1$. Then,

$$A(s) = k_1\mathrm{Ai}(s) + k_2\mathrm{Bi}(s), \tag{5.35}$$

with

$$k_1 = \pi\left[\frac{A_0'}{A_0^2}\tilde{\delta}^{-1/3}\mathrm{Bi}(s_0) + A_0\mathrm{Bi}'(s_0)\right], \quad k_2 = -\pi\left[\frac{A_0'}{A_0^2}\tilde{\delta}^{-1/3}\mathrm{Ai}(s_0) + A_0\mathrm{Ai}'(s_0)\right]. \tag{5.36}$$

Now, since $s_0 \gg 1$, we can approximate $\mathrm{Ai}(s_0)$ and $\mathrm{Bi}(s_0)$ by

$$\mathrm{Ai}(s_0) \approx \frac{1}{2\sqrt{\pi}}s_0^{-1/4}e^{-\frac{2}{3}s_0^{3/2}}, \qquad \mathrm{Bi}(s_0) \approx \frac{1}{\sqrt{\pi}}s_0^{-1/4}e^{\frac{2}{3}s_0^{3/2}}. \tag{5.37}$$

Using the previous expressions we have

$$\lim_{\tilde{\delta}\to 0^+}\frac{k_2}{k_1} = \lim_{\tilde{\delta}\to 0^+} -\frac{\mathrm{Ai}(s_0)}{\mathrm{Bi}(s_0)} = \lim_{\tilde{\delta}\to 0^+} -\frac{1}{2}e^{-\frac{4}{3}s_0^{3/2}} = 0, \tag{5.38}$$

and consequently equation (5.35) becomes

$$A(s) \approx k_1\mathrm{Ai}(s), \quad s = \mathcal{O}(1), \quad 0 < \tilde{\delta} \ll 1. \tag{5.39}$$

Similarly, approximations given in (5.37) imply

$$\lim_{\tilde{\delta}\to 0^+} \tilde{\delta}^{1/3} k_1 = \lim_{\tilde{\delta}\to 0^+} \pi \frac{A_0'}{A_0^2} \mathrm{Bi}(s_0) \tag{5.40}$$

$$\approx \lim_{\tilde{\delta}\to 0^+} \pi \frac{A_0'}{A_0^2} \frac{1}{\sqrt{\pi}} s_0^{-1/4} e^{\frac{2}{3} s_0^{3/2}} \tag{5.41}$$

$$= \lim_{\tilde{\delta}\to 0^+} \frac{\sqrt{\pi} A_0'}{A_0^2} \tilde{\delta}^{1/6} \beta_0^{-1/4} e^{\frac{2}{3}\frac{\beta_0^{3/2}}{\tilde{\delta}}} = \infty. \tag{5.42}$$

By numerical integration is shown in [21, 22] that as $\tilde{\delta} \to 0^+$,

$$s(t;\delta) \approx \begin{cases} \mathcal{O}(s_0), & \text{if } 0 \le t < T_c, \\ s', & \text{if } t > T_c, \end{cases} \tag{5.43}$$

where $s' \approx -2.338$ is the first negative root of $\mathrm{Ai}(s)$. Therefore, in terms of the equations (5.39) and (5.43) the expanding velocity $L_t(t;\delta)$ satisfies

$$\lim_{\tilde{\delta}\to 0^+} L_t(t;\delta) \approx \lim_{\tilde{\delta}\to 0^+} \tilde{\delta}^{1/3} k_1 \mathrm{Ai}'(s') = \infty, \tag{5.44}$$

and consequently the post-collapse expanding velocity becomes infinite as $\tilde{\delta} \to 0^+$. This fact proves the second limit in the equation (5.29). The rest of conclusions is supported in [21, 22] by numerical simulations. □

5.3.1 Wave-maximum

It is clear that the maximum of solutions of the damped NLS (5.1) depends on $\delta > 0$. We can use the reduced equations to estimate the δ-dependence of the maximum of such solutions. Indeed, for ψ a solution of the damped NLS (5.1), we define

$$|\psi|^2_{\max\max} := \max_{x,t} |\psi(x,t)|^2. \tag{5.45}$$

Since ψ approaches the $\psi_{R^{(0)}}$ profile, we have

$$|\psi|^2_{\max\max} = 3^{1/4} A^d_{\max}, \tag{5.46}$$

where $A_{\max} = \max_t A(t)$ with $A(t) = 1/L(t)$. Hence, by equations (5.37) and (5.39) follows

$$A(s) \approx k_1 \mathrm{Ai}(s) \tag{5.47}$$

$$\approx \pi \frac{A_0'}{A_0^2} \tilde{\delta}^{-1/3} \mathrm{Bi}(s_0)\mathrm{Ai}(s) \tag{5.48}$$

$$\approx \pi \frac{A_0'}{A_0^2} \tilde{\delta}^{-1/3} \frac{1}{\sqrt{\pi}} s_0^{-1/4} e^{\frac{2}{3}s_0^{3/2}} \mathrm{Ai}(s) \tag{5.49}$$

$$= \sqrt{\pi} \frac{A_0'}{A_0^2} \tilde{\delta}^{-1/6} \beta_0^{-1/4} e^{\frac{2\beta_0^{3/2}}{2\tilde{\delta}}} \mathrm{Ai}(s). \tag{5.50}$$

The Airy function $\mathrm{Ai}(s)$ attains its absolute maximum (≈ 0.54) at $s \approx -1.0$. Therefore, the maximum of $A(s)$ is

$$A_{\max} \approx 0.54\sqrt{\pi} \frac{A_0'}{A_0^2} \beta_0^{-1/4} \tilde{\delta}^{-1/6} \exp\left(\frac{2}{3}\frac{\beta_0^{3/2}}{\tilde{\delta}}\right). \tag{5.51}$$

In other words, the maximum of $|\psi|^2$ increases exponentially with decreasing δ [21, 23].

5.3.2 Wave dissipation

The last question that we will address in this chapter is about the amount of mass dissipated in an individual collapse. Fibich in [16] established the following estimate for the mass loss in a collapsing event for the two-dimensional NLS equation (5.1):

$$\Delta M \sim \int_{\tau(s_0)}^{\tau(s')} \tilde{\delta} d\tau \sim N\left(\beta_0 - \tilde{\delta}^{2/3} s'\right), \tag{5.52}$$

where $s' \approx -2.338$ is the first negative root of $\mathrm{Ai}(s)$. Therefore, in the limit $\delta \to 0^+$, the amount of mass loss is equal to $N\beta_0 = M_{\text{collapse}}(0) - M_c$, i.e., the excess mass above critical of the collapsing core of the solution.

Dyachenko et al. in [13] treated the general critical d-dimensional NLS with the supercritical perturbation $i\delta|\psi|^p\psi$ where $p > 4/d$. In this context was established that the amount of dissipated mass scales as

$$\Delta M \sim \left[\log\log\frac{1}{\delta}\right]^{-2}. \tag{5.53}$$

Therefore, in this case no mass is dissipated in the limit of vanishing damping.

5.4 Concluding remarks

In this chapter we saw that reduced system suggested the following facts:

1. Continuation of explicit and generic solutions share the phase-loss property.

2. Post-collapse velocity of the expanding core for explicit solutions is finite. In contrast, generic solutions have an infinite velocity expanding core, implying the instantaneous interaction between the collapsing core and the tail. Consequently, the validity of the reduced system breaks down shortly after the collapse.

3. The exponential growth of the maximum of generic solutions as $\delta \to 0^+$.

4. In the limit $\delta \to 0^+$, the amount of mass $M_{\text{collapse}}(0) - M_c$ is dissipated in the two-dimensional NLS.

Chapter 6

Fourth-Order Split Step Method

In this chapter we introduce the numerical method used in the numerical simulations. We conducted numerical simulations of the damped/undamped NLS in one dimension by employing the fourth-order split step method similar to the one described in [10, 68] (see description below).

In order to guarantee that the undamped NLS solution ($\delta = 0$) blows up in finite time, we have chosen a periodic initial condition with initial mass greater than the critical one, and a negative initial Hamiltonian. In such non-dissipative case, by monitoring the conservation of mass (L^2 norm), Hamiltonian conservation and the linear momentum allowed to check the consistency of the method, see Figure 6.2. The Hamiltonian appeared less conserved because the two terms of the Hamiltonian go to infinity, and consequently the numerical evaluation of it suffers from cancellation of significant digits (Figure 6.2:(c)). In the dissipative case, consistency was checked by using the mass balance equation (6.19) (Figure 6.3).

Singularity is a local phenomenon in which the ψ_x becomes unbounded close the collapse time. Therefore, for efficient computation we adaptively change the spatial resolution. Indeed, the spatial grid step was decreased by two with Fourier interpolation when the spectrum was reaching the largest wavenumbers. This adaptive scheme was used for simulations for the damped/undamped NLS.

In the next sections, we will provide a more detailed information about the initial condition and numerical simulations.

6.1 Numerical method

Consider the critical one-dimensional NLS equation

$$i\psi_t(x,t) + \psi_{xx} + (1+i\delta)|\psi|^4\psi = 0, \quad \delta \geq 0, \tag{6.1}$$

where $x \in [-\pi, \pi]$ with periodic boundary conditions and $t \geq 0$. As we mentioned before, to simulate the NLS equation (6.1) we used the fourth-order split step method [10, 68]. The main idea of the method is to split the NLS (6.1) into the linear and nonlinear part, and by alternatively solving each of these parts, we approximate the solution of the whole equation (6.1). In fact, the equation (6.1) can be written as

$$\psi_t = (\hat{L} + \hat{N})\psi, \tag{6.2}$$

where $\hat{L}$ and $\hat{N}$ are the linear and nonlinear operators defined as

$$\hat{L}\psi = i\psi_{xx}, \qquad \hat{N}\psi = i(1+i\delta)|\psi|^4\psi. \tag{6.3}$$

Given the time step Δt, the solution $\psi(t+\Delta t) = e^{\Delta t(\hat{N}+\hat{L})}\psi(t)$ is approximated by the expression [10, 68]

$$\psi(t+\Delta t) = e^{c_1\Delta t\hat{N}}e^{d_1\Delta t\hat{L}}e^{c_2\Delta t\hat{N}}e^{d_2\Delta t\hat{L}}e^{c_2\Delta t\hat{N}}e^{d_1\Delta t\hat{L}}e^{c_1\Delta t\hat{N}}\psi(t), \tag{6.4}$$

where

$$c_1 = \frac{1}{2(2-2^{1/3})}, \quad c_2 = \frac{1-2^{1/3}}{2(2-2^{1/3})}, \quad d_1 = \frac{1}{2-2^{1/3}}, \quad d_2 = \frac{-2^{1/3}}{2-2^{1/3}}. \tag{6.5}$$

The nonlinear part $e^{c_j\Delta t\hat{N}}$ is approximated by

$$e^{c_j\Delta t\hat{N}}\psi(t) \approx e^{ic_j\Delta t(1+i\delta)|\psi(t)|^4}\psi(t), \quad j = 1, 2. \tag{6.6}$$

For the linear part $e^{c_j\Delta t\hat{L}}$, we have the exact solution

$$e^{c_j\Delta t\hat{L}}\psi(t) = \mathcal{F}^{-1}\left[e^{-ic_j\Delta tk^2}\mathcal{F}[\psi(t)]\right], \quad j = 1, 2, \tag{6.7}$$

where $\mathcal{F}$ and $\mathcal{F}^{-1}$ denote the Fourier transform and its inverse respectively. Equation (6.7) was computed by using the fast Fourier transform (FFT) algorithm implemented in MATLAB. The resulting method has spectral accuracy in space and fourth order in time.

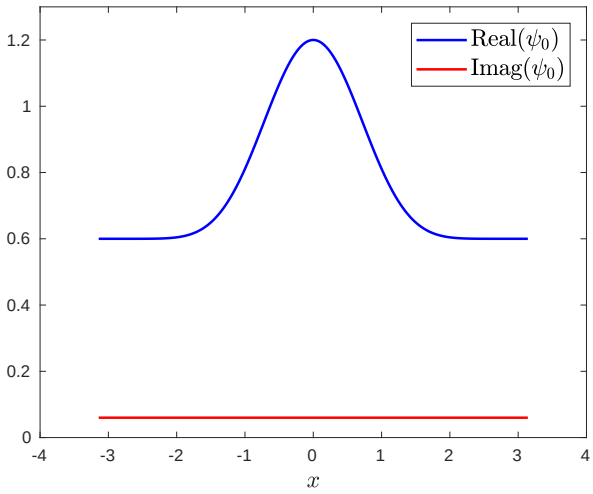

Figure 6.1: Real and imaginary parts of the initial condition (6.8).

Due to the locality of the singularity, we used an adaptive time/spatial meshing. We started the simulations with the spatial grid size $\Delta x = 2\pi/2^{12}$. It was decreased by two with the Fourier interpolation for the solution each time, when the spectrum was reaching the largest wavenumbers, so that the discretization error was kept at the level of round-off noise. At the end of simulations, we reached the resolution up to 2^{23} points. For the time step, we used the relation $\Delta t = 0.2(\Delta x)^2/\pi$ in order to avoid numerical instability [10].

We solved the NLS (6.1) with the periodic initial condition

$$\psi_0(x) = 0.6\left[1 + \cos^8(x/2) + 0.1i\right]. \tag{6.8}$$

In the Figure 6.1 is shown the real and imaginary parts of this initial state. Such initial condition has initial mass

$$M(0) = \int_{-\pi}^{\pi} |\psi_0|^2 dx \approx 3.96577, \tag{6.9}$$

which corresponds to 45.76% above the critical mass $M_c = \frac{\sqrt{3}\pi}{2} \approx 2.7207$. The Hamiltonian of (6.8) is

$$H(0) = \int_{-\pi}^{\pi} |\psi_{0,x}|^2 dx - \frac{1}{3}\int_{-\pi}^{\pi} |\psi_0|^6 dx \approx -0.6888, \tag{6.10}$$

and then the solution for the undamped NLS ($\delta = 0$) blows up in finite time, with critical time estimated numerically as $T_c \approx 1.4826$. The initial linear momentum is

$$P(0) = i\int_{-\pi}^{\pi} \left(\psi_0\psi_{0,x}^* - \psi_0^*\psi_{0,x}\right) dx = 0. \tag{6.11}$$

The NLS (6.1) was solved with the same initial condition and the values of

$$\delta = 10^{-2}, 5 \times 10^{-3}, 2.5 \times 10^{-3}, 10^{-3}, 5 \times 10^{-4} \text{ and } 0. \tag{6.12}$$

6.2 Consistency and accuracy checks

In this section we present the approach used in the simulations to monitor the consistency and the accuracy of the numerical method. The consistency of the solution for the NLS (6.1), was monitored by checking the associated conservation laws in the non-dissipative case, and by the mass balance equation

$$\frac{d}{dt}\int_{-\pi}^{\pi} |\psi|^2 dx = -2\delta \int_{-\pi}^{\pi} |\psi|^6 dx, \tag{6.13}$$

in the dissipative one. The corresponding accuracy of the method for $\delta \geq 0$ was tracked through the spectrum of the solution. In the next sections, we will treat the two cases, damped and undamped NLS, separately.

6.2.1 Non-dissipative case

In Chapter 2, we saw that the undamped NLS ($\delta = 0$) conserves the quantities: mass (L^2 norm)

$$M(t) = \int_{-\pi}^{\pi} |\psi|^2 dx, \tag{6.14}$$

linear momentum

$$P(t) = i\int_{-\pi}^{\pi} \left(\psi\psi_x^* - \psi^*\psi_x\right) dx, \tag{6.15}$$

and Hamiltonian

$$H(t) = \int_{-\pi}^{\pi} |\psi_x|^2 dx - \frac{1}{3}\int_{-\pi}^{\pi} |\psi|^6 dx. \tag{6.16}$$

Consequently, in the absence of dissipation the consistency of the method was monitored by checking these conservation laws. In Figure 6.2 we show the time evolution of these three quantities. One can observe in the Figures 6.2:(a)-(b) that $M(t)$ and $P(t)$ are conserved in the whole time interval. Similarly, the dynamics of the Hamiltonian $H(t)$ is shown in Figure 6.2:(c). In this case the Hamiltonian appears not conserved,

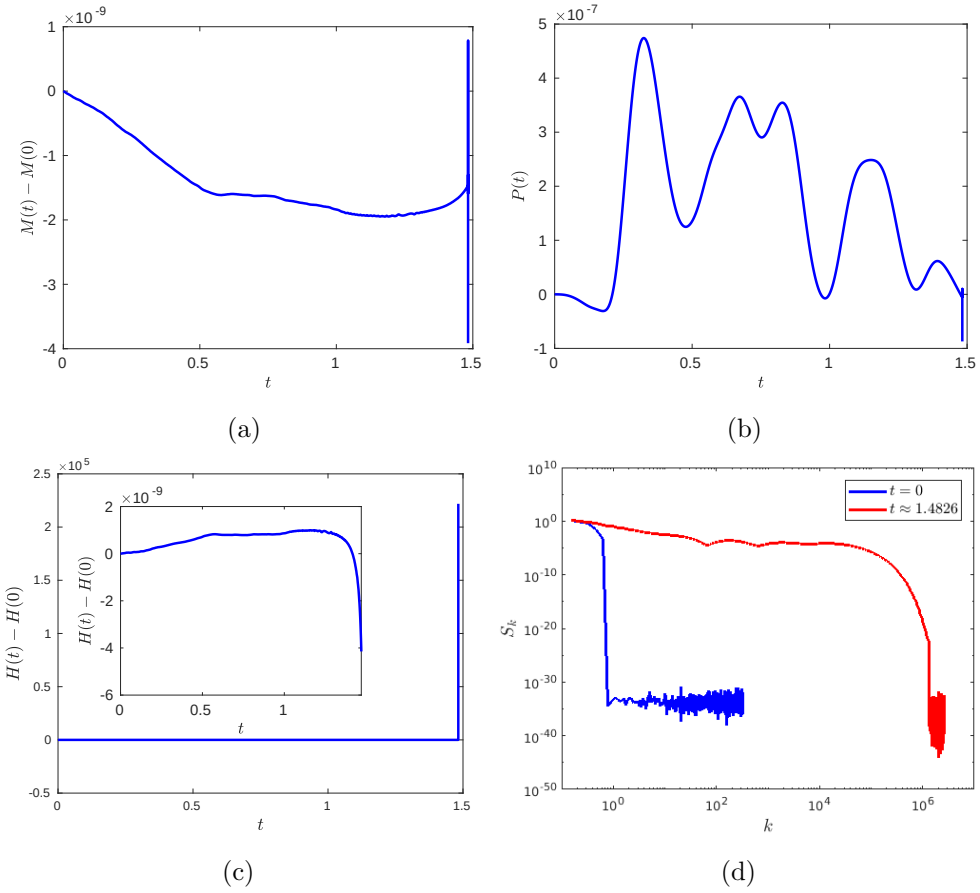

Figure 6.2: Verification of the conservation laws for the one-dimensional unperturbed NLS equation ($\delta = 0$). (a) Mass conservation. (b) Linear momentum conservation. (c) Hamiltonian conservation. As it is expected, the Hamiltonian appears less conserved due to the fact that both $\|\psi_x\|_2$ and $\|\psi\|_6$ becomes infinite close the collapsing time, and in this way the numerical evaluation is affected from cancellation of significant digits. The inset displays the Hamiltonian in the time interval $[0, 1.47]$, indicating clearly the Hamiltonian conservation in the first instants of the dynamics. (d) Spectrum S_k of the solution in the instants $t = 0$ and $t \approx 1.4826$.

but this is only a numerical issue caused by the cancellation of significant digits of the unbounded terms $\|\psi_x\|_2$ and $\|\psi\|_6$ in the definition of the Hamiltonian. This is well-known fact, see, e.g., [17]. The unbounded grow of these terms only occurs for times close to T_c. Therefore, the Hamiltonian conservation is checked in the non-blowup stage, as it is shown in the inset of Figure 6.2:(c).

To maintain the accuracy of the numerical method we have monitored the spec-

trum,

$$S_k = |\hat{\psi}(k)|^2 + |\hat{\psi}(-k)|^2, \tag{6.17}$$

where $\hat{\psi}(k) = \mathcal{F}[\psi](k)$ is the Fourier transform, of the solution all the time. Figure 6.2:(d) displays the spectrum S_k, of the initial condition (6.8) versus the spectrum of the solution at the final time $t \approx 1.4826$.

6.2.2 Dissipative case

In the dissipative NLS mass and Hamiltonian are not conserved. Instead, we can monitor the consistency of the method by the mass balance equation (6.13) or its equivalent form

$$\int_{-\pi}^{\pi} |\psi(x,t)|^2 dx = -2\delta \int_0^t \left(\int_{-\pi}^{\pi} |\psi(x,t')|^6 dx \right) dt' + \int_{-\pi}^{\pi} |\psi_0(x)|^2 dx. \tag{6.18}$$

Also, it can be written as

$$M(t) = -2\delta \int_0^t \|\psi(t')\|_6^6 dt' + M(0). \tag{6.19}$$

In Figure 6.3 we have verified the equation (6.19) for the simulations with different values of δ. The accuracy of the method was monitored by the spectrum of the solution all the time. Figure 6.4 displays the spectrum of the solution for the initial condition and for the solution at the last time.

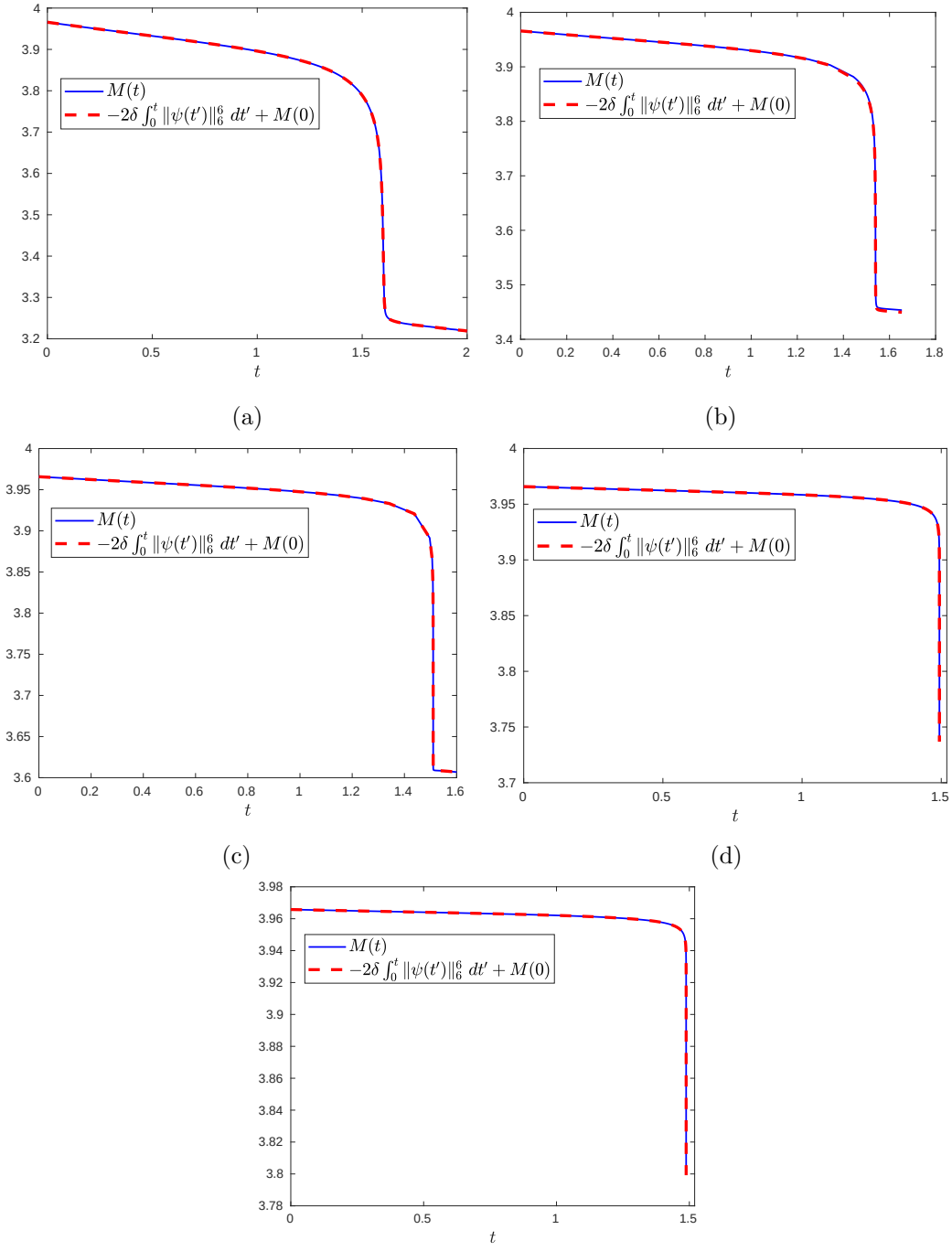

Figure 6.3: Verification of the equation (6.19) for (a) $\delta = 10^{-2}$. (b) $\delta = 5 \times 10^{-3}$. (c) $\delta = 2.5 \times 10^{-3}$. (d) $\delta = 10^{-3}$. (e) $\delta = 5 \times 10^{-4}$.

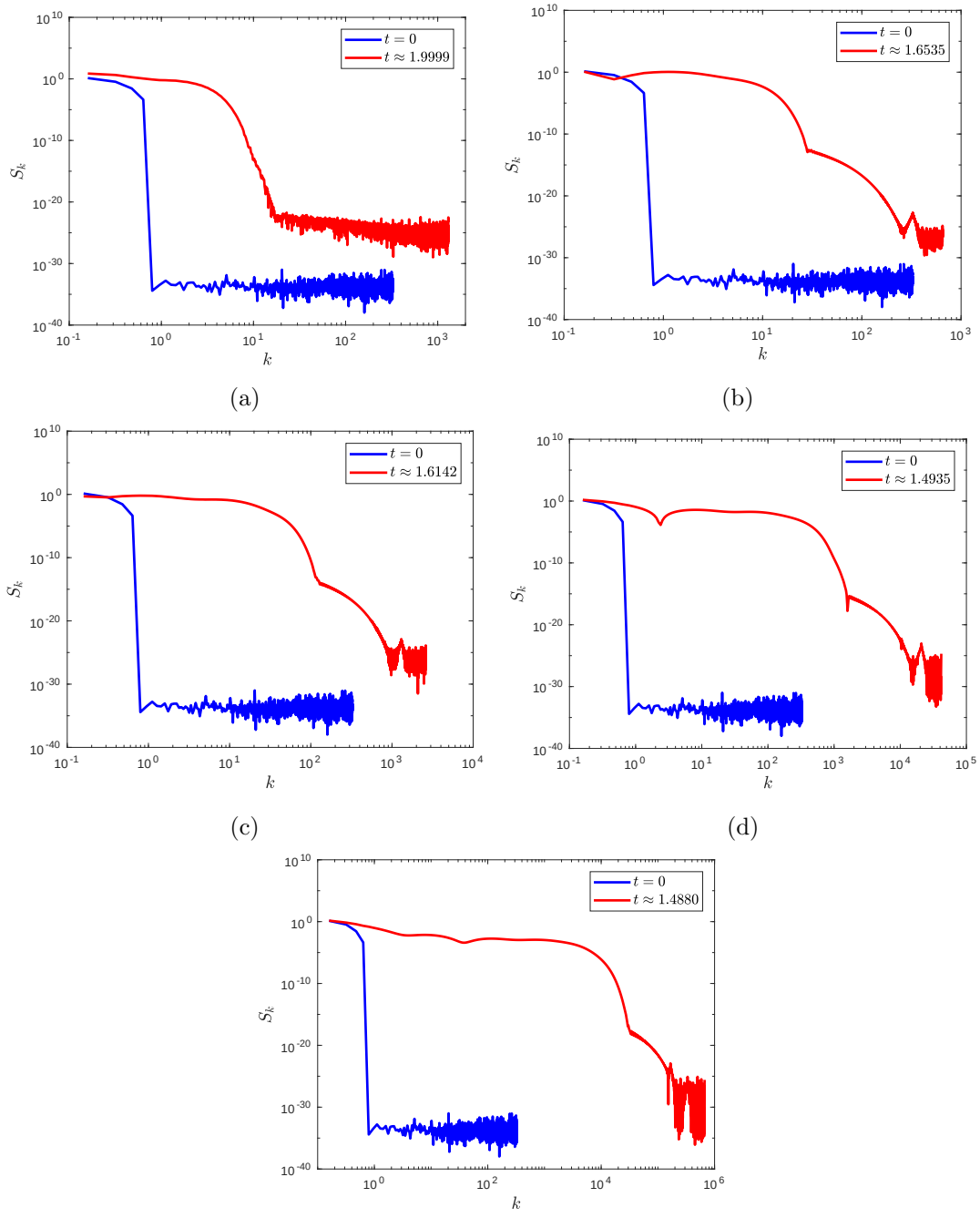

Figure 6.4: Spectrum S_k of the solution at the initial and final time for (a) $\delta = 10^{-2}$. (b) $\delta = 5 \times 10^{-3}$. (c) $\delta = 2.5 \times 10^{-3}$. (d) $\delta = 10^{-3}$. (e) $\delta = 5 \times 10^{-4}$.

6.3 Concluding remarks

In this chapter we described the numerical method used in the numerical simulations for the NLS (6.1). We summarize this chapter as follows:

1. The fourth-order split step method was used to carry out the numerical simulations.

2. Consistency of the numerical method was checked by monitoring the conservation laws in the undamped NLS, and the mass balance equation for the dissipative case.

3. The accuracy of the method was maintained by using Fourier interpolation, in such way that the error of Fourier transform was kept at the level of round-off noise.

Chapter 7

Simulation of the NLS Equation: Blowup Dynamics

In Chapters 2 and 3, we saw that the blowup dynamics of NLS solutions with total mass slightly above the critical one, can be described by a system of ODEs called reduced system, see Theorem 2.6 and Proposition 3.1. Both results stablish that under certain conditions the collapsing core of the solution can be approximated by the universal radial $\psi_{R^{(0)}}$ profile, where the solution width is governed by the reduced system. In these order of ideas, one objective of the present chapter is to check, by the direct simulation of the NLS, such universality and the validity of the reduced system. Then, we proceed with the analysis of the solution tail, in which we reasonable verified the predicted power laws [4, 5].

The numerical simulation presented here corresponds to the one-dimensional NLS equation

$$i\psi_t(x,t) + \psi_{xx} + |\psi|^4\psi = 0, \tag{7.1}$$

where $x \in [-\pi, \pi]$, $t > 0$ and subjected to periodic boundary conditions and the initial condition

$$\psi_0(x) = 0.6\left[1 + \cos^8(x/2) + 0.1i\right]. \tag{7.2}$$

In the last chapter we saw that the initial Hamiltonian is negative, and consequently, solution blows up at the finite time, which we estimate numerically as $T_c \approx 1.4826$.

7.1 Verification of the universal profile

In this section we will verify the convergence of the collapsing core toward the universal profile. In one dimension, the universal $\psi_{R^{(0)}}$ profile has the explicit form:

$$\psi_{R^{(0)}}(x,t) = \frac{3^{1/4}}{L^{1/2}(t)} \operatorname{sech}^{1/2}(2\xi) \exp\left(i\tau + i\frac{L_t}{L}\frac{x^2}{4}\right), \tag{7.3}$$

with

$$\xi = \frac{x}{L(t)}, \qquad \tau = \int_0^t \frac{ds}{L^2(s)}, \tag{7.4}$$

for some unknown function $L(t)$. Therefore, the intention of this section is to verify (7.3)-(7.4).

Firstly, we show in Figure 7.1:(a) that indeed the solution of the initial value problem (7.1)-(7.2), blows up at T_c. As can be observed in such figure, the profile of $|\psi|^2$ becomes narrower and higher as time approaches the critical time $T_c \approx 1.4826$. The narrowess of $|\psi|^2$ is explained by the fact that the collapsing core convergences toward the delta function in the limit $t \to T_c$, see Lemma 2.10. The increasing amplitude of $|\psi|^2$ is also expected because the L^∞ norm of ψ becomes infinity at the singularity, see Lemma 2.1. In order to verify (7.3), we need to check that in the inner zone, $|\psi|^2$ and the phase of the solution, $\theta(x,t) = \arg\psi$, can be approximated as

$$|\psi|^2 \approx \frac{3^{1/2}}{L(t)} \operatorname{sech}(2\xi), \qquad \theta(x,t) \approx \tau(t) + \frac{L_t}{4L}x^2, \tag{7.5}$$

where the solution width $L(t)$ is computed by the relation

$$L(t) = \frac{\sqrt{3}}{|\psi(0,t)|^2}. \tag{7.6}$$

Figure 7.1:(b) corresponds to the first part of (7.5). It shows the comparison between the profile of $L^{1/2}|\psi|$ and the ground state $R^{(0)}(x) = 3^{1/4}\operatorname{sech}^{1/2}(2x)$ for the time $t = 1.4825$. The good agreement between both graphs in the region $|\xi| \ll 6$ supports the first part of (7.5). The second part of (7.5) is verified in Figure 7.1:(c), in which $\theta(x,t)$ is compared with the quadratic expression in the renormalized variable $\xi = x/L$ for $t = 1.4825$. Here the function τ was computed by $\tau = \theta(0,t)$. Therefore, we conclude that the NLS solution collapses with the $\psi_{R^{(0)}}$ profile. Since $1/L(t)$ becomes infinity as $t \to T_c$ (see Figure 7.2 below), then τ goes to infinity at the same time. Hence, a consequence of the

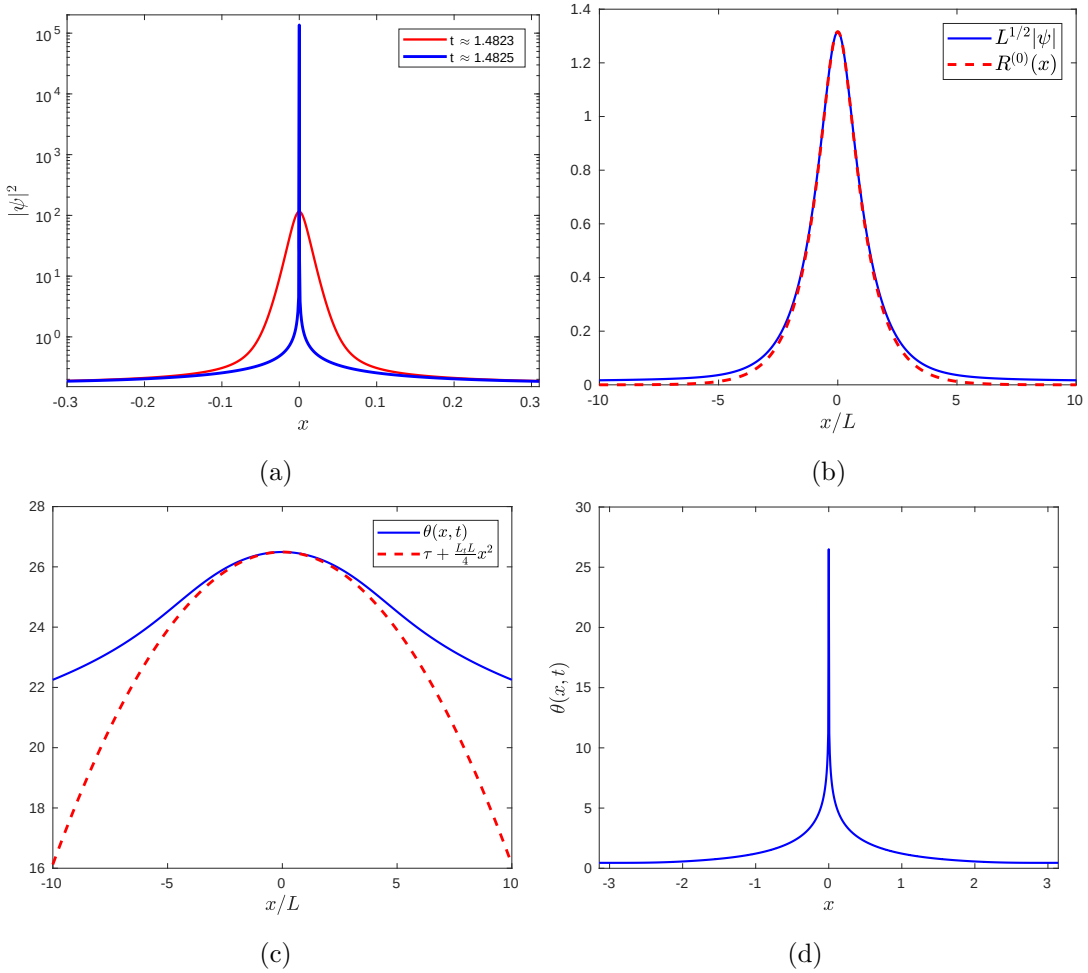

Figure 7.1: (a) Profile of $|\psi|^2$ for times close the collapsing time $T_c \approx 1.4826$. (b) Comparison between the rescaled profile $L^{1/2}|\psi|$ and $R^{(0)}(x) = 3^{1/4}\,\mathrm{sech}^{1/2}(2x)$ for $t = 1.4825$. (c) Verification of the quadratic phase of the solution at $t = 1.4825$: $\theta(x,t)$ vs $\tau(t) + \frac{L_t}{4L}x^2$. (d) Profile of the phase of the solution $\theta(x,t)$ as function of x, at the time $t = 1.4825$.

solution collapsing with the $\psi_{R^{(0)}}$ profile, is that the phase $\theta(x,t)$ becomes singular at the critical time as well, as it is verified in the Figure 7.1:(d).

7.2 Verification of the reduced system

In the last section we have verified numerically that the solution of the problem (7.1)-(7.2) collapses with the universal profile (7.3)-(7.4). Now, the aim of the present

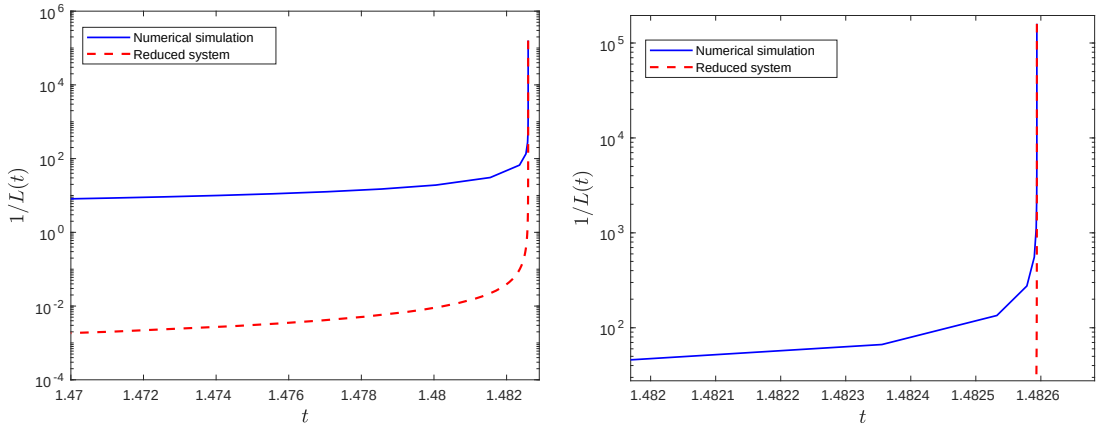

(a) (b)

Figure 7.2: (a) Comparison of the function $1/L(t)$ obtained from the numerical simulation and the reduced system. (b) Dynamics of $1/L(t)$ close the blowup instant. It indicates, as it is expected, that reduced system is valid only when the dynamics becomes adiabatic, i.e., close to the collapsing time.

section is to verify the reduced system governing the blow up dynamics, i.e.,

$$\beta_t = -\frac{\nu(\beta)}{L^2}, \qquad \beta = -L^3 L_{tt}, \tag{7.7}$$

where $\nu(\beta) = c_\beta e^{-\pi/\sqrt{\beta}}$ with $c_\beta = 1024/\pi^3$. As was mentioned before, the solution width $L(t)$ can be computed from our numercal simulation by the relation (7.6).

The intention is compare the solution width L obtained from the reduced equations (7.7) with the relation (7.6). For that purpose, we have solved (7.7) backward in time taking as initial conditions the values of $L(t)$ and $\beta(t)$ at the last time of the simulation, accomplished by (7.6) and $\beta = -L^3 L_{tt}$ respectively. In Figure 7.2 one sees the behavior of $1/L(t)$ obtained from the numerical simulation and the corresponding one from the reduced system. In Figure 7.2:(b) one sees a reasonable agreement of both graphs close to the collapsing time, but far away of it reduced equations do not capture the earlier dynamics, as it is expected.

7.3 Solution tail

In the previous sections we verified numerically the universality of the collapsing core and the validity of the reduced system in describing the blowup dynamics of our

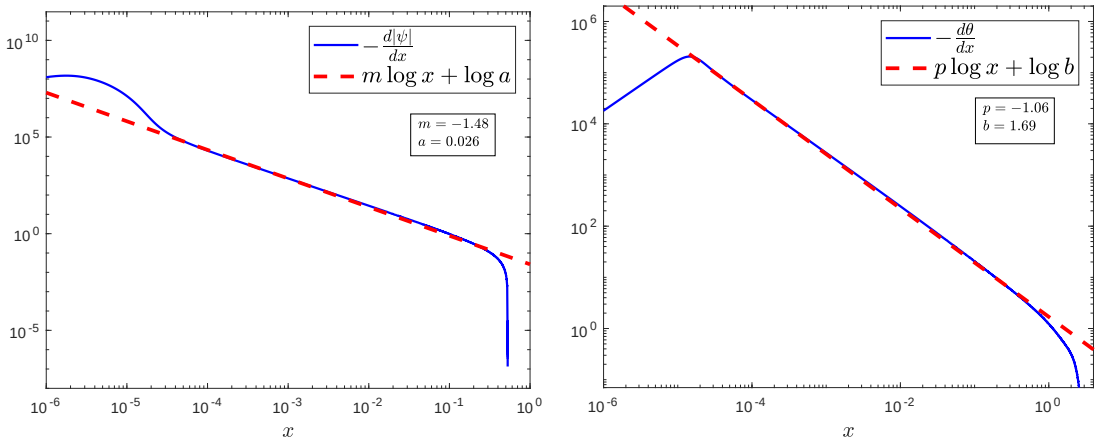

(a) (b)

Figure 7.3: (a) First space derivative of $|\psi|$ for $x > 0$ at the time last time of the simulation. It suggests the power law $\frac{d}{dx}|\psi| \approx -ax^m$ in the region $10^{-5} < x < 1$ with $a \approx 0.026$ and $m \approx -1.48$. (b) Derivative of the phase of the solution for $x > 0$ at the time last time of the simulation. This figure supports the power law $\frac{d}{dx}\theta \approx -bx^p$ for $10^{-5} < x < 1$ with $b \approx 1.69$ and $p \approx -1.06$.

initial value problem (7.1)-(7.2). In these terms, our numerical simulation corroborated the dynamics established in the Theorem 2.6.

Now, in this present section, the intention is to show the observed behavior of the solution tail in our numerical simulation. Indeed, in the Figure 7.3 are displayed in a log-log scale the first space derivatives of $|\psi|$ and θ for $x > 0$ and at the last time of the simulation. Both figures suggest that derivatives of $|\psi|$ and θ follow a power law for times close to T_c. More specifically, Figure 7.3:(a) suggests that the solution tail satisfies the power law

$$\frac{d}{dx}|\psi| \approx -ax^m, \quad \text{for} \quad 10^{-5} < x < 1 \quad \text{and} \quad a \approx 0.026,\ m \approx -1.48. \tag{7.8}$$

In a similar way, one has from the Figure 7.3:(b) that the phase of the tail satisfies

$$\frac{d}{dx}\theta \approx -bx^p, \quad \text{for} \quad 10^{-5} < x < 1 \quad \text{and} \quad b \approx 1.69,\ p \approx -1.06. \tag{7.9}$$

The asymptotic form of the solution tail can be found, e.g., [4, 5]. In these works was established that the part of the solution tail closest to the collapsing core satisfies

$$\frac{d}{dx}|\psi_{\text{tail}}| \approx C(\beta)x^{-3/2}, \quad C(\beta) < 0, \tag{7.10}$$

where $C(\beta)$ decays exponentially in β, and the phase of the tail obeys

$$\frac{d}{dx}\theta_{\text{tail}} \approx D(\beta)x^{-1}, \quad D(\beta) < 0, \tag{7.11}$$

where $D(\beta)$ becomes infinite as $\beta \to 0$. Therefore, the previous power laws obtained from our numerical simulation are in agreement with (7.10)-(7.11).

7.4 Concluding remarks

In this chapter we verified numerically that:

1. The solution of the initial value problem (7.1)-(7.2) collapses following the predicted universal $\psi_{R^{(0)}}$ profile (see Section 7.1).

2. The validation of the reduced system governing the blowup dynamics of the problem (7.1)-(7.2) (see Section 7.2).

3. The reasonable verification of the theoretical power laws for the solution tail (see Section 7.3).

Chapter 8

Breakdown of the Adiabatic Approximation in the Damped NLS Dynamics

In Chapter 4 we presented a theory to treat the damped NLS equation based on the adiabatic approximation (modulation theory). This theory assumes that after the singularity, solution remains in the fundamental state $\psi_{R^{(0)}}$. Afterwards, in Chapter 5 and in the framework of the modulation theory, some well known continuation results for the explicit and generic singular solutions were presented (Proposition 5.1 and 5.2). Both continuation results are informal and based on numerical simulations carried out by Fibich and Klein in [21, 22]. Continuation result for the generic solution was supported in [21, 22] by simulating the one-dimensional damped NLS by using as initial conditions small perturbations of the explicit blowup solution, with mass approximately $2.5\% - 10.25\%$ above the critical one. In [21, 22] the authors reported the invalidity of the reduced system shortly after the collapse. This invalidity of the reduced system was justified by the infinite pre-collapse velocity, which result as a consequence of the solution collapsing with the loglog law (Theorem 2.6).

In this chapter we will present the first part of our results related to the damped NLS. In fact, the aim of the current chapter is to see how well the adiabatic approximation (modulation theory) describes the first instants of the post-blowup dynamics, taking into account that our initial condition is not too close to the ground state $R^{(0)}$,

i.e., initial condition is not a perturbation of the explicit solution and its mass is approximately 45.76% above the critical mass. Our findings also support the breakdown of the adiabatic approach soon after the maximum of the solution. Indeed, our results show a clear deviation of the dynamics predicted by the reduced system. We hypothesize that this deviation can be the result of the increase influx of mass into the collapsing core, which is neglected in the derivation of the reduced system. Also, in this chapter we will check some of the adiabatic approach based predictions as the δ-dependence of the wave maximum, and the zero-limit dissipation (Subsections 5.3.1 and 5.3.2).

The numerical simulations presented in this chapter corresponds to the damped NLS equation

$$i\psi_t(x,t) + \psi_{xx} + (1+i\delta)|\psi|^4\psi = 0, \tag{8.1}$$

where $x \in [-\pi, \pi]$, $t > 0$ and with the initial condition

$$\psi_0(x) = 0.6\left[1 + \cos^8(x/2) + 0.1i\right]. \tag{8.2}$$

8.1 Verification of the universal profile

In this section, we will verify the regularization mechanism in the damped NLS (8.1), and the convergence of the core of the solution to the universal $\psi_{R^{(0)}}$ profile. As we saw in the previous chapter, $\psi_{R^{(0)}}$ has the form

$$\psi_{R^{(0)}}(x,t) = \frac{3^{1/4}}{L^{1/2}(t)}\,\mathrm{sech}^{1/2}(2\xi)\exp\left(i\tau + i\frac{L_t}{L}\frac{x^2}{4}\right), \tag{8.3}$$

with

$$\xi = \frac{x}{L(t)}, \qquad \tau = \int_0^t \frac{ds}{L^2(s)}, \tag{8.4}$$

for some function $L(t)$, governed by the reduced system which can be computed numerically by the relation

$$L(t) = \frac{\sqrt{3}}{|\psi(0,t)|^2.} \tag{8.5}$$

Figure 8.1:(a) plots the maxima of the squared modulus of the function ψ as function of the time for different values of δ, i.e.,

$$|\psi(t)|^2_{\max} := \max_x |\psi(x,t)|^2. \tag{8.6}$$

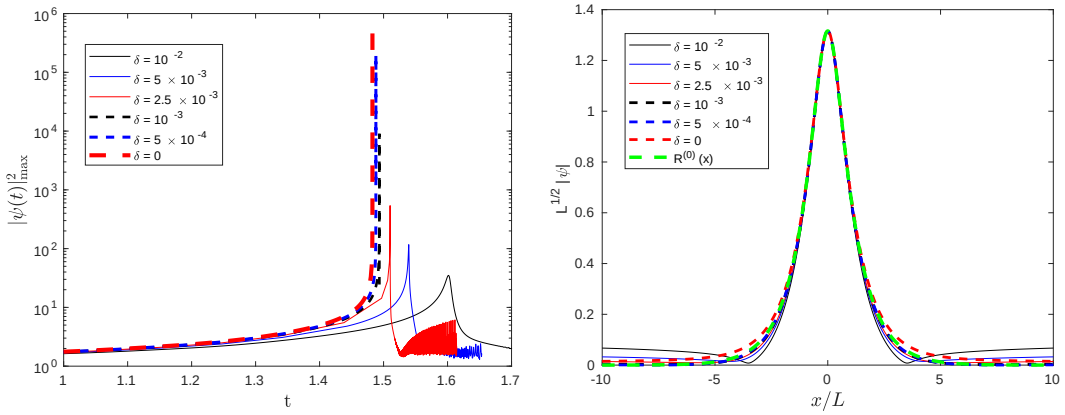

(a) (b)

Figure 8.1: (a) Time evolution of $|\psi(t)|^2_{\max}$ for different values of δ. As it is expected, the dynamics shows that for the smaller $\delta > 0$, the sooner and higher is the peak of $|\psi(t)|^2_{\max}$ verifying that indeed the nonlinear dissipation term regularizes the solution. It also shows the convergence to the non-dissipative case, $\delta = 0$, in the pre-blowup dynamics. (b) Comparison between the rescaled profile $L^{1/2}|\psi(x/L,t)|$ of the dissipative solution and the ground state $R^{(0)}(x)$ at the time $t_{\max}$.

One can observe, as it is expected that adding the small damping term to the NLS equation implies that the singularity is cured, and it allows to continue the solution after the collapse, see Theorem 4.1. A clear convergence to the unperturbed NLS, $\delta = 0$, for times before the blowup is showed in the same figure. The convergence in Figure 8.1:(a) is manifested by noting that the peak is located earlier and its amplitude is larger as δ decreases. In order to verify the convergence of the core region to the universal profile (8.3)-(8.4), we have compared the rescaled profile $L^{1/2}|\psi(x/L,t)|$ with the ground state $R^{(0)}(x)$ at the time $t_{\max}$, where the solution attains its maximum value, as can be seen in Figure 8.1:(b). It is clear that the δ-dependent time $t_{\max}$, converges to T_c when δ going to zero.

As it is displayed in Figure 8.1:(b), the quasi self-similar collapsing core becomes closer of $R^{(0)}(x)$ for smaller $\delta > 0$. The justification of why in the Figure 8.1:(b) the collapsing core corresponding to $\delta = 5 \times 10^{-4}$ is closer to $R^{(0)}(x)$ than for the case $\delta = 0$, follows from the physical interpretation of β. In Corollary 4.1 we saw that β is proportional to the excess mass above M_c of the collapsing core. Since that $\beta \approx 0.0943$ at the last time of the simulation for $\delta = 0$, and $\beta \approx -0.0470$ for $\delta = 5 \times 10^{-4}$, it

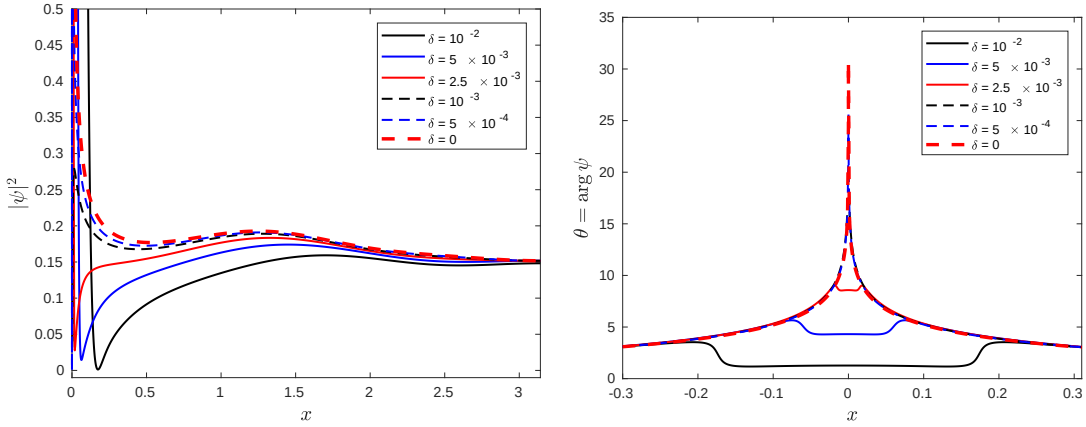

(a) (b)

Figure 8.2: (a) Profile of $|\psi|^2$ for $x > 0$ at the time $t_{\max}$ and various values of δ. It manifests the convergence of the solution tail provided δ going to zero. (b) Phase of the solution, $\theta = \arg\psi$, at $t_{\max}$ for each δ. The behavior observed of θ as δ decreases supports the convergence to the undamped case.

indicates that a considerable amount of mass above the critical one is contained in the collapsing core in the undamped NLS, meanwhile in the damped case, the amount of mass is less than the critical mass. We point out that the resolution reached for the undamped NLS is of order 2^{23}e.

In Figure 8.2 we have plotted the profile of $|\psi|^2$ and the phase $\theta = \arg\psi(x,t)$ for various δ at the time $t_{\max}$. In the corresponding Figure 8.2:(a) the profile of $|\psi|^2$ for $x > 0$ is shown. Here a clear convergence of the solution tail as δ decreases is observed. Likewise, the convergence of the phase of the solution can be observed in the Figure 8.2:(b).

8.2 Wave-maximum

In Chapter 5, it was established based on the modulation theory, that the maximum of $|\psi|^2$, $|\psi|^2_{\max\max}$, increases exponentially with decreasing δ, see Subsection 5.3.1. In the one-dimensional case, such behavior is

$$|\psi|^2_{\max\max} \sim \exp(\text{const}/\delta), \qquad \text{const} = \text{const}(\psi_0) > 0. \tag{8.7}$$

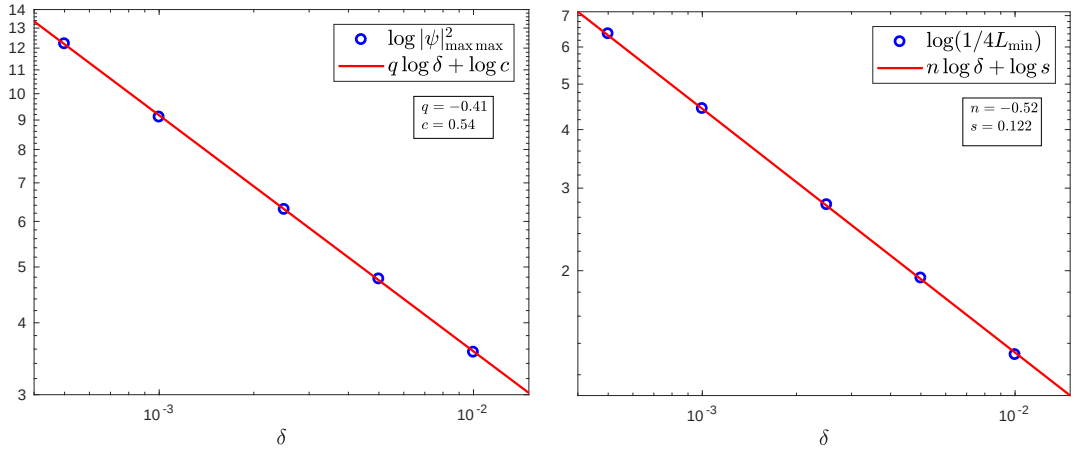

(a) (b)

Figure 8.3: (a) $\log|\psi|^2_{\max\max}$ as function of δ in a log-log scale. It shows that $|\psi|^2_{\max\max}$ behaves like a exponential of a power of δ, i.e., $|\psi|^2_{\max\max}\sim\exp(c\delta^q)$ with $c\approx 0.54$ and $q\approx -0.41$. (b) Solution of the reduced system (8.8)-(8.9) for $\delta=10^{-2}, 5\times10^{-3}, 2.5\times10^{-3}, 10^{-3}, 5\times10^{-4}$ and initial conditions corresponding to the blowup solution at time $t\approx 1.4$, i.e., $L(1.4)\approx 0.3112$, $\beta(1.4)\approx 0.4473$ and $L_t(1.4)\approx -2.6454$. The maximum of the function $1/L(t)$, $1/L_{\min}$, as function of δ satisfies the law $1/L_{\min}\sim 4\exp(s\delta^n)$ with $s\approx 0.122$ and $n\approx -0.52$. Therefore, both results are in a qualitative agreement with the exponential growth of the maximum, but our measurements do no confirm numerically the theoretical prediction (-1) for the power of δ.

In the present section, by using our numerical simulations for the different values of δ, we will estimate the δ-dependence of the maximum of $|\psi|^2$, and compare it with the theoretical estimate (8.7). In addition, the previous estimates are compared with the δ-dependence of the maximum obtained by solving numerically the corresponding reduced system:

$$\beta_t+\frac{\nu(\beta)}{L^2}=-\frac{c_1\delta}{L^2},\qquad \beta=-L^3L_{tt}, \tag{8.8}$$

where

$$\nu(\beta):=\begin{cases} c_\beta e^{-\pi/\sqrt{\beta}}, & \beta>0,\\ 0, & \beta\le 0,\end{cases} \tag{8.9}$$

with $c_1=192/\pi^2$ and $c_\beta=1024/\pi^3$.

In Figure 8.3 are displayed the results obtained by (a) the numerical simulations and (b) the reduced system (8.8)-(8.9). The graph shown in the Figure 8.3:(a) indicates

that $|\psi|^2_{\max\max}$ follows the asymptotic law

$$|\psi|^2_{\max\max} \sim \exp(c\delta^q) \quad \text{where} \quad c \approx 0.54,\ q \approx -0.41. \tag{8.10}$$

Therefore, our numerical measurements also suggest an exponential growth of the wave-maximum with decreasing δ as predicted by the adiabatic theory, but the power of δ estimated in our analysis (≈ -0.41) is different from the theoretical prediction (-1).

In order to compare the previous result with the reduced equations (8.8)-(8.9), we have solved it for each δ with the initial conditions $L(1.4) \approx 0.3112$, $\beta(1.4) \approx 0.4473$ and $L_t(1.4) \approx -2.6454$, obtained from the inviscid NLS. Here, the values for L and β were computed by (8.5) and $\beta = -L^3 L_{tt}$ respectively. Derivatives of L were calculated by finite differences. The result of solving (8.8)-(8.9) with the previous initial conditions is presented in Figure 8.3:(b). According to the result shown in such figure, the maximum of the function $1/L(t)$, $1/L_{\min}$, scales as

$$1/L_{\min} \sim 4\exp(s\delta^n), \quad \text{where} \quad s \approx 0.122,\ n \approx -0.52. \tag{8.11}$$

Consequently, it also suggests the exponential asymptotic law

$$|\psi|^2_{\max\max} \sim 4\sqrt{3}\exp(s\delta^n) \quad \text{where} \quad s \approx 0.122,\ n \approx -0.52. \tag{8.12}$$

One observes that, although the three predictions for the wave-maximum are in a qualitative agreement, powers of δ in (8.10) and (8.12) are not close the theoretical estimate. We point out that such theoretical estimate is determined by solving the reduced system with a linear approximation for $\beta(\tau)$, see Section 5.3. As we will observe in Figures 8.4:(d)-(f), $\beta(\tau)$ becomes straighter as δ decreases. Although our $\beta(\tau)$ for the two smaller δ are close to the linear approximation, our measurements do not test numerically the theoretical estimate for the power of δ.

8.3 Breakdown of the adiabatic approximation

As was mentioned before, the main goal of the present chapter is address the validity of the adiabatic approach in the post-blowup dynamics. In the numerical studies carried out in [21, 22], the authors reported the lack of validity of the reduced system shortly after the arrest of the collapse, see Section 5.3. The breakdown of the

reduced equations was attributed to the infinite velocity of the expanding core, L_t, when δ going to zero. In the current section, we pretend to show a more detailed evidences of this fact, and a plausible explanation of such invalidity.

In order to accomplish our goal, we will compare direct simulations of the damped NLS (8.1) with the solution of the reduced system (8.8)-(8.9). From the direct simulations of the NLS (8.1), we compute the corresponding functions $L(t)$ and $\beta(t)$ through (8.5) and $\beta = -L^3 L_{tt}$, respectively. Here, the variable $\tau(t)$ is obtained by $\tau = \arg\psi(0,t) = \theta(0,t)$. Now, to determine the initial conditions for the reduced system (8.8)-(8.9), we proceeded as follows: the minimum value of the function $L(t)$ computed previously, was taken as its initial condition. The minimum value of $L(t)$ and the instant where it attains it, were approximated by the best fitted quadratic function. The values of β and τ at the time computed previously, were obtained by using the "spline" algorithm implemented in MATLAB. Finally, we solved forward and backward the reduced system.

Figure 8.4 plots the functions $1/L(t)$ and $\beta(\tau)$ obtained from the numerical simulations and reduced system for various δ. Evidently, adiabatic approximation describes well the collapse dynamics as long as δ decreases, see Figures 8.4:(a)-(c). These figures show a quantitative agreement of the function $1/L(t)$ in a vicinity of $t_{\max}$. At the bottom of Figure 8.4, it is displayed the function $\beta(\tau)$ and here τ_β is such that $\beta(\tau_\beta) = 0$. Figures 8.4:(d)-(f) show that for the smaller δ, $\beta(\tau)$ is almost straight as it is expected in the adiabatic regime with $\beta(\tau)$ non-positive. However, after a certain moment, $\beta(\tau)$ starts to have marked deviation from the linear dynamics forecasted by the adiabatic approximation. This deviation manifests the breakdown of the adiabatic approximation.

In these order of ideas, we have defined the breakdown time τ_{break}, and consequently t_{break}, as the time where the relative error between the functions $\beta(\tau)$ is approximately 50%. The times t_{break} and τ_{break} were plotted by blue dots in the graphs of $1/L(t)$ and $\beta(\tau)$ respectively. Therefore, our numerical simulations indicate that breakdown of the adiabatic approach occurs shortly after the peak, and the time-interval in which it is valid collapses with δ going to zero, see Figures 8.4:(a)-(c). It is in concordance with what was reported in [21, 22].

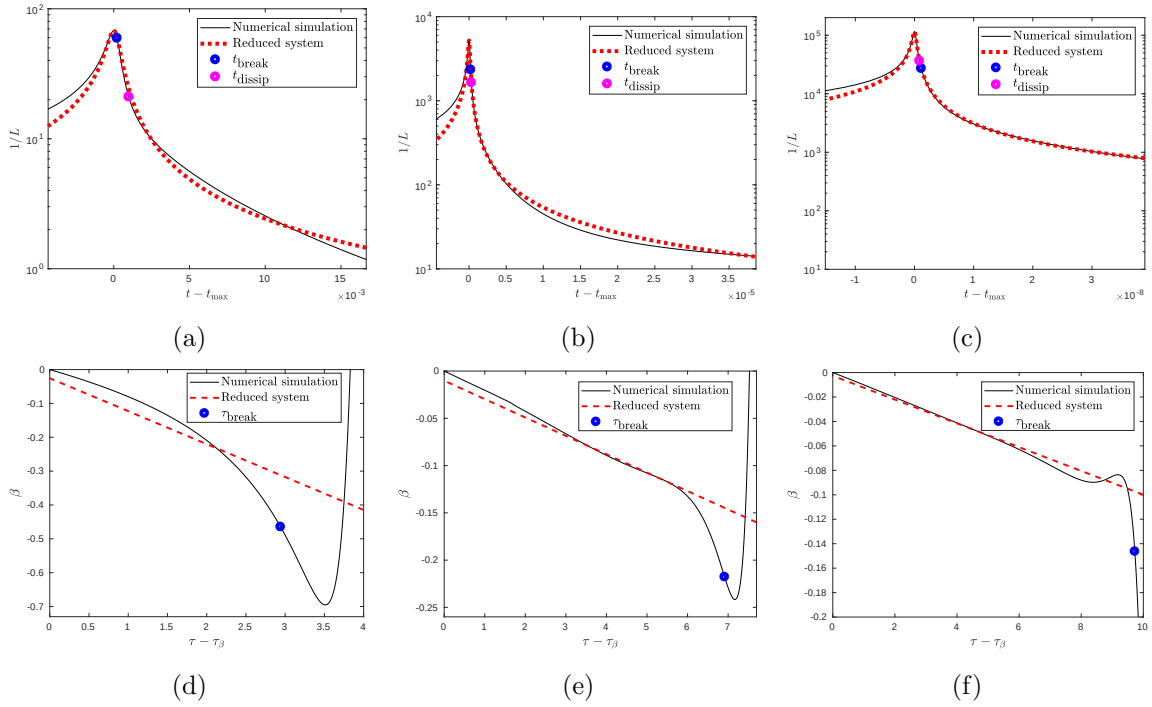

Figure 8.4: Comparison between the solution of the reduced system (8.8)-(8.9) and direct numerical simulations of the damped NLS for (a) $\delta = 5\times10^{-3}$, (b) $\delta = 10^{-3}$ and (c) $\delta = 5\times10^{-4}$. In Figures 8.4:(a)-(c), one sees a good agreements among the functions $1/L(t)$ in a neighborhood of $t_{\max}$ for δ decreasing. In contrast, in Figures 8.4:(d)-(f) we have plotted the functions $\beta(\tau)$. In such figures, one observes that $\beta(\tau)$, as δ goes down, becomes closer the linear behavior predicted by the adiabatic approximation. But, after a certain time, a prominent deviation to the linear approximation is noticed. Therefore, we defined the break down time τ_{break}, and by consequence t_{break}, as the time where the relative error among the functions $\beta(\tau)$ is approximately 50%. The location of t_{break} on the function $1/L(t)$ adverts the invalidity of the adiabatic approach shortly after the peak, and the interval of validity collapsing with δ decreasing.

Adiabatic dynamics take place in the renormalized wavefunction

$$\Psi(\xi,\tau) = \sqrt{L(t)}\psi(x,t)\exp\left(-i\tau - i\frac{L_t}{4L}x^2\right), \tag{8.13}$$

satisfying the equation (4.16). In the modulation theory, the initial weak interaction (mass transfer) between the collapsing core and the tail is neglected. Therefore, due that adiabatic approximation breaks down, the first thing that one can check is this

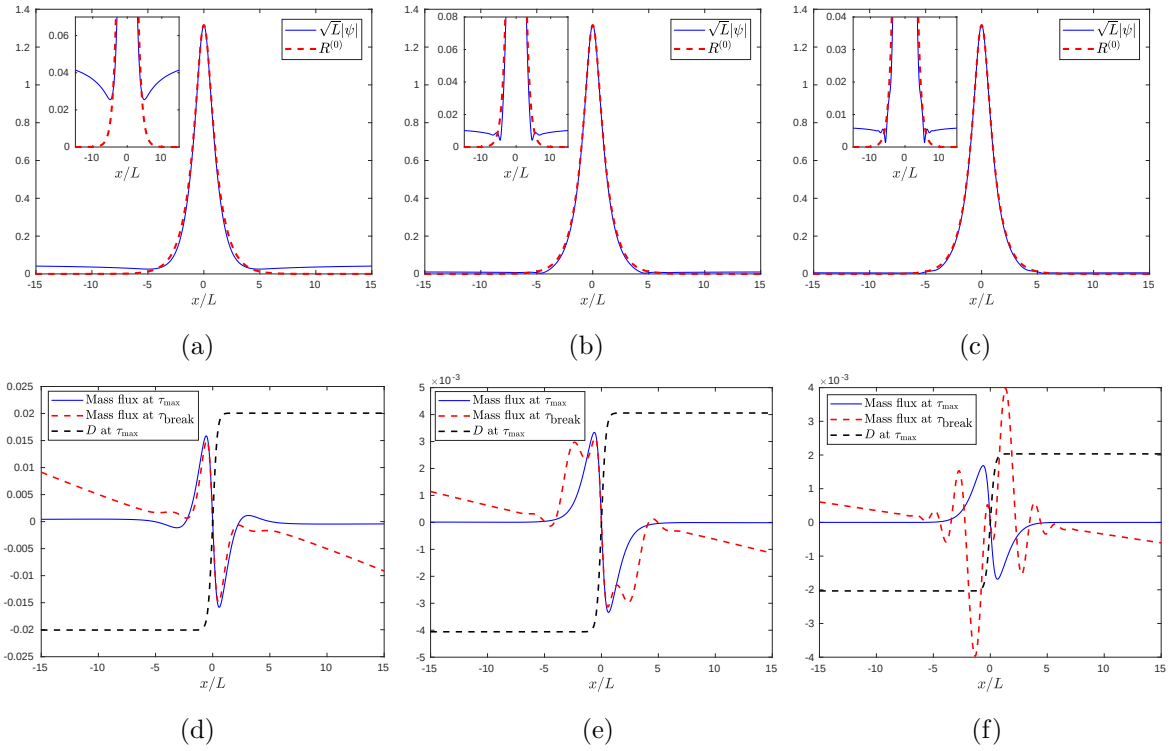

Figure 8.5: At the top is displayed the rescaled profile $\sqrt{L}|\psi(x/L,t)|$ vs $R^{(0)}(x)$ at t_{break} for (a) $\delta = 5\times10^{-3}$, (b) $\delta = 10^{-3}$ and (c) $\delta = 5\times10^{-4}$. The good agreement between the graphs suggests the validity of the universal $\psi_{R^{(0)}}$ profile at the breakdown time t_{break}. At the bottom, are displayed the mass flux $J(\xi,\tau)$ and the dissipation term $D(\xi,\tau)$ for the corresponding values of δ. In these three last figures, one observes that at t_{break} the influx of mass becomes of the same order as dissipation. Since in the adiabatic theory only dissipated effects are taking into account, we hypothesize that such influx of mass is causing the invalidity of the reduced system.

mass transfer. The mass balance equation in the renormalized variables for the interval $[-\xi_0,\xi_0]$ is

$$\frac{d}{d\tau}\int_{-\xi_0}^{\xi_0}|\Psi(\xi,\tau)|^2d\xi = -\,J(\xi,\tau)|_{-\xi_0}^{\xi_0} - D(\xi,\tau)|_{-\xi_0}^{\xi_0}\,, \tag{8.14}$$

where

$$J(\xi,\tau) = \frac{1}{i}\left(\Psi^*\Psi_\xi - \Psi_\xi^*\Psi\right), \tag{8.15}$$

is the mass flux, and

$$D(\xi,\tau) = 2\delta\int_0^{\xi}|\Psi(\xi',\tau)|^6d\xi' \tag{8.16}$$

is the dissipation term. For an efficient numerical computation of $J(\xi,\tau)$, we used the relation

$$J(\xi,\tau)=\frac{1}{i}L^2\left(\psi^*\psi_x-\psi_x^*\psi\right)-L_tLx|\psi(x,t)|^2. \tag{8.17}$$

The advantage of this relation is that it allows to compute the derivative of ψ with a spectral accuracy, due to the periodicity of the problem in the original variables.

In Figure 8.5 was displayed the mass flux $J(\xi,\tau)$ and the dissipation $D(\xi,\tau)$, as well as the profile of the solution at τ_{break} for $\delta=5\times10^{-3}$, $\delta=10^{-3}$ and $\delta=5\times10^{-4}$. The figures shown in the top of Figure 8.5, indicate that at the breakdown instant t_{break}, the collapsing core of the solution maintains yet the universal $\psi_{R^{(0)}}$ profile given in (8.3)-(8.4). Meanwhile, at such moment the formation of some small oscillations around the collapsing core is displayed in the corresponding insets of the same figures. Consequently, solution initially ingresses the non-adiabatic regime maintaining the universal $\psi_{R^{(0)}}$ profile. In the bottom of Figure 8.5, is displayed the mass flux $J(\xi,\tau)$. In order to observe how the flux changes in the passage from adiabatic to non-adiabatic regime, we have plotted it at the times $t_{\max}$ and t_{break}. Also, the dissipation is displayed in such figures. Since dissipation at $\tau_{\max}$ and τ_{break} are almost the same (it becomes important only in the collapse), we have plotted it at the collapse moment. Figures 8.5:(d)-(f) suggest an increasing influx of mass into the inner zone of the solution, $|\xi|\ll 6$, in the interval $[\tau_{\max},\tau_{\text{break}}]$, see also Table 8.1 below. In contrast with the mass flux at $\tau_{\max}$, where the theory works, the mass flux becomes comparable with the dissipation at the breakdown time τ_{break}. Since after the collapse the adiabatic theory assumes a dominant dissipative effect (mass transfer is neglected), our *hypothesis* is that the invalidity of the adiabatic approximation is due to this increasing influx of mass into the inner core after the arrest of the collapse. In these terms, the small oscillations shown in the insets of Figures 8.5:(a)-(c) is the result of this "strong" core-tail interaction (mass transfer).

With the objective to study the dynamics of $J(\xi,\tau)$ in the inner zone of $\Psi(\xi,\tau)$, we will focus in the net mass flux, $J_{\text{net}}(\xi,\tau)=-2J(\xi,\tau)$ with $\xi\geq 0$, flowing in through the boundaries of the interval $[-6,6]$. In Table 8.1, we have tabulated the approximate values of $J_{\text{net}}(6,\tau)$ at $\tau_{\max}$ and τ_{break} for each δ. The last column in Table 8.1 corresponds to the quotient $J_{\text{net}}(6,\tau_{\text{break}})/J_{\text{net}}(6,\tau_{\max})$. It provides a clear evidence of growing of

	δ	$\tau_{\max}$	τ_{break}	break/max
$J_{\text{net}}(6,\tau)$	5×10^{-3}	5.2×10^{-4}	4.2×10^{-3}	8.1
	10^{-3}	3.1×10^{-5}	6.4×10^{-4}	2.06×10
	5×10^{-4}	2×10^{-6}	2.2×10^{-4}	1.1×10^{2}

Table 8.1: Net mass flux J_{net} flowing in through the boundaries of $[-6,6]$ for various values of δ.

influx of mass at τ_{break}, in comparison with the flux at $\tau_{\max}$, as long as δ is going down. In [21] the breakdown of the adiabatic regime was attributed to the post-collapse infinite velocity of the expanding core, L_t. That infinite velocity was justified through the infinite velocity of the log log collapse before the singularity. Based on our observations, we think that the breakdown of the adiabatic regime is the result of the rapid growth of the mass flux.

8.4 Wave-dissipation

The aim of this section is address the amount of mass dissipated in a single collapse event. For that purpose, for each $\delta > 0$ we computed the total mass

$$M(t) = \int_{-\pi}^{\pi} |\psi(x,t)|^2 dx, \tag{8.18}$$

for all the time. In Figure 8.6:(a) we have plotted the time evolution of the mass $M(t)$ (L^2 norm) for various δ, and we can observe, as it is expected, that dissipation becomes important only in the collapse event. In these terms, the amount of dissipated mass is defined as

$$\Delta M = M(0) - M(t_{\text{dissip}}), \tag{8.19}$$

where t_{dissip} is a time after $t_{\max}$, and corresponding to the instant where the dissipative effect is almost unimportant. In our analysis, t_{dissip} was defined as the time where the derivative of $M(t)$ reaches approximately the 10% of its maximum absolute value. The location of t_{dissip} on the graphs of $M(t)$ is presented in Figure 8.6:(a), as well as in the

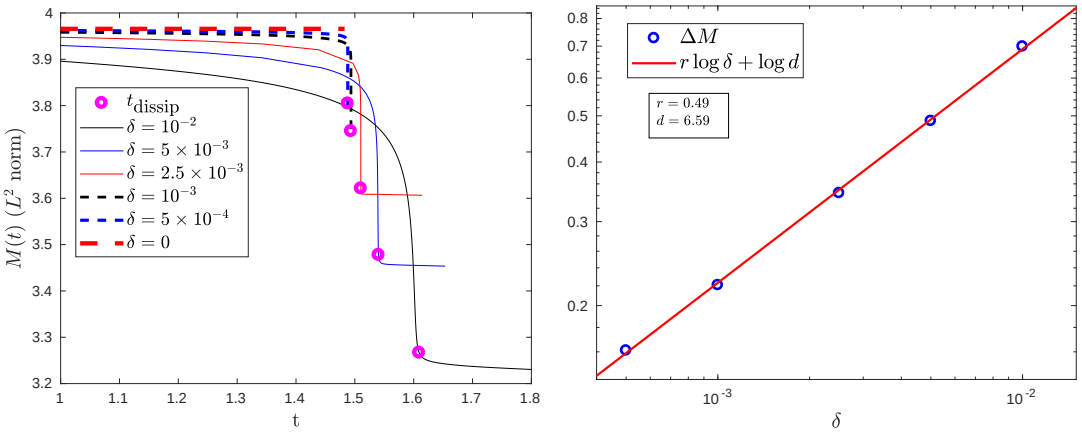

(a) (b)

Figure 8.6: (a) Time-evolution of mass $M(t)$ (L^2 norm) for different values of δ. The time t_{dissip} corresponds to the moment where the first derivative of $M(t)$ is approximately 10% of its maximum absolute value. (b) The δ-dependence of the amount of mass dissipated within a collapse $\Delta M = M(0) - M(t_{\text{dissip}})$. Numerical simulations support the scaling $\Delta M \sim d\delta^r$ with $d \approx 6.59$ and $r \approx 0.49$. Consequently, our measurements indicate that in the limit $\delta \to 0^+$ no mass is dissipated in the collapse.

Figures 8.4:(a)-(c). These last figures indicate that both times t_{break} and t_{dissip} are very close, which is intuitively expected due to the fast defocusing process. The result of our analysis is presented in the Figure 8.6:(b). According to such figure, ΔM scales like

$$\Delta M \sim d\delta^r \quad \text{with} \quad d \approx 6.59, \quad r \approx 0.49. \tag{8.20}$$

We point out that taking different percentages for the definition of t_{dissip} does not change the qualitative structure of the scaling (8.20). Therefore, the power law (8.20) indicates that in the limit of vanishing damping no mass is dissipated in the collapse. This fact is opposite to the theoretical prediction established in Subsection 5.3.2 for the two-dimensional damped NLS, in which the expected amount of mass loss is equal to $M_{\text{collapse}}(0) - M_c$.

8.5 Concluding remarks

In this chapter we provided a detailed numerical study of the one-dimensional damped NLS (8.1) and the reduced system (8.8)-(8.9). Then, we can highlight the following results:

1. We verified numerically that the singularity in the NSL model is cured by adding the small nonlinear damping term given in (8.1) (Section 8.1).

2. We verified the approaching of the collapsing core toward the universal $\psi_{R^{(0)}}$ profile as δ is getting small (Section 8.1).

3. The exponential growth of the maximum of the solution as δ decreases, i.e., $|\psi|^2_{\max\max} \sim \exp(k\delta^m)$ where $k > 0$ is a constant depending of the initial condition. Direct numerical simulations of the NLS (8.1) suggest the value $m \approx -0.41$, meanwhile the reduced system produces $m \approx -0.52$. Therefore, our findings are in qualitative agreement with the predicted exponential growing for the wave-maximum, but do not verify the theoretical estimate for the power of δ, $m = -1$ (Section 8.2).

4. The invalidity of the adiabatic approximation (modulation theory) soon after the maximum of the soluion, and the collapse of the interval of validity with $\delta \to 0$. Our findings suggest that the breakdown of the adiabatic approach is possibly due to the increasing influx of mass into the inner zone of the solution, which is comparable with the dissipation (Section 8.3).

5. The validity of the universal profile $\psi_{R^{(0)}}$ in the non-adiabatic regime (Section 8.3).

6. The non loss of mass in the zero-limit dissipation. Indeed, our numerical simulations suggest a power law scaling for the amount of dissipatived mass in a single collapse $\Delta M \sim d\delta^r$ with $d \approx 6.59$ and $r \approx 0.49$ (Section 8.4).

Chapter 9

Post-Adiabatic Dynamics

We saw in the previous chapter that adiabatic approximation breaks down very soon after the arrest of the collapse, and that this invalidity of the adiabatic approach is possibly caused by the increasing influx of mass in the inner core of the solution (Section 8.3).

The goal of this chapter is to describe the post-blowup dynamics at instants after the breakdown of the adiabatic stage. We will show clear evidences that after the end of the adiabatic phase a quasi-linear regime is developed, see Section 9.1. In the subsequent Section 9.2, the numerical verification of the validity of the universal $\psi_{R^{(0)}}$ profile, after removing some oscillations, in the linear regime is shown. Finally, our results suggest that in a free-space problem, in the limit of vanishing damping the total collapsed mass M_c is instantly radiated to infinity at the critical time, see Section 9.3. Therefore, we emphasize in the importance of the boundary conditions used in the problem formulation.

9.1 Quasi-linear regime.

Numerical simulations for the damped NLS (8.1)-(8.2) indicate the generation of small oscillations around the collapsing core short after the invalidity of the adiabatic stage. When the solution defocuses, the amplitude and the number of these outgoing fluctuations increase and "pollute" the inner core of the solution. In Figure 9.1:(a) we have plotted some snapshots of $|\psi|^2$ for $\delta = 10^{-3}$ at different instants of the defocusing

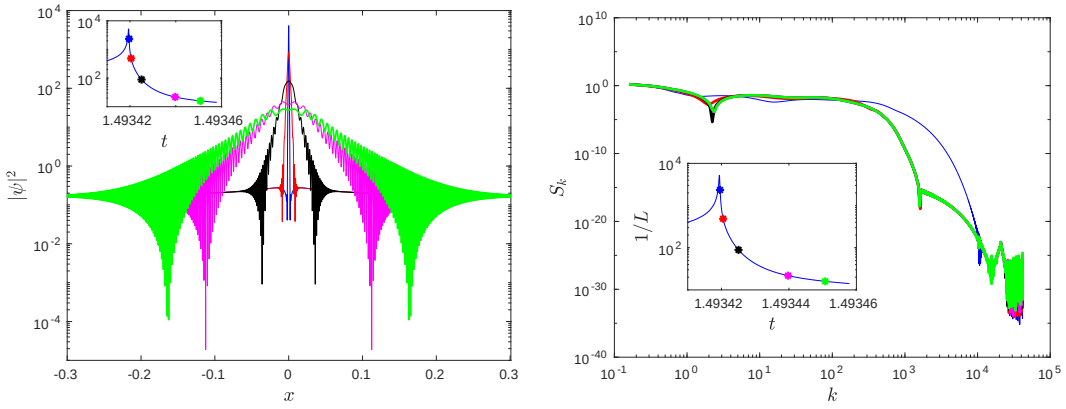

(a) (b)

Figure 9.1: (a) Profile of $|\psi|^2$ for $\delta = 10^{-3}$ at different instants of time in the non-adiabatic dynamics. The first profile corresponds to the time t_{break}. The outgoing oscillations propagate involving the whole collapsing core. The inset shows the function $1/L(t)$ and the instants considered in post-blowup dynamics. These oscillations indicate a dominant dispersive effect. (b) Spectra of the solution. The quasi unmodified spectra support that the dynamics is almost linear.

process, starting at the breakdown time t_{break}. In the corresponding inset the function $1/L(t)$ and the times considered are displayed. Here the function $L(t)$ was computed by using the relation $L(t) = \sqrt{3}/|\psi(0,t)|^2$.

The generation of these oscillations strongly suggests a dispersive-dominated regime in the post-adiabatic dynamics. Indeed, one can see in Figure 9.1:(b) the almost unchanged spectra of the solution S_k (see definition in (6.17)) in the prescribed regime: the spectrum corresponding to the red, black, pink and green instants are almost identical, but different from the spectrum at the blue instant near the peak. Figure 9.1:(b) indicates a quasi-linear regime in which the dispersive term dominates the nonlinear one. This quasi-linear regime was also reported in [56], by a numerical study of the two-dimensional critical NLS with a supercritical nonlinear damping.

In order to reinforce the evidences of this quasi-linear regime, we complement the previous indicia by checking directly the evolution of the dispersive and nonlinear terms. In Figure 9.2 we have compared the terms $|\psi_{xx}|$ and $|\psi|^5$. In the first instants

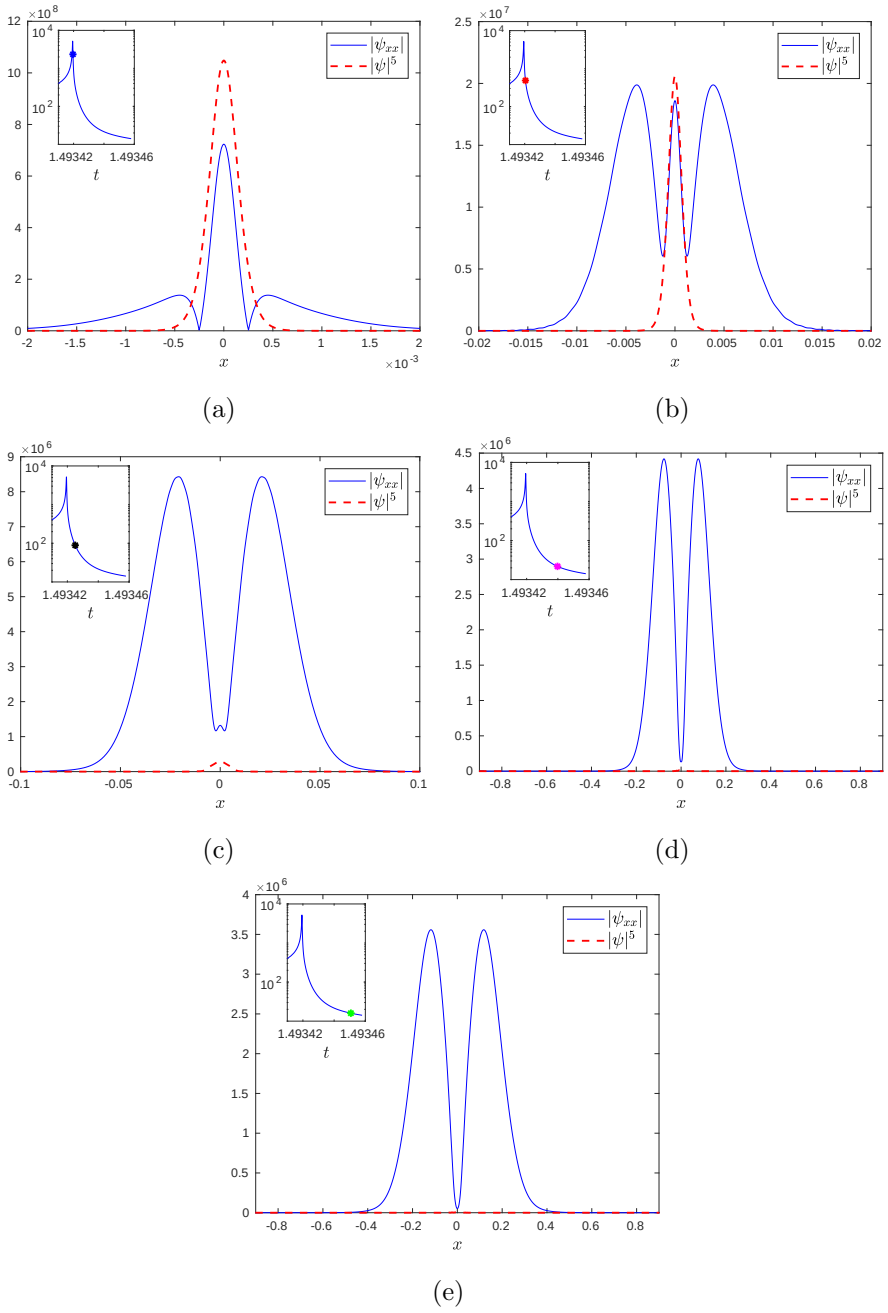

Figure 9.2: Comparison between the dispersive term $|\psi_{xx}|$ and the nonlinear term $|\psi|^5$ for $\delta = 10^{-3}$ at different moments after the breakdown of the adiabatic stage. As time runs, the delicate balance between both terms is replaced by a dispersive-dominated stage caused by the rapid defocusing process.

in the defocusing process both terms compensate each other, as it expected. Afterwhile, $|\psi_{xx}|$ becomes dominant over $|\psi|^5$, in such a way that the space-interval in which the former strongly dominates the latter expands in time, as can be observed in Figure 9.2.

Despite both terms decrease when the solution defocuses, the fast decay of the

nonlinear term induces a quasi-linear dynamics. Consequently, in that stage the resulting dynamics of the solution is approximately described by the linear Schrödinger equation.

9.2 Persistence of the universal profile $\psi_{R^{(0)}}$

So far, we have observed two stages in the post-blowup dynamics: an adiabatic regime, in which the inner core of the solution follows asymptotically the profile $\psi_{R^{(0)}}$ subjected to the reduced equations (8.8)-(8.9), and a quasi-linear stage, caused by the fast decay of the peak of the solution. In such linear regime reduced equations are not valid. Now, the goal is to show the validity of $\psi_{R^{(0)}}$ in the linear regime. Recall that the universal $\psi_{R^{(0)}}$ profile is given by

$$\psi_{R^{(0)}}(x,t) = \frac{3^{1/4}}{L^{1/2}(t)} \operatorname{sech}^{1/2}(2\xi) \exp\left(i\tau + i\frac{L_t}{L}\frac{x^2}{4}\right), \tag{9.1}$$

with $\xi = x/L(t)$ for some unknown function $L(t)$. We will start by verifying the hyperbolic secant profile $R^{(0)}(\xi) = 3^{1/4}\operatorname{sech}^{1/2}(2\xi)$, i.e.,

$$|\psi(x,t)| \approx \frac{1}{L^{1/2}(t)} R^{(0)}(\xi). \tag{9.2}$$

Due to the strong interference between the inner core and the tail in the linear regime, collapsing core is typically "polluted" by small oscillations. Therefore, in order to verify (9.2), we need to clean up the profile of $|\psi|$. We define $\phi_{\max}(x)$ as the resulting function to subtract from $\psi(x, t_{\max})$ its inner core, i.e.,

$$\phi_{\max}(x) := \begin{cases} \psi(x, t_{\max}), & |x| \geq 6L(t_{\max}), \\ 0, & |x| \ll 6L(t_{\max}). \end{cases} \tag{9.3}$$

In other words, $\phi_{\max}(x)$ is almost all the extra mass (mass above M_c) contained in the solution. Then, taking advantage of the linearity, almost all the oscillations contained in ψ will be removed by subtracting from it the function $\phi_{\max}(x)$. In Figure 9.3:(a) we have displayed the profile of $|\psi|$ for $\delta = 10^{-3}$ in a certain moment of the linear regime. The left and right inset correspond to $1/L(t)$ and $|\phi_{\max}(x)|$ respectively. In Figure 9.3:(b), the cleaned profile $|\psi - \phi_{\max}|$ is compared with the rescaled ground state

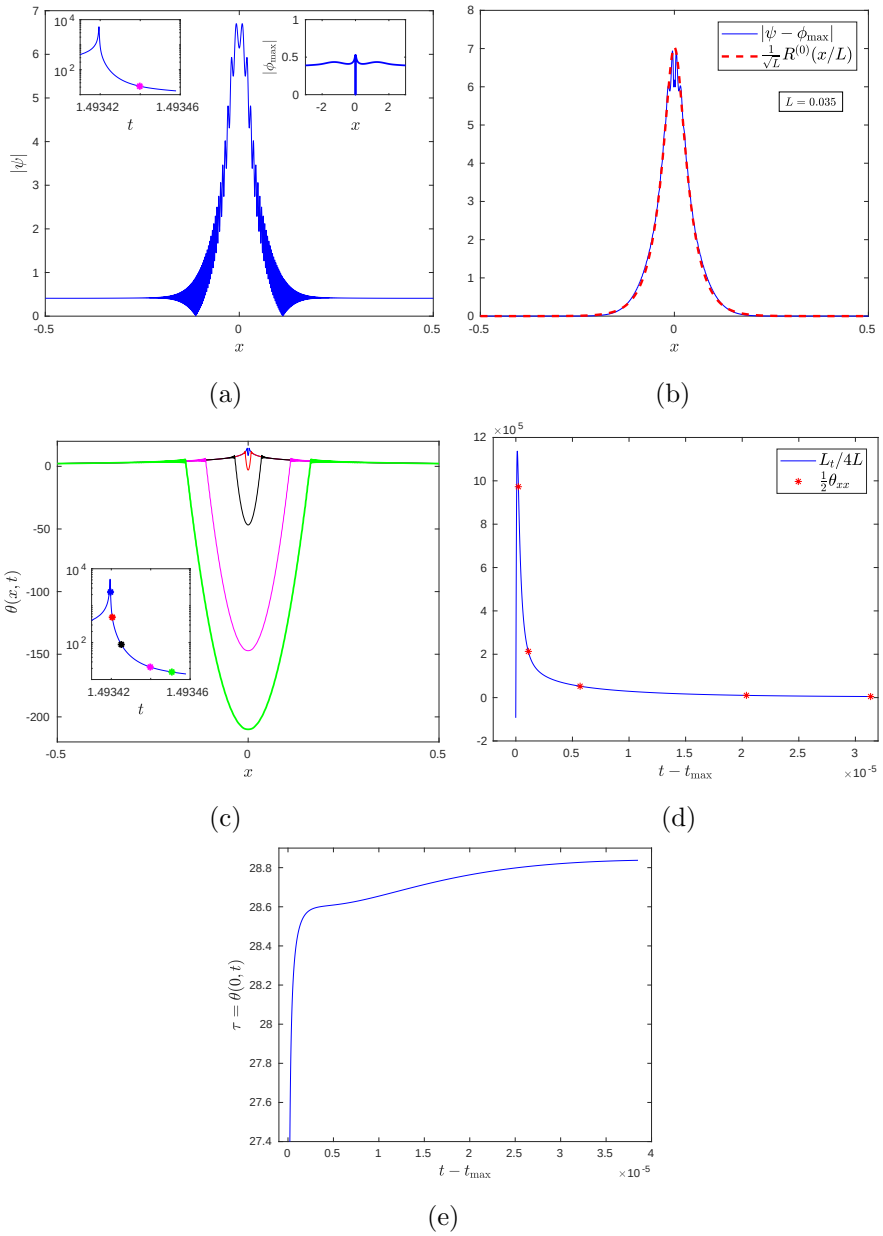

Figure 9.3: Verification of the universal profile $\psi_{R^{(0)}}$ in the linear regime of the post-blowup dynamics. (a) Profile of $|\psi|$ for $\delta = 10^{-3}$ at certain moment in the linear stage. In the right inset is displayed the extra mass $\phi_{\max}(x)$, obtained taking away from $\psi(x, t_{\max})$ its inner core. (b) Comparison between the cleaned profile $|\psi - \phi_{\max}|$, and the rescaled ground state $R^{(0)}$. Then, the collapsing core shape is modulated by $R^{(0)}$. (c) Phase of the solution $\theta(x,t)$ at different moments in the post-adiabatic dynamics. (d) Leading coefficients of the quadratic functions, $\frac{1}{2}\theta_{xx}$, plotted on the graph of $L_t/4L$ with $L(t)$ computed by the relation $L(t) = \sqrt{3}/|\psi(0,t)|^2$. (e) Dynamics of the accumulative phase $\tau = \theta(0,t)$.

$\frac{1}{\sqrt{L}}R^{(0)}(x/L)$ with $L \approx 0.035$ is shown. One sees that indeed almost all the extra mass is removed in that process, and the comparison corroborates (9.2).

The next step in the verification of the universal profile (9.1), is to check that the phase of the solution $\theta = \arg\psi(x,t)$, is approximated by the quadratic expression

$$\theta(x,t) \approx \tau + \frac{L_t}{4L}x^2. \tag{9.4}$$

In fact, as can be seen in Figure 9.3:(c), the phase of the solution as function of x, through the post-blowup dynamics behaves like a parabola in a vicinity of $x = 0$. In the bottom row, Figure 9.3:(d), one can see the good agreement between the leading coefficients of these quadratic functions, $\frac{1}{2}\theta_{xx}$, with the term $L_t/4L$ computed by using the relation $L(t) = \sqrt{3}/|\psi(0,t)|^2$. Consequently, the quadratic phase (9.4) is verified. In conclusion, after removing some oscillations, the collapsing core of the solution can be approximated by the universal profile $\psi_{R^{(0)}}$. The validity of the $\psi_{R^{(0)}}$ profile in the linear regime was an unexpected finding. As it is well known, in the adiabatic stage of the collapsing process dispersion and nonlinearity are almost balanced (exactly balanced in the explicit case). Therefore, in the profile $\psi_{R^{(0)}}$ the dispersion and nonlinearity are balanced, but the numerical simulations manifested also the validness of it in the dispersive-dominated regime.

The time evolution of $\tau = \theta(0,t)$ through the post-blowup dynamics is displayed in Figure 9.3:(e).

9.3 Conjecture: Instantaneous radiation of the critical mass

In the previous section we observed a linear regime in the post-adiabatic stage. Due to the increase defocusing process as δ decreases, one expects that such linear regime begins sooner (closer the peak) and becomes faster in the limit $\delta \to 0$. In this stage the dynamics can be described by the linear Schrödinger equation

$$i\psi_t + \psi_{xx} = 0. \tag{9.5}$$

Therefore, the localized part of the solution (collapsing core) spread out due to the dominant dispersion effect, i.e., each Fourier mode travels at different velocities. As it

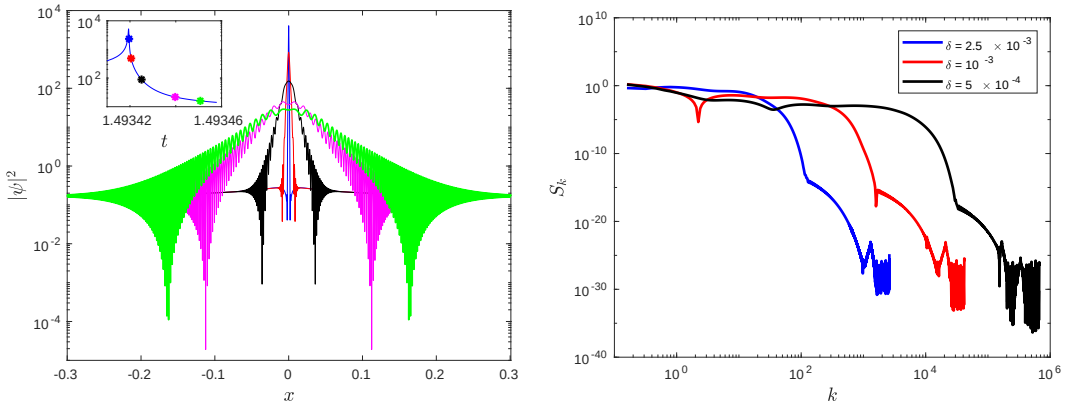

(a) (b)

Figure 9.4: (a) Profiles of $|\psi|^2$ for $\delta = 10^{-3}$ in the defocusing process. This shows the radiation of the collapsed mass toward the boundary of the domain. (b) Spectra of the solution for various values of δ. A tendency to the formation of small scales as δ decreases is observed. Consequently, our measurements suggest that in the limit of vanishing damping, all the critical mass M_c is instantly radiated to infinity (in the free-space domain) at the blowup time.

well known, the dispersion relation associated to the equation (9.5) is given by

$$w(k) = k^2. \tag{9.6}$$

Consequently, the mass of the collapsing core tends to be radiated outward, and therefore towards the domain boundary, through the higher frequencies and at the velocity (group velocity)

$$v_{\mathrm{g}} = 2k. \tag{9.7}$$

Figure 9.4:(a) (same Figure 9.1:(a)) displays the profile of $|\psi|^2$ at different moments of the defocusing process for $\delta = 10^{-3}$. The snapshots clearly show the radiation of the mass of the collapsing core carry out through the outgoing waves.

In Figure 9.4:(b) we have plotted the spectrum S_k of the solution for the three smaller $\delta = 2.5 \times 10^{-3}, 10^{-3}, 5 \times 10^{-4}$ at certain instants of the post-adiabatic stage. It indicates that after the arrest of collapse the spectrum exhibits the rapid formation of smaller scales (larger k) as long as δ decreases. Therefore, by (9.7) we *conjecture* that in the limit of vanishing dissipation the collapsed mass M_c is instantly radiated.

For example, if the solution is considered in a free-space, $x \in \mathbb{R}$, the mass is instantly radiated to infinity at the collapsing time.

By virtue of the mass radiation process, the boundary conditions assumed play a crucial role in order to have a well-defined post-blowup dynamics. Probably, in order to have a better description of the dynamics a kind of absorbing boundary conditions should be used in physical applications and numerical simulations.

9.4 Concluding remarks

In this chapter we provided a detailed numerical study of the post-blowup dynamics in the framework of the damped NLS equation (8.1), when the adiabatic approximation is broken. The main results were:

1. The numerical observation of a quasi linear regime in the post-adiabatic dynamics (Section 9.1). This fact was verified through the almost unchanged spectrum of the solution, and reinforced by the direct comparison of the terms $|\psi_{xx}|$ and $|\psi|^5$ demostrating the domination of the dispersive term over the nonlinearity one.

2. The numerical verification of the universal $\psi_{R^{(0)}}$ profile in the linear regime (Section 9.2). This was a surprising result taking into account that $\psi_{R^{(0)}}$ almost balanced dispersion and nonlinearity in the adiabatic stage.

3. The observation of the fast outgoing radiation of mass from the inner core of the damped NLS solution in the post-adiabatic dynamics (Section 9.3). Consequently, we conjecture that in the limit of vanishing damping the collapsed mass M_c is instantly radiated toward the domain boundary, or equivalently to infinity in the free-space domain. In order to avoid an undesired interference with the dynamics in the interior of the domain, an absorbing boundary conditions should be considered instead of the periodic boundary conditions used in our simulations.

Chapter 10

Conclusions

In this thesis we have provided a systematic numerical study of the post-blowup dynamics of singular solutions in the framework of the one-dimensional critical focusing damped NLS equation. In this work the damped/undamped NLS was solved under an initial condition with mass approximately 45.76% above the critical mass, in contrast to the numerical simulations carried out in [21, 22], where the initial mass ranged between $2.5\% - 10.25\%$ above the critical one.

In regards to the damped NLS, some predictions based on the adiabatic approach have been compared with the results obtained form our direct numerical simulations. The expected exponential growth of the maximum of the solution was verified in our simulations, but our simulations provide different power laws of δ in the exponential expression. Also, our measurements indicated that no mass is dissipated in a single collapse event in the limit δ going to zero, different to the expected finite amount of dissipated mass in the two-dimensional problem [16]. Our findings were in agreement with [21, 22], showing the invalidity of the adiabatic approximation shortly after the arrest of the collapse. We provide a numerical evidence that it could be caused by the increasing influx of mass into the inner core of the solution.

After the adiabatic regime, valid close to the maximum of the solution, a quasi linear stage was observed as a consequence of the rapid defocusing process. Interestly, the validity of the universal profile $\psi_{R^{(0)}}$, after removing the interference oscillations caused by the extra mass, was verified in such linear regime. This dynamics is accompanied of an outward mass radiation process. In these terms, and knowing that

periodic boundary conditions allow that the mass radiated enter from the other side of the domain, we highlight the importance of using a kind of absorbing boundary conditions in order to prevent any unwanted interference with the dynamics in the interior of the domain. In addition, our observations suggested that in the limit δ going to zero, the critical mass is instantly radiated to infinity (in the case of the free-space domain) at the collapsing time.

Some recent works, see, e.g., [10, 31, 42], have considered some perturbations of the NLS equation in the study of dissipation by singularity events in the framework of turbulent dissipation. A fundamental objective of these kind of works is try to understand the strong turbulece based of the assumption that it could be the consequence of spatio-temporal singularities. We expect that the detailed theory of the blowup and post-blowup dynamics, to which our study contributes, will help for understanding properties of turbulent spectra observed in these applications.

Appendices

Appendix A

Perturbation Analysis for $U = R^{(0)} + \epsilon h$

In this appendix we will provide some results that are useful in the derivation of the reduced system for both unperturbed and perturbed cases. In both derivations, the main assumption is that the collapsing core of the solution is approximated by the ground state $R^{(0)}$. Consequently, it is needed a perturbation analysis around $R^{(0)}$ with small expansion parameters β and δ. Therefore, in this appendix we will focus in the analysis of the perturbation $U = R^{(0)} + \epsilon h$ with $|\epsilon| \ll 1$.

The main result in this section is the following lemma:

Lemma A.1. *Let $U(\boldsymbol{x};\epsilon)$ be a real function in $H^1(\mathbb{R}^d)$ that satisfies the equation*

$$\Delta U - U + |U|^{\frac{4}{d}}U + \epsilon w(U) = 0, \tag{A.1}$$

where $w(U)$ is real, and let $H(U) = \int |\nabla U|^2 d\boldsymbol{x} - \frac{d}{d+2}\int |U|^{\frac{4}{d}+2} d\boldsymbol{x}$. Then,

$$H(U) = \epsilon \int w(U)\left[\frac{d}{2}U + \boldsymbol{x}\cdot\nabla U\right] d\boldsymbol{x}. \tag{A.2}$$

Let

$$U(\boldsymbol{x}) = R^{(0)}(r) + \epsilon h(\boldsymbol{x}) + \mathcal{O}(\epsilon^2), \qquad |\epsilon| \ll 1, \tag{A.3}$$

where $r = |\boldsymbol{x}|$, and $R^{(0)}$ is the ground state of

$$\Delta R - R + |R|^{\frac{4}{d}}R = 0. \tag{A.4}$$

Then h is the solution of

$$L_+ h = -w(R^{(0)}), \qquad L_+ := \Delta - 1 + \left(\frac{4}{d} + 1\right) |R^{(0)}|^{\frac{4}{d}}. \tag{A.5}$$

In addition, the following integral identities hold:

$$\int R^{(0)} h d\boldsymbol{x} = -\frac{1}{2} \int w(R^{(0)}) \left[\frac{d}{2} R^{(0)} + r \frac{dR^{(0)}}{dr}\right] d\boldsymbol{x}, \tag{A.6}$$

$$\int \nabla R^{(0)} \nabla h d\boldsymbol{x} = \frac{1}{2} \int w(R^{(0)}) r \frac{dR^{(0)}}{dr} d\boldsymbol{x}, \tag{A.7}$$

$$\int |R^{(0)}|^{\frac{4}{d}} R^{(0)} h d\boldsymbol{x} = -\frac{d}{4} \int w(R^{(0)}) R^{(0)} d\boldsymbol{x}. \tag{A.8}$$

Therefore,

$$\|U\|_2^2 = \|R^{(0)}\|_2^2 + 2\epsilon \int R^{(0)} h \boldsymbol{x} + \mathcal{O}(\epsilon^2), \tag{A.9}$$

and

$$H(U) = \epsilon \int w(R^{(0)}) \left[\frac{d}{2} R^{(0)} + r \frac{dR^{(0)}}{dr}\right] d\boldsymbol{x} + \mathcal{O}(\epsilon^2). \tag{A.10}$$

Proof. We first derive some identities for U. Multiplying the equation (A.1) by U and integrate by parts, we get that

$$-\int (\nabla U)^2 d\boldsymbol{x} - \int |U|^2 d\boldsymbol{x} + \int |U|^{\frac{4}{d}+2} d\boldsymbol{x} + \epsilon \int w(U) U d\boldsymbol{x} = 0. \tag{A.11}$$

Similarly, if we multiply the equation (A.1) by $\boldsymbol{x} \cdot \nabla U$ and integrate by parts, we have

$$\begin{aligned} -\int \nabla (\boldsymbol{x} \cdot \nabla U) \cdot \nabla U d\boldsymbol{x} + \int \boldsymbol{x} \cdot \left(-\nabla \frac{U^2}{2} + \nabla \frac{|U|^{4/d+2}}{4/d+2}\right) d\boldsymbol{x} \\ + \epsilon \int w(U) \boldsymbol{x} \cdot \nabla U d\boldsymbol{x} = 0. \end{aligned} \tag{A.12}$$

Now, to evaluate the first integral in the last expression we use the vectorial relation

$$\nabla(\boldsymbol{x} \cdot \nabla U) = \nabla U + (\boldsymbol{x} \cdot \nabla) \nabla U. \tag{A.13}$$

Indeed, by (A.13) and integration by parts one has

$$-\int \nabla (\boldsymbol{x} \cdot \nabla U) \cdot \nabla U d\boldsymbol{x} = -\int [\nabla U + (\boldsymbol{x} \cdot \nabla) \nabla U] \cdot \nabla U d\boldsymbol{x} \tag{A.14}$$

$$= -\int \left[(\nabla U)^2 + \boldsymbol{x} \cdot \nabla \frac{(\nabla U)^2}{2}\right] d\boldsymbol{x} \tag{A.15}$$

$$= \left(-1 + \frac{d}{2}\right) \int (\nabla U)^2 d\boldsymbol{x}. \tag{A.16}$$

Therefore,

$$-\int \nabla\left(\boldsymbol{x}\cdot\nabla U\right)\cdot\nabla U d\boldsymbol{x}=\left(-1+\frac{d}{2}\right)\int(\nabla U)^2 d\boldsymbol{x}. \tag{A.17}$$

For the second integral in (A.12), the integration by parts implies

$$\int \boldsymbol{x}\cdot\left(-\nabla\frac{U^2}{2}+\nabla\frac{|U|^{4/d+2}}{4/d+2}\right)d\boldsymbol{x}=\frac{d}{2}\int U^2 d\boldsymbol{x}-\frac{d}{4/d+2}\int|U|^{4/d+2}d\boldsymbol{x}. \tag{A.18}$$

Then, by (A.17) and (A.18) equation (A.12) becomes

$$\begin{aligned}\frac{d-2}{2}\int(\nabla U)^2 d\boldsymbol{x}+\frac{d}{2}\int|U|^2 d\boldsymbol{x}-\frac{d}{4/d+2}\int|U|^{4/d+2}d\boldsymbol{x} \\ +\epsilon\int w(U)\boldsymbol{x}\cdot\nabla U d\boldsymbol{x}=0.\end{aligned} \tag{A.19}$$

The last identity required is obtained multiplying equation (A.4) (with $R=R^{(0)}$) by U, and integrating by parts:

$$-\int\nabla R^{(0)}\nabla U d\boldsymbol{x}-\int UR^{(0)}d\boldsymbol{x}+\int U|R^{(0)}|^{4/d}R^{(0)}d\boldsymbol{x}=0. \tag{A.20}$$

In these terms, the rest of the proof is use the identities (A.1), (A.11), (A.19) and (A.20) to derive the desired results. Indeed, multiplying (A.11) by $d/2$ and adding (A.19) one gets

$$-\int|\nabla U|^2 d\boldsymbol{x}+\frac{d}{2+d}\int|U|^{4/d+2}d\boldsymbol{x}+\epsilon\int w(U)\left[\frac{d}{2}U+\boldsymbol{x}\cdot\nabla U\right]d\boldsymbol{x}=0, \tag{A.21}$$

or equivalently,

$$-H(U)+\epsilon\int w(U)\left[\frac{d}{2}U+\boldsymbol{x}\cdot\nabla U\right]d\boldsymbol{x}=0, \tag{A.22}$$

proving the equation (A.2).

The next step is prove (A.5). If we substitute (A.3) into (A.1), and collecting powers of ϵ, we get

$$\begin{aligned}\left(\Delta R^{(0)}-R^{(0)}+|R^{(0)}|^{4/d}R^{(0)}\right)+\epsilon\left(\Delta h-h+\left(\frac{4}{d}+1\right)|R^{(0)}|^{4/d}h+w(R^{(0)})\right) \\ +\mathcal{O}(\epsilon^2).\end{aligned} \tag{A.23}$$

Therefore, h satisfies the equation

$$\Delta h-h+\left(\frac{4}{d}+1\right)|R^{(0)}|^{4/d}h+w(R^{(0)})=0. \tag{A.24}$$

Now, we will derive the integral identities (A.6)-(A.8). They are derived by taking the $\mathcal{O}(\epsilon)$ terms from (A.11), (A.19) and (A.20) and solving the linear system obtained. In fact, substituting (A.3) into (A.11), and collecting powers of ϵ we have

$$\begin{aligned}&\left[-\int(\nabla R^{(0)})^2 d\boldsymbol{x}-\int|R^{(0)}|^2 d\boldsymbol{x}+\int|R^{(0)}|^{4/d+2} d\boldsymbol{x}\right] \\ &+\epsilon\left[-2\int\nabla R^{(0)}\nabla h d\boldsymbol{x}-2\int R^{(0)} h d\boldsymbol{x}+(4/d+2)\int|R^{(0)}|^{4/d}R^{(0)} h d\boldsymbol{x}\right] \\ &+\epsilon\int w(R^{(0)})R^{(0)} d\boldsymbol{x}+\mathcal{O}(\epsilon^2)=0\end{aligned} \tag{A.25}$$

Therefore, the equation for the $\mathcal{O}(\epsilon)$ terms is

$$\begin{aligned}-2\int\nabla R^{(0)}\nabla h d\boldsymbol{x}-2\int R^{(0)} h d\boldsymbol{x}+(4/d+2)\int|R^{(0)}|^{4/d}R^{(0)} h d\boldsymbol{x} \\ +\int w(R^{(0)})R^{(0)} d\boldsymbol{x}=0.\end{aligned} \tag{A.26}$$

Similarly, if we substitute (A.3) into (A.19) we get

$$\begin{aligned}&\left[\frac{d-2}{2}\int(\nabla R^{(0)})^2 d\boldsymbol{x}+\frac{d}{2}\int|R^{(0)}|^2 d\boldsymbol{x}-\frac{d}{4/d+2}\int|R^{(0)}|^{4/d+2} d\boldsymbol{x}\right] \\ &+\epsilon\left[(d-2)\int\nabla R^{(0)}\nabla h d\boldsymbol{x}+d\int R^{(0)} h d\boldsymbol{x}-d\int|R^{(0)}|^{4/d}R^{(0)} h d\boldsymbol{x}\right] \\ &+\epsilon\int w(R^{(0)})r\frac{dR^{(0)}}{dr} d\boldsymbol{x}+\mathcal{O}(\epsilon^2)=0,\end{aligned} \tag{A.27}$$

where we have used the identity $\boldsymbol{x}\cdot\nabla R^{(0)}=r\frac{dR^{(0)}}{dr}$. Consequently, the $\mathcal{O}(\epsilon)$ term is

$$\begin{aligned}(d-2)\int\nabla R^{(0)}\nabla h d\boldsymbol{x}+d\int R^{(0)} h d\boldsymbol{x}-d\int|R^{(0)}|^{4/d}R^{(0)} h d\boldsymbol{x} \\ +\int w(R^{(0)})r\frac{dR^{(0)}}{dr} d\boldsymbol{x}=0.\end{aligned} \tag{A.28}$$

From (A.3) and (A.20) one has

$$\begin{aligned}&\left[-\int(\nabla R^{(0)})^2 d\boldsymbol{x}-\int|R^{(0)}|^2 d\boldsymbol{x}+\int|R^{(0)}|^{4/d+2} d\boldsymbol{x}\right] \\ &+\epsilon\left[-\int\nabla R^{(0)}\nabla h d\boldsymbol{x}-\int R^{(0)} h d\boldsymbol{x}+\int|R^{(0)}|^{4/d}R^{(0)} h d\boldsymbol{x}\right]+\mathcal{O}(\epsilon^2)=0.\end{aligned} \tag{A.29}$$

Then,

$$-\int\nabla R^{(0)}\nabla h d\boldsymbol{x}-\int R^{(0)} h d\boldsymbol{x}+\int|R^{(0)}|^{4/d}R^{(0)} h d\boldsymbol{x}=0. \tag{A.30}$$

Note that if we define $x=\int\nabla R^{(0)}\nabla h d\boldsymbol{x}$, $y=\int R^{(0)} h d\boldsymbol{x}$, $z=\int|R^{(0)}|^{4/d}R^{(0)} h d\boldsymbol{x}$, $a=\int w(R^{(0)})R^{(0)} d\boldsymbol{x}$ and $b=\int w(R^{(0)})r\frac{dR^{(0)}}{dr} d\boldsymbol{x}$, the equations (A.26), (A.28) and

(A.30) can be written as

$$\begin{aligned} -x - y + z &= 0, \\ -2x - 2y + (4/d + 2)z &= -a, \\ (d-2)x + dy - dz &= -b, \end{aligned} \tag{A.31}$$

with the solution

$$x = \frac{b}{2}, \quad y = -\frac{b}{2} - \frac{d}{4}a, \quad z = -\frac{d}{4}a. \tag{A.32}$$

Therefore,

$$\int R^{(0)} h d\boldsymbol{x} = -\frac{1}{2}\int w(R^{(0)}) \left[\frac{d}{2}R^{(0)} + r\frac{dR^{(0)}}{dr}\right] d\boldsymbol{x}, \tag{A.33}$$

$$\int \nabla R^{(0)} \nabla h d\boldsymbol{x} = \frac{1}{2}\int w(R^{(0)}) r\frac{dR^{(0)}}{dr} d\boldsymbol{x}, \tag{A.34}$$

$$\int |R^{(0)}|^{\frac{4}{d}} R^{(0)} h d\boldsymbol{x} = -\frac{d}{4}\int w(R^{(0)}) R^{(0)} d\boldsymbol{x}. \tag{A.35}$$

The equation (A.9) is easily verified, and (A.10) comes from substituting (A.3) into (A.2) and using the relation $\boldsymbol{x} \cdot \nabla R^{(0)} = r\frac{dR^{(0)}}{dr}$. □

Corollary A.1. *The results of Lemma A.1 remain unchanged if we replace equation (A.1) with the equation*

$$\Delta U - U + |U|^{\frac{4}{d}} U + \epsilon w(U) = \mathcal{O}(\epsilon^2). \tag{A.36}$$

Proof. The $\mathcal{O}(\epsilon^2)$ right-hand side does not affect the equations for the $\mathcal{O}(1)$ and $\mathcal{O}(\epsilon)$ terms in the proof of Lemma A.1. □

A.1 Perturbation $\Psi_0 = R^{(0)} + \beta g$

In this section we will use Lemma A.1 and Corollary A.1 to prove the following integral identity:

Lemma A.2. $\int_0^\infty R^{(0)} g \xi^{d-1} d\xi = \frac{1}{8}\int_0^\infty \xi^2 |R^{(0)}|^2 \xi^{d-1} d\xi$.

Proof. We cannot apply Lemma A.1 with $U = \Psi_0$ directly, because $\Psi_0 \notin L^2$, see e.g., [17]. Therefore, we proceed as follows. Let $\tilde{\Psi}_0 := R^{(0)} + \beta g$. Since $R^{(0)}$ and g decay exponentially, $\tilde{\Psi}_0 \in H^1$. In these terms, we can apply Lemma A.1 with $U = \tilde{\Psi}_0$. Multiplying by β the equation (B.7) and adding the result to (A.4) (with $R = R^{(0)}$) we get

$$\Delta\tilde{\Psi}_0 - \tilde{\Psi}_0 + \beta\left(\frac{4}{d}+1\right)|R^{(0)}|^{4/d}g + |R^{(0)}|^{4/d}R^{(0)} + \frac{1}{4}\beta\xi^2 R^{(0)} = 0. \tag{A.37}$$

Consequently,

$$\begin{aligned}
&\Delta\tilde{\Psi}_0 - \tilde{\Psi}_0 + |\tilde{\Psi}_0|^{4/d}\tilde{\Psi}_0 + \frac{1}{4}\beta\xi^2\tilde{\Psi}_0 && \text{(A.38)}\\
&\quad = |\tilde{\Psi}_0|^{4/d}\tilde{\Psi}_0 - |R^{(0)}|^{4/d}R^{(0)} - \beta\left(\frac{4}{d}+1\right)|R^{(0)}|^{4/d}g + \frac{1}{4}\beta\xi^2\left(\tilde{\Psi}_0 - R^{(0)}\right) && \text{(A.39)}\\
&\quad = |R^{(0)}|^{4/d}R^{(0)} + \beta\left(\frac{4}{d}+1\right)|R^{(0)}|^{4/d}g - |R^{(0)}|^{4/d}R^{(0)} && \text{(A.40)}\\
&\quad - \beta\left(\frac{4}{d}+1\right)|R^{(0)}|^{4/d}g + \frac{1}{4}\beta\xi^2(\beta g) + \mathcal{O}(\beta^2) && \text{(A.41)}\\
&\quad = \mathcal{O}(\beta^2). && \text{(A.42)}
\end{aligned}$$

The right-hand side is $\mathcal{O}(\beta^2)$ for $0 \le \xi < \infty$, because it consists of the exponentially decreasing functions $R^{(0)}$ and g. In other words, one has

$$\Delta\tilde{\Psi}_0 - \tilde{\Psi}_0 + |\tilde{\Psi}_0|^{4/d}\tilde{\Psi}_0 + \frac{1}{4}\beta\xi^2\tilde{\Psi}_0 = \mathcal{O}(\beta^2), \tag{A.43}$$

and we can apply Corollary A.1 with $U = \tilde{\Psi}_0$, $\epsilon = \beta$, $w(U) = \frac{1}{4}\xi^2 U$ and $h = g$. Hence, by the identity (A.6) (in radial form) and integration by parts, we get

$$\begin{aligned}
\int_0^\infty R^{(0)} h r^{d-1} dr &= -\frac{1}{2}\int_0^\infty w(R^{(0)})\left[\frac{d}{2}R^{(0)} + r\frac{dR^{(0)}}{dr}\right] r^{d-1} dr && \text{(A.44)}\\
&= -\frac{1}{8}\int_0^\infty r^2 R^{(0)}\left[\frac{d}{2}R^{(0)} + r\frac{dR^{(0)}}{dr}\right] r^{d-1} dr && \text{(A.45)}\\
&= -\frac{1}{8}\int_0^\infty r^2\left(R^{(0)}r^{d/2}\right)_r\left(R^{(0)}r^{d/2}\right) dr && \text{(A.46)}\\
&= -\frac{1}{8}\int_0^\infty \frac{r^2}{2}\frac{d}{dr}(R^{(0)}r^{d/2})^2 dr && \text{(A.47)}\\
&= \frac{1}{8}\int_0^\infty r^2|R^{(0)}|^2 r^{d-1} dr. && \text{(A.48)}
\end{aligned}$$

□

Therefore, in the non-radial form one has

$$\int R^{(0)} g d\boldsymbol{x} = \frac{1}{8} \int |\boldsymbol{x}|^2 |R^{(0)}|^2 d\boldsymbol{x} = \frac{N}{2}, \tag{A.49}$$

where

$$N = \frac{1}{4} \int |\boldsymbol{x}|^2 |R^{(0)}|^2 d\boldsymbol{x}. \tag{A.50}$$

Appendix B

Proof of Proposition 3.1: Details

In this appendix we will provide details of the derivation of the reduced system established in the Proposition 3.1. Indeed, the steps of the proof are:

1. Let us introduce the *quasi self-similar transformation* (generalized lens transformation)

$$\psi(r,t) = \frac{1}{L^{d/2}(t)}\Psi(\xi,\tau)\exp\left(i\tau(t) + i\frac{L_t}{L}\frac{r^2}{4}\right), \tag{B.1}$$

where ξ and τ are given by (3.5). Substituting this ansatz into the NLS equation (3.2), yields the following equation for Ψ as

$$i\Psi_\tau(\xi,\tau) + \Psi_{\xi\xi} + \frac{d-1}{\xi}\Psi_\xi - \Psi + |\Psi|^{\frac{4}{d}}\Psi + \frac{1}{4}\beta(t)\xi^2\Psi = 0, \tag{B.2}$$

with $\beta(t) = -L^3 L_{tt}$. In this way, we have derived the first equation of the reduced system. Now, by (3.3) one has $\Psi \approx R^{(0)}$ for $0 \le \xi \le \xi_c$ with $0 \le \xi_c \ll \beta^{-1/2}$, i.e., this approximation is valid only in the region where $\beta\xi^2$ is small.

2. Expanding the solution of (B.2) as

$$\Psi = \Psi_0 + \Psi_1 + \Psi_2 + \cdots, \qquad \Psi_0 \gg \Psi_1 \gg \Psi_2 \cdots, \tag{B.3}$$

one expects that $\Psi(\xi,\tau) \approx \Psi_0(\xi,\tau) \approx R^{(0)}(\xi)$ for $0 \le \xi \le \xi_c$. Therefore, it is assumed that Ψ is quasi stationary, i.e., $\Psi_\tau \approx \Psi_{0,\tau} = o(1)$. Hence, the leading-order equation for Ψ_0 in the collapsing core region is given by

$$\Psi_{0,\xi\xi} + \frac{d-1}{\xi}\Psi_{0,\xi} - \Psi_0 + |\Psi_0|^{\frac{4}{d}}\Psi_0 + \frac{1}{4}\beta\xi^2\Psi_0 = 0, \qquad 0 \le \xi \le \xi_c, \tag{B.4}$$

with the radial condition $\Psi_0'(0) = 0$. It is noted that for $\beta = 0$, equation for Ψ_0 reduces to equation (3.6) for $R^{(0)}$. Then, the fact that $\Psi_0 \approx R^{(0)}$ implies that $\beta \to 0$. Hence, we will assume that β is small.

3. Since $0 < \beta \ll 1$, we can expand Ψ_0 in terms of β, i.e.,

$$\Psi_0(\xi;\beta) = R^{(0)}(\xi) + \beta g(\xi) + \mathcal{O}(\beta^2), \qquad g = \Psi_{0,\beta}(\xi;0). \tag{B.5}$$

Substituting this last expansion in (B.4) and collecting powers of β we have

$$(R^{(0)})'' + \frac{d-1}{\xi}(R^{(0)})' - R^{(0)} + |R^{(0)}|^{\frac{4}{d}}R^{(0)} + \beta\left(L_+ g + \frac{\xi^2}{4}R^{(0)}\right) + \mathcal{O}(\beta^2) = 0, \tag{B.6}$$

where $L_+ g = g'' + \frac{d-1}{\xi}g' - g + (4/d+1)|R^{(0)}|^{4/d}g$. Therefore, the function g satisfies

$$L_+ g + \frac{\xi^2}{4}R^{(0)} = 0, \qquad g'(0) = 0, \quad g(\infty) = 0, \tag{B.7}$$

and $g(\xi) \sim A_g \xi^3 R^{(0)}(\xi)$ as $\xi \to \infty$, where A_g is a constant, see [17]. Then, by Lemma 2.4 both $R^{(0)}$ and g decay exponentially as $\xi \to \infty$.

The expansion (B.5) allow us to obtain the following result:

Lemma B.1 ([43])**.** *Let $M_{collapse}^{radial}$ denote the radial mass of the collapsing core, i.e.,*

$$M_{collapse}^{radial} = \int_0^{\xi_c L(t)} |\psi|^2 r^{d-1} dr. \tag{B.8}$$

Then,

$$M_{collapse}^{radial} = M_c^{radial} + \beta N^{radial} + \mathcal{O}(\beta^2), \qquad 0 < \beta \ll 1, \tag{B.9}$$

where

$$M_c^{radial} = \int_0^{\infty} |R^{(0)}|^2 r^{d-1} dr, \qquad N^{radial} = \frac{1}{4}\int_0^{\infty} r^2 |R^{(0)}|^2 r^{d-1} dr. \tag{B.10}$$

Proof. Since the expansion (B.5) consists of the exponentially-decreasing functions $R^{(0)}$ and g, it is uniform in $0 \le \xi \le \xi_c$, i.e., there exists a constant C, such that

$$|\Psi_0 - R^{(0)} - \beta g| \le C\beta^2, \qquad 0 \le \xi \le \xi_c. \tag{B.11}$$

Therefore, we have

$$\int_0^{\xi_c} |\Psi_0|^2 \xi^{d-1} d\xi = \int_0^{\xi_c} |R^{(0)}|^2 \xi^{d-1} d\xi + 2\beta \int_0^{\xi_c} R^{(0)} g \xi^{d-1} d\xi + \mathcal{O}(\beta^2). \quad \text{(B.12)}$$

Due to the exponential decay of $R^{(0)}$, the value of $M_{\text{collapse}}^{\text{radial}}$ has an exponentially small change replacing ξ_c by $\beta^{-1/2}$:

$$\begin{aligned}
\int_0^{\beta^{-1/2}L(t)} |\psi|^2 r^{d-1} dr &= \int_0^{\xi_c L(t)} |\psi|^2 r^{d-1} dr + \int_{\xi_c L(t)}^{\beta^{-1/2}L(t)} |\psi|^2 r^{d-1} dr && \text{(B.13)} \\
&\approx M_{\text{collapse}}^{\text{radial}} + \int_{\xi_c}^{\beta^{-1/2}} |R^{(0)}|^2 \xi^{d-1} d\xi && \text{(B.14)} \\
&\approx M_{\text{collapse}}^{\text{radial}} + \frac{A_R^2}{2} \left(e^{-2\xi_c} - e^{-2/\sqrt{\beta}} \right) && \text{(B.15)} \\
&= M_{\text{collapse}}^{\text{radial}} + \mathcal{O}(e^{-2\xi_c}). && \text{(B.16)}
\end{aligned}$$

Therefore, in this proof we can use $\xi_c = \beta^{-1/2}$ in the definition of $M_{\text{collapse}}^{\text{radial}}$. Now, this fact allow us to maintain the validity of the equation (B.12) by substituting ξ_c with infinity. Indeed,

$$\begin{aligned}
\int_0^{\infty} |R^{(0)}|^2 \xi^{d-1} d\xi &= \int_0^{\xi_c} |R^{(0)}|^2 \xi^{d-1} d\xi + \int_{\xi_c}^{\infty} |R^{(0)}|^2 \xi^{d-1} d\xi && \text{(B.17)} \\
&= \int_0^{\xi_c} |R^{(0)}|^2 \xi^{d-1} d\xi + 2A_R^2 e^{-2/\sqrt{\beta}} && \text{(B.18)} \\
&= \int_0^{\xi_c} |R^{(0)}|^2 \xi^{d-1} d\xi + \mathcal{O}\left(e^{-2/\sqrt{\beta}} \right). && \text{(B.19)}
\end{aligned}$$

and

$$\begin{aligned}
\int_0^{\infty} R^{(0)} g \xi^{d-1} d\xi &= \int_0^{\xi_c} R^{(0)} g \xi^{d-1} d\xi + \int_{\xi_c}^{\infty} R^{(0)} g \xi^{d-1} d\xi && \text{(B.20)} \\
&= \int_0^{\xi_c} R^{(0)} g \xi^{d-1} d\xi + \frac{1}{8} A_g A_R^2 e^{-2\xi_c} \left(4\xi_c^3 + 6\xi_c^2 + 6\xi_c + 3 \right) && \text{(B.21)} \\
&= \int_0^{\xi_c} R^{(0)} g \xi^{d-1} d\xi + \mathcal{O}(\beta^{-3/2} e^{-2/\sqrt{\beta}}). && \text{(B.22)}
\end{aligned}$$

In other words, the error of replacing ξ_c with infinity is exponentially small in β. Consequently, by Lemma A.2 we have

$$\begin{aligned}
\int_0^{\xi_c} |\Psi_0|^2 \xi^{d-1} d\xi &= \int_0^{\infty} |R^{(0)}|^2 \xi^{d-1} d\xi + 2\beta \int_0^{\infty} R^{(0)} g \xi^{d-1} d\xi + \mathcal{O}(\beta^2) && \text{(B.23)} \\
&= M_c^{\text{radial}} + \frac{\beta}{4} \int_0^{\infty} \xi^2 |R^{(0)}|^2 \xi^{d-1} d\xi + \mathcal{O}(\beta^2) && \text{(B.24)} \\
&= M_c^{\text{radial}} + \beta N^{\text{radial}} + \mathcal{O}(\beta^2). && \text{(B.25)}
\end{aligned}$$

Finally, using the fact

$$M^{\text{radial}}_{\text{collapse}} = \int_0^{\xi_c L(t)} |\psi|^2 r^{d-1} dr = \int_0^{\xi_c} |\Psi|^2 \xi^{d-1} d\xi \approx \int_0^{\xi_c} |\Psi_0|^2 \xi^{d-1} d\xi, \quad \text{(B.26)}$$

we get the desired result. □

As a consequence of the previous result we have the physical interpretation of the function β:

Corollary B.1. *β is proportional to the excess mass above M_c of the collapsing core, i.e.,*

$$\beta \approx \frac{M^{radial}_{collapse} - M^{radial}_{c}}{N^{radial}} = \frac{M_{collapse} - M_c}{N}, \quad \text{(B.27)}$$

with

$$M_{collapse} = \int_{|\boldsymbol{x}| \le \xi_c L(t)} |\psi|^2 d\boldsymbol{x}, \qquad M_c = \int |R^{(0)}|^2 d\boldsymbol{x}, \quad \text{(B.28)}$$

and

$$N = \frac{1}{4} \int |\boldsymbol{x}|^2 |R^{(0)}|^2 d\boldsymbol{x}. \quad \text{(B.29)}$$

Similarly, from equation (B.9) we get

$$\frac{d}{dt} M^{\text{radial}}_{\text{collapse}} \approx \beta_t N^{\text{radial}}. \quad \text{(B.30)}$$

4. In this step the idea is compute the rate of change of the mass of the collapsing core. Indeed, we have the following result:

Lemma B.2. *The rate of change of the mass of the collapsing core is*

$$\frac{d}{dt} M^{radial}_{collapse} = \frac{1}{L^2} \left[i\xi^{d-1} \Psi^* \Psi_\xi + c.c. \right]_{\xi = \xi_c}, \quad \text{(B.31)}$$

where c.c. stands for complex conjugate.

Proof. By definition,

$$\frac{d}{dt} M^{\text{radial}}_{\text{collapse}} = \frac{d}{dt} \int_0^{r_c(t)} |\psi|^2 r^{d-1} dr, \qquad r_c(t) = L(t)\xi_c, \quad \text{(B.32)}$$

$$= r_c'(t) |\psi|^2 r_c^{d-1} + \int_0^{r_c} \frac{d}{dt} |\psi|^2 r^{d-1} dr, \qquad r_c' = \frac{L_t}{L} r_c. \quad \text{(B.33)}$$

Now, by using the radial NLS (3.2) and integrations by parts, one gets

$$\int_0^{r_c} \frac{d}{dt}|\psi|^2 r^{d-1} dr = \int_0^{r_c} \left(\psi_t \psi^* + \psi \psi_t^*\right) r^{d-1} dr \tag{B.34}$$

$$= i \int_0^{r_c} \left(\psi^* \psi_{rr} - \psi \psi_{rr}^*\right) r^{d-1} dr \tag{B.35}$$

$$+ i(d-1) \int_0^{r_c} \left(\psi_r \psi^* - \psi \psi_r^*\right) r^{d-2} dr \tag{B.36}$$

$$= \left[i\psi^* \psi_r r^{d-1} - i\psi \psi_r^* r^{d-1}\right]_{r=0}^{r=r_c} \tag{B.37}$$

$$+ i(d-1) \int_0^{r_c} \left(\psi_r^* \psi - \psi_r \psi^*\right) r^{d-2} dr \tag{B.38}$$

$$+ i(d-1) \int_0^{r_c} \left(\psi_r \psi^* - \psi \psi_r^*\right) r^{d-2} dr \tag{B.39}$$

$$= \left[i\psi^* \psi_r r^{d-1} + c.c.\right]_{r=0}^{r=r_c}. \tag{B.40}$$

Therefore,

$$\frac{d}{dt} M_{\text{collapse}}^{\text{radial}} = \left[\frac{L_t}{L} r^d |\psi|^2 + \left[i\psi^* \psi_r r^{d-1} + c.c.\right]\right]_{r=0}^{r=r_c}. \tag{B.41}$$

In terms of the transformation (B.1),

$$\psi_r = i\frac{L_t}{L}\frac{r}{2}\psi + \frac{\Psi_\xi}{L^{d/2+1}} \exp\left(i\tau + i\frac{L_t}{L}\frac{r^2}{4}\right), \tag{B.42}$$

and

$$\psi^* \psi_r = i\frac{L_t}{L}\frac{r}{2}|\psi|^2 + \frac{1}{L^{d+1}} \Psi^* \Psi_\xi. \tag{B.43}$$

Substituting the last expression in (B.41) gives:

$$\frac{d}{dt} M_{\text{collapse}}^{\text{radial}} = \left[\frac{L_t}{L} r^d |\psi|^2 - \frac{L_t}{L} r^d |\psi|^2 + i\frac{r^{d-1}}{L^{d+1}} \left(\Psi^* \Psi_\xi - \Psi \Psi_\xi^*\right)\right]_{r=0}^{r=r_c} \tag{B.44}$$

$$= \left[\frac{i}{L^2} \xi^{d-1} \left(\Psi^* \Psi_\xi - \Psi \Psi_\xi^*\right)\right]_{r=0}^{r=r_c}. \tag{B.45}$$

□

5. In this stage, the goal is compute the right-hand side of (B.31). Doing that by replacing the expansion (B.5) we get zero, because $R^{(0)}$ and g are real. Therefore, the strategy will be use the WKB approximation to evaluate Ψ_0. To do that, we note that equation (B.4) can be written as

$$\Psi_{0,\xi\xi} + \frac{d-1}{\xi} \Psi_{0,\xi} - V(\xi)\Psi_0 = 0, \qquad V(\xi) = 1 - \frac{1}{4}\beta\xi^2 - |\Psi_0|^{\frac{4}{d}}. \tag{B.46}$$

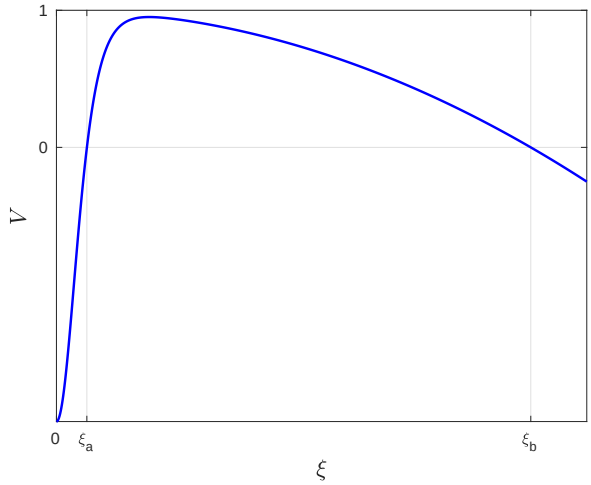

Figure B.1: Illustration of the potential $V(\xi)$ in (B.46)

Since $\Psi_0 \approx R^{(0)}$ for $0 \leq \xi \ll \beta^{-1/2}$, we have

$$V(\xi) \approx 1 - |R^{(0)}|^{\frac{4}{d}}, \qquad 0 \leq \xi \ll \beta^{-1/2}. \tag{B.47}$$

Also, by the fact that $R^{(0)}(0) > 1$, we have $V(0) < 0$. In addition, considering that $R^{(0)}$ is monotonically decreasing, potential V changes sign at the turning point $\xi_a = \mathcal{O}(1)$, where $R^{(0)}(\xi_a) \approx 1$, see Figure B.1. Now, since the ground state $R^{(0)}$ decays exponentially,

$$V(\xi) \approx 1 - \frac{1}{4}\beta\xi^2, \qquad \xi \gg 1. \tag{B.48}$$

Therefore, $V(\xi) \approx 1$ in the overlap region $1 \ll \xi \ll \beta^{-1/2}$, and changes its sign at the second turning point $\xi_b \approx 2\beta^{-1/2}$. Since in the classically inaccessible region $[\xi_a, \xi_b]$ where $V > 0$, the solution Ψ_0 has an exponential decay, if we set ξ_c in the definition of $M^{\text{radial}}_{\text{collapse}}$ to be just past the second turning point to the right i.e. $0 < \xi_c - \xi_b \ll 1$, this would only result in an exponentially small change in the value of $M^{\text{radial}}_{\text{collapse}}$.

To find the asymptotic behaviour of Ψ_0 for $\xi > \xi_c$, we introduce

$$s := \delta\xi, \qquad \delta := \frac{\beta^{1/2}}{2} \ll 1. \tag{B.49}$$

In these terms equation (B.46) reads,

$$\Psi_{0,ss} + \frac{d-1}{s}\Psi_{0,s} - \frac{1}{\delta^2}V(s)\Psi_0 = 0, \qquad V(s) = 1 - s^2 - |\Psi_0|^{\frac{4}{d}}, \tag{B.50}$$

and the turning points became $s_a = \delta\xi_a = \mathcal{O}(\delta)$ and $s_c \approx 1$. By Lemma 2.4 we get

$$\Psi_0 \approx R^{(0)} \sim A_R \left(\frac{s}{\delta}\right)^{-\frac{d-1}{2}} e^{-s/\delta}, \qquad \delta \ll s \ll 1. \tag{B.51}$$

Then, for $s \gg \delta$, the nonlinearity becomes negligible, i.e., $V(s) \approx 1 - s^2$. It implies that in that regime equation (B.50) is linear and we can approximate it by using the WKB method. In order to apply the Lemma 3.1 with $Q = -V \approx s^2 - 1$ for $s \gg \delta$, we note that $Q(s_c) = 0$ and $Q'(s_c) = 2$. Then,

$$\Psi_0 \approx \Psi_0^{\text{WKB,right}}, \qquad s - 1 \gg \delta^{2/3}, \quad \delta \to 0, \tag{B.52}$$

where

$$\Psi_0^{\text{WKB,right}} = \frac{1}{s^{\frac{d-1}{2}} Q^{\frac{1}{4}}(s)} \left(a_1 e^{-\frac{i}{\delta}\int_1^s \sqrt{Q}} + a_2 e^{\frac{i}{\delta}\int_1^x \sqrt{Q}}\right). \tag{B.53}$$

To determine completely the last expression for $\Psi_0^{\text{WKB,right}}$, it is necessary to compute the values of the constants a_1 and a_2. To compute a_1, we must force ψ to satisfy the frozen state (3.7), i.e.,

$$\psi_{tail}(r,t) \approx \phi(r) \in L^2, \qquad as \quad t \to T_c. \tag{B.54}$$

Then, a_2 is computed by considering the WKB expansion to the left of the turning point $s_c \approx 1$.

Lemma B.3. *If ψ satisfies the frozen state (B.54), then $a_1 = 0$.*

Proof. In the region $s \gg 1$, we have $Q(s) \approx s^2$ and equation (B.53) reads

$$\Psi_0^{\text{WKB,right}} \approx \frac{1}{s^{\frac{d}{2}}} \left(a_1 e^{-i\frac{s^2}{2\delta}} + a_2 e^{i\frac{s^2}{2\delta}}\right), \qquad s \gg 1. \tag{B.55}$$

Considering that

$$\psi \approx \frac{\Psi_0}{L^{\frac{d}{2}}} e^{i\tau + i\frac{L_t}{4L} r^2}, \qquad \frac{s^2}{2\delta} = \frac{\beta^{1/2}}{4} \frac{r^2}{L^2}, \tag{B.56}$$

and by the condition $s \gg 1$ we get $r \gg 2L/\beta^{1/2}$ and

$$\psi \approx \frac{1}{s^{\frac{d}{2}}}\left(a_1 e^{-i\frac{s^2}{2\delta}} + a_2 e^{i\frac{s^2}{2\delta}}\right)\frac{1}{L^{\frac{d}{2}}} e^{i\tau + i\frac{L_t}{4L}r^2} \tag{B.57}$$

$$= \frac{1}{(\delta\xi)^{1/2}}\left[a_1 e^{i\left(\frac{L_t}{L}-\frac{\beta^{1/2}}{L^2}\right)\frac{r^2}{4}} + a_2 e^{i\left(\frac{L_t}{L}+\frac{\beta^{1/2}}{L^2}\right)\frac{r^2}{4}}\right]\frac{e^{i\tau}}{L^{\frac{d}{2}}} \tag{B.58}$$

$$= \frac{e^{i\tau}}{(\delta r)^{1/2}}\left[a_1 e^{i\left(\frac{L_t L-\beta^{1/2}}{L^2}\right)\frac{r^2}{4}} + a_2 e^{i\left(\frac{L_t L+\beta^{1/2}}{L^2}\right)\frac{r^2}{4}}\right]. \tag{B.59}$$

Now, we will prove that

$$\lim_{t\to T_c}\frac{LL_t-\beta^{1/2}}{L^2} = -\infty, \qquad \lim_{t\to T_c}\frac{LL_t+\beta^{1/2}}{L^2} < \infty. \tag{B.60}$$

In fact, let us assume first β a positive constant. Then, multiplying the equation

$$L_{tt} = -\frac{\beta}{L^3} \tag{B.61}$$

by $2L_t$, integrate and multiplying by L^2 we get

$$L^2L_t^2 = \beta + a_0L^2, \qquad a_0 = \text{constant}. \tag{B.62}$$

Since $L > 0$ and $L_t < 0$, we have

$$\lim_{t\to T_c} LL_t = -\sqrt{\beta}. \tag{B.63}$$

Therefore,

$$\lim_{t\to T_c}\frac{LL_t+\sqrt{\beta}}{L^2} = \lim_{t\to T_c}\frac{L^2L_t^2-\beta}{L^2(LL_t-\sqrt{\beta})} = \lim_{t\to T_c}\frac{a_0L^2}{L^2(LL_t-\sqrt{\beta})} = -\frac{a_0}{2\sqrt{\beta}}, \tag{B.64}$$

and

$$\lim_{t\to T_c}\frac{LL_t-\sqrt{\beta}}{L^2} = \lim_{t\to T_c}\frac{-2\sqrt{\beta}}{L^2} = -\infty. \tag{B.65}$$

In the case that β is not constant one can verify that while both L and β go to zero as $t \to T_c$, changes in β are exponentially slower than in L, see e.g., [17], and the previous relations remain valid. Therefore, ψ_{tail} satisfies the frozen state (B.54), and thus avoids having infinitely-fast oscillations, only if $a_1 = 0$. □

The value of other coefficient a_2 is established in the following result.

Lemma B.4. *The coefficient a_2 is given by the expression*

$$a_2 = A_R \delta^{\frac{d-1}{2}} e^{\frac{\pi}{4\delta} + \frac{i\pi}{4}}. \tag{B.66}$$

Proof. The idea is use the WKB approximation to the left of the turning point $s_c \approx 1$. Indeed we have,

$$\Psi_0 \approx \Psi_0^{\text{WKB,left}}, \quad \{s \gg 1\} \cap \{1 - s \gg \delta^{2/3}\}, \quad \delta \to 0, \tag{B.67}$$

where

$$\Psi_0^{\text{WKB,left}} = \frac{1}{s^{\frac{d-1}{2}} |Q|^{\frac{1}{4}}} \left(b_1 e^{-\frac{i}{\delta} \int_1^s \sqrt{|Q|}} + b_2 e^{\frac{i}{\delta} \int_1^x \sqrt{|Q|}} \right), \tag{B.68}$$

$|Q| \approx 1 - s^2$ and $b_1,\ b_2$ are constants. In order to determine d_1 and d_2 we need to connect the right with the left approximation. The connection formula is [35, 3]:

$$b_1 = a_2 e^{-i\frac{\pi}{4}}, \qquad b_2 = 0. \tag{B.69}$$

Hence,

$$\Psi_0^{\text{WKB,left}} = \frac{a_2 e^{-i\frac{\pi}{4}}}{s^{\frac{d-1}{2}} |Q|^{1/4}} e^{-\frac{1}{\delta} \int_1^s \sqrt{|Q|}}. \tag{B.70}$$

In particular, for $\delta \ll s \ll 1$ we have $|Q| \approx 1$ and

$$\Psi_0^{\text{WKB,left}} \approx \frac{a_2 e^{-i\frac{\pi}{4}}}{s^{\frac{d-1}{2}}} e^{-\frac{1}{\delta}\left(\int_1^0 \sqrt{1-s^2} ds + \int_0^s \sqrt{1-s^2} ds\right)} \approx \frac{a_2}{s^{\frac{d-1}{2}}} e^{-i\frac{\pi}{4} - \frac{\pi}{4\delta} - \frac{s}{\delta}}, \tag{B.71}$$

where we have used $\int_0^s \sqrt{1-s^2} ds \approx s$. Matching this expansion for $\Psi_0^{\text{WKB,left}}$ with the expansion $\Psi_0 \approx A_R e^{-\frac{s}{\delta}} \left(\frac{s}{\delta}\right)^{-\frac{d-1}{2}}$, gives

$$a_2 = A_R \delta^{\frac{d-1}{2}} e^{\frac{\pi}{4\delta} + \frac{i\pi}{4}}. \tag{B.72}$$

□

Consequently, rewritting $\Psi_0^{\text{WKB,right}}$ in terms of ξ gives

$$\Psi_0^{\text{WKB,right}} = \frac{a_2}{(\delta\xi)^{\frac{d-1}{2}} Q^{1/4}} e^{i \int_{\xi_c}^{\xi} \sqrt{Q}}, \qquad \xi - \xi_c \gg \beta^{-1/6}. \tag{B.73}$$

Now, substituting this last expression into the right-hand side of (B.31) we get,

$$\frac{1}{L^2} \left(i\xi^{d-1} \Psi^* \Psi_\xi + c.c. \right) \approx -\frac{1}{L^2} \frac{2|a_2|^2}{\delta^{d-1}} = -\frac{2A_R^2}{L^2} e^{-\pi/\sqrt{\beta}}. \tag{B.74}$$

Therefore,

$$\frac{d}{dt} M_{\text{collapse}}^{\text{radial}} \approx -\frac{2A_R^2}{L^2} e^{-\pi/\sqrt{\beta}}. \tag{B.75}$$

6. Finally, using equation (B.30), we obtain the second equation of the reduced system:

$$\beta_t = -\frac{2A_R^2}{N^{\text{radial}}L^2}e^{-\frac{\pi}{\sqrt{\beta}}}. \tag{B.76}$$

Appendix C

Proof of Proposition 4.1: Details

In this appendix, we will provide the details of the derivation of the reduced system established in the Proposition 4.1. Indeed, the steps are:

1. Derivation the reduced equations will comes from balance of mass

$$\frac{d}{dt}\int |\psi|^2 d\boldsymbol{x} = -2\delta \int |\psi|^{4/d+2}\boldsymbol{x}. \tag{C.1}$$

Since we are assuming that the perturbation is small, the adiabatic dynamics of the perturbed NLS is assumed to be the same of the undamped NLS. In these terms, solution of the NLS equation (4.1) can be splitted as

$$\psi = \begin{cases} \psi_{\text{collapse}}, & \text{if } 0 \leq |\boldsymbol{x}| \leq \xi_c L(t), \\ \psi_{\text{tail}}, & \text{if } |\boldsymbol{x}| \geq \xi_c L(t), \end{cases} \tag{C.2}$$

with $\xi_c = \mathcal{O}(1)$ and $\xi_c \gg 1$. Therefore, the total mass of the solution consists of the sum of the mass of the collapsing core ψ_{collapse} plus the mass of the tail ψ_{tail}, i.e.,

$$\int |\psi|^2 d\boldsymbol{x} = M_{\text{collapse}} + M_{\text{tail}}, \tag{C.3}$$

where

$$M_{\text{collapse}} = \int_{|\boldsymbol{x}|<\xi_c L(t)} |\psi|^2 d\boldsymbol{x}, \qquad M_{\text{tail}} = \int_{|\boldsymbol{x}|>\xi_c L(t)} |\psi|^2 d\boldsymbol{x}. \tag{C.4}$$

Now, the rate of mass change (C.1) becomes

$$\frac{d}{dt}M_{\text{collapse}} + \frac{d}{dt}M_{\text{tail}} = -2\delta \int |\psi|^{\frac{4}{d}+2} d\boldsymbol{x}. \tag{C.5}$$

The idea in the next steps is approximate the equation (C.5).

2. We will begin computing the term $\frac{d}{dt}M_{\text{collapse}}$. For that purpose, we introduce the generalized lens transformation

$$\psi(\boldsymbol{x},t)=\frac{1}{L^{d/2}(t)}\Psi^{\delta}(\boldsymbol{\xi},\tau)\exp\left(i\tau(t)+i\frac{L_t}{L}\frac{r^2}{4}\right), \tag{C.6}$$

where $\boldsymbol{\xi}$ and τ are given by (4.7). If we substitute (C.6) in the perturbed NLS (4.1), the equation for Ψ^{δ} is

$$i\Psi^{\delta}_{\tau}+\Delta_{\boldsymbol{\xi}}\Psi^{\delta}-\Psi^{\delta}+(1+i\delta)|\Psi^{\delta}|^{\frac{4}{d}}\Psi^{\delta}+\frac{1}{4}\beta(t)|\boldsymbol{\xi}|^2\Psi^{\delta}=0, \tag{C.7}$$

with $\beta(t)=-L^3L_{tt}$. Now, by the assumption that $\psi_{\text{collapse}}\approx\psi_{R^{(0)}}$, we have $\Psi^{\delta}\approx R^{(0)}$ for $\boldsymbol{\xi}=\mathcal{O}(1)$.

3. As in the unperturbed case, we expand

$$\Psi^{\delta}=\Psi^{\delta}_0+\Psi^{\delta}_1+\Psi^{\delta}_2+\cdots, \tag{C.8}$$

and we assume that $\Psi^{\delta}_0(\boldsymbol{\xi},\tau)=\Psi^{\delta}_0(\boldsymbol{\xi};\beta(\tau))$, and that Ψ^{δ}_0 satisfies the stationary equation

$$\Delta_{\boldsymbol{\xi}}\Psi^{\delta}_0-\Psi^{\delta}_0+|\Psi^{\delta}_0|^{\frac{4}{d}}\Psi^{\delta}_0+\frac{1}{4}\beta|\boldsymbol{\xi}|^2\Psi^{\delta}_0=0. \tag{C.9}$$

We did not add the complex perturbation because we assume that, as in the unperturbed case, Ψ^{δ}_0 is essentially real for $\boldsymbol{\xi}=\mathcal{O}(1)$.

4. Since we are in the regimen $|\beta|\ll 1$, and $0<\delta\ll 1$, we can expand the function Ψ^{δ}_0 as

$$\Psi^{\delta}_0(\boldsymbol{\xi};\beta)=R^{(0)}(\boldsymbol{\xi})+\beta g(\boldsymbol{\xi})+\delta h(\boldsymbol{\xi},\tau)+\mathcal{O}(\beta^2,\beta\delta,\delta^2). \tag{C.10}$$

Inserting this last expansion into the equation (C.9), and collecting powers of β and δ, one has

$$\Delta R^{(0)}-R^{(0)}+|R^{(0)}|^{4/d}R^{(0)}+\beta\left(L_+g+\frac{|\boldsymbol{\xi}|^2}{4}R^{(0)}\right)+\delta L_+h+\mathcal{O}(\beta^2,\beta\delta,\delta^2), \tag{C.11}$$

where $L_+=\Delta-1+\left(\frac{4}{d}+1\right)|R^{(0)}|^{4/d}$. Hence, the functions g and h satisfy

$$L_+g+\frac{|\boldsymbol{\xi}|^2}{4}R^{(0)}=0,\quad \nabla g(0,\tau)=0,\quad g(\infty,\tau)=0, \tag{C.12}$$

and

$$L_+ h = 0, \quad \nabla h(0,\tau) = 0, \quad h(\infty,\tau) = 0. \tag{C.13}$$

Here the function h decays exponentially for $|\boldsymbol{\xi}| \to \infty$, see e.g., [17, 25], and satisfies the relation

$$\int R^{(0)} h d\boldsymbol{\xi} = 0. \tag{C.14}$$

This integral identity comes from applying Lemma A.1 to equation (C.9) with $\beta = 0$ and $w(U) \equiv 0$. Now, the expansion (C.10) allow us to stablish the following result:

Lemma C.1. *Let conditions 1-2 hold. Then,*

$$M_{collapse} = M_c + N\beta(t) + \mathcal{O}(\beta^2, \beta\delta, \delta^2). \tag{C.15}$$

Proof. By the definition of M_{collapse} and the expansion (C.10), one gets

$$\begin{aligned} M_{\text{collapse}} &= \int_{0\le|\boldsymbol{x}|\le\xi_c L(t)} |\psi|^2 d\boldsymbol{x} && \text{(C.16)}\\ &\approx \int_{0\le|\boldsymbol{\xi}|\le\xi_c} |\Psi_0^\delta|^2 d\boldsymbol{\xi} && \text{(C.17)}\\ &= \int_{0\le|\boldsymbol{\xi}|\le\xi_c} \left(R^{(0)} + \beta g + \delta h\right)^2 d\boldsymbol{\xi} + \mathcal{O}(\beta^2, \beta\delta, \delta^2). && \text{(C.18)} \end{aligned}$$

Since $R^{(0)}$, g and h decay exponentially, we can replace ξ_c by infinity, as we did in the unperturbed case, and we get

$$\begin{aligned} M_{\text{collapse}} &= \int |R^{(0)}|^2 d\boldsymbol{\xi} + 2\beta \int R^{(0)} g d\boldsymbol{\xi} + 2\delta \int R^{(0)} h d\boldsymbol{\xi} + \mathcal{O}(\beta^2, \beta\delta, \delta^2) && \text{(C.19)}\\ &= M_c + 2\beta \int R^{(0)} g d\boldsymbol{\xi} + 2\delta \int R^{(0)} h d\boldsymbol{\xi} + \mathcal{O}(\beta^2, \beta\delta, \delta^2) && \text{(C.20)}\\ &= M_c + \beta N + \mathcal{O}(\beta^2, \beta\delta, \delta^2), && \text{(C.21)} \end{aligned}$$

where in the last equality we have used the relation (C.14) and the Lemma A.2 in the non-radial form. □

As consequence of the previous lemma, we have again the interpretation for β:

Corollary C.1. *β is proportional to the excess mass above M_c of the collapsing core, i.e.,*

$$\beta \approx \frac{M_{collapse} - M_c}{N}. \tag{C.22}$$

We point out that this interpretation for β is not valid for other perturbations of the NLS, see e.g., [17, 25]. Also, Lemma C.1 implies the relation

$$\frac{d}{dt} M_{\text{collapse}} \approx N\beta_t. \tag{C.23}$$

5. In addition, since the perturbation is small, the mass radiation from the high-intensity core to the background is still given, to leading order, by (B.75). Hence,

$$\frac{d}{dt} M_{\text{tail}} \approx \frac{N\nu(\beta)}{L^2}. \tag{C.24}$$

The rate of change of the total mass becomes

$$\frac{d}{dt} \int |\psi|^2 d\boldsymbol{x} = \frac{d}{dt} M_{\text{collapse}} + \frac{d}{dt} M_{\text{tail}} \tag{C.25}$$

$$\approx N\beta_t + \frac{N\nu(\beta)}{L^2}. \tag{C.26}$$

6. In order to approximate the right-hand side of (C.1), we use the fact that $\psi_{\text{collapse}} \approx \psi_{R^{(0)}}$:

$$-2\delta \int |\psi|^{4/d+2} d\boldsymbol{x} \approx -\frac{2\delta}{L^2} \int \frac{1}{L^d} |R^{(0)}|^{4/d+2} d\boldsymbol{x} \tag{C.27}$$

$$= -\frac{2\delta}{L^2} \int |R^{(0)}|^{4/d+2} d\boldsymbol{\xi} \tag{C.28}$$

$$= -\frac{2\delta c_d}{L^2}, \tag{C.29}$$

where $c_d = \|R^{(0)}\|_{4/d+2}^{4/d+2}$.

7. Finally, form the balance equation we get the second equation of the reduced system:

$$\beta_t + \frac{\nu(\beta)}{L^2} = -\frac{2\delta c_d}{NL^2}. \tag{C.30}$$

Bibliography

[1] S. Akhmanov, A. Sukhorukov, and R. Khokhlov, *Self-focusing and self-trapping of intense light beams in a nonlinear medium*, JETP, 23 (1966), pp. 1025–1033.

[2] D. Anderson, M. Bonnedal, and M. Lisak, *Self-trapped cylindrical laser beams*, Phys. Fluids, 22 (1979), pp. 1838–1840.

[3] C. Bender and S. Orszag, *Advanced Mathematical Methods for Scientists and Engineers*, McGraw-Hill, New York, 1978.

[4] L. Berge and D. Pesme, *Time dependent solutions of wave collapse*, Physics Lett. A, 166 (1992), pp. 116–122.

[5] ——, *Non-self-similar collapsing solutions of the nonlinear Schrödinger at the critical dimension*, Physical Review E, 48, No. 2 (1993), pp. 684–687.

[6] J. Bourgain and W. Wang, *Construction of blowup solutions for the nonlinear Schrödinger equation with critical nonlinearity*, Ann. Scuola Norm. Sup. Pisa Cl. Sci. (4), 25 (1997), pp. 197–215.

[7] R. Boyd, *Nonlinear Optics*, Elsevier, Boston, 2008.

[8] T. Cazenave, *Semilinear Schrödinger Equations*, New York University, Courant Institute of Mathematical Sciences, New York, 2003.

[9] T. Cazenave and F. Weissler, *The cauchy problem for the critical nonlinear Schrödinger equation in H^s*, Nonlin. Anal., 14 (1990), pp. 807–836.

[10] Y. Chung and P. Lushnikov, *Strong collapse turbulence in a quintic nonlinear Schrödinger equation*, Phys. Rev. E, 84 (2011).

[11] M. Cross and P. Hohenberg, *Pattern formation outside of equilibrium*, Rev. Mod. Phys., 65 (1993), p. 851.

[12] M. Desaix, D. Anderson, and M. Lisak, *Variational approach to collapse of optical pulses*, J. Opt. Soc. Am. B, 8 (1991), pp. 2082–2086.

[13] S. Dyachenko, A. Newell, A. Pushkarev, and V. Zakharov, *Optical turbulence: weak turbulence, condensates and collapsing filaments in the nonlinear Schrödinger equation*, Physica D, 57 (1992), pp. 96–160.

[14] F. Ferlaino, S. Knoop, M. Berninger, W. Harm, J. D'Incao, H. Nagerl, and R. Grimm, *Evidence for universal four-body states tied to an efimov trimer*, Phys. Rev. Lett., 102 (2009), p. 140401.

[15] G. Fibich, *An adiabatic law for self-focusing of optical beams*, Opt. Lett., 21 (1996), pp. 1735–1737.

[16] G. Fibich, *Self-focusing in damped nonlinear Schrödinger equation*, SIAM J. Appl. Math., 61, No 5 (2001), pp. 1680–1705.

[17] ——, *The Nonlinear Schrödinger Equation: Singular solutions and optical collapse*, Springer, 2015.

[18] G. Fibich, N. Gavish, and X. Wang, *New singular solutions of the nonlinear Schrödinger equation*, Physica D, 211 (2005), pp. 193–220.

[19] ——, *Singular ring solutions of critical and supercritical nonlinear Schrödinger equation*, Physica D, 231 (2007), pp. 55–86.

[20] G. Fibich and B. Ilan, *Vectorial and random effects in self-focusing and in multiple filamentation*, Physica D, 157 (2001), pp. 112–146.

[21] G. Fibich and M. Klein, *Continuations of the nonlinear Schrödinger equation beyond the singularity*, Nonlinearity, 24 (2011), pp. 2003–2045.

[22] ——, *Numerical-damping continuation of the nonlinear Schrödinger equation-a numerical study*, Physica D, 241 (2012), pp. 519–527.

[23] G. Fibich and D. Levy, *Self-focusing in the complex Ginzburg-Landau limit of the critical nonlinear Schrödinger equation*, Physics Letters A, 249 (1998), pp. 286–294.

[24] G. Fibich and B. Llan, *Self-focusing of elliptic beams: an example of the failure of the aberrationless approximation*, J. Opt. Soc. Am. B, 17 (2000), pp. 1749–1758.

[25] G. Fibich and G. Papanicolaou, *A modulation theory for self-focusing in the perturbed critical nonlinear Schrödinger equation*, Phys. Lett. A, 239 (1998), pp. 167–173.

[26] ——, *Self-focusing in the perturbed and unperturbed nonlinear Schrödinger equation in critical dimension*, SIAM J. Applied Math., 60 (1999), pp. 183–240.

[27] G. Fraiman, *Asymptotic stability of manifold of self-similar solutions in self-focusing*, Sov. Phys. JETP, 61 (1985), pp. 228–233.

[28] J. Gerton, D. Strekalov, I. Prodan, and R. Hulet, *Direct observation of growth and collapse of a Bose-Einstein condensate with attractive interactions*, Nature, 408 (2000), pp. 692–695.

[29] J. Ginibre and G. Velo, *On a class of Schrödinger equations. iii: Special theories in dimensions 1, 2 and 3*, Ann. Inst. H. Poincaré, Sec. A, 28 (1978), pp. 287–316.

[30] R. Glassey, *On the blowing up of solutions to the cauchy problem for nonlinear Schrödinger equations*, J. Math. Phys., 18, No. 9 (1977), pp. 1794–1797.

[31] C. Josserand, Y. Pomeau, and S. Rica, *Finite-time localized singularities as a mechanism for turbulent dissipation*, Phys. Rev. Fluids, 5 (2020), p. 054607.

[32] T. Kato, *On nonlinear Schrödinger equations,*, Ann. Inst. H. Poincaré, Phys. Théor, 46 (1987), pp. 113–129.

[33] P. Kelley, *Self-focusing of optical beams*, Phys. Rev. Lett., 15 (1965), pp. 1005–1008.

[34] E. Kuznetsov and S. Turitsyn, *Talanov transformations in self-focusing problems and instability of stationary waveguides*, Physics Lett., 112 A, No. 6-7 (1985), pp. 273–275.

[35] L. Landau and E. Lifshitz, *Quantum mechanics*, Pergamon Press, Oxford, 1977.

[36] M. Landman, G. Papanicolaou, C. Sulem, and P. Sulem, *Rate of blowup for solutions of the nonlinear Schrödinger equation at critical dimension*, Phys. Rev. A, 38 (1988), pp. 3837–3843.

[37] M. Landman, G. Papanicolaou, C. Sulem, P. Sulem, and X. Wang, *Stability of isotropic singularities for the nonlinear Schrödinger equation*, Physica D, 47 (1991), pp. 393–415.

[38] B. LeMesurier, G. Papanicolaou, C. Sulem, and P. Sulem, *Local structure of the self-focusing singularity of the nonlinear Schrödinger equation*, Physica D, 32 (1988), pp. 210–226.

[39] J. Lin and W. Strauss, *Decay and scattering of solutions of a nonlinear Schrödinger equation*, J. Funct. Anal., 30 (1978), pp. 245–263.

[40] F. Linares and G. Ponce, *Introduction to Nonlinear Dispersive Equations*, Springer, 2009.

[41] P. Lushnikov, S. Dyachenko, and N. Vladimirova, *Beyond leading-order logarithmic scaling in the catastrophic self-focusing of a laser beam in Kerr media*, Physical Review A, 88 (2013), p. 013845.

[42] P. Lushnikov and N. Vladimirova, *Non-gaussian statistics of multiple filamentation*, Optics Letters, 35 (2010), pp. 1965–1967.

[43] V. Malkin, *On the analytical theory for stationary self-focusing of radiation*, Physica D, 64 (1993), pp. 251–266.

[44] J. Marburger, *Self-focusing: theory*, Prog. Quant. Electr., 4 (1975), pp. 35–110.

[45] F. Merle, *Limit behavior of saturated approximations of nonlinear Schrödinger equation*, Commun. Math. Phys., 149 (1992), pp. 377–414.

[46] ——, *On uniqueness and continuation properties after blow-up time of self-similar solutions of nonlinear Schrödinger equation with critical exponent and critical mass*, Commun. Pure Appl. Math., 45 (1992), pp. 203–254.

[47] F. Merle and P. Raphael, *Sharp upper bound on the blow-up rate for the critical nonlinear Schrödinger equation*, Geom. Funct. Anal., 13 (2003), pp. 591–642.

[48] ——, *On universality of blow-up profile for L^2 critical nonlinear Schrödinger equation*, Invent. Math., 156 (2004), pp. 565–672.

[49] ——, *Blow-up dynamics and upper bound on the blow-up rate for the critical nonlinear Schrödinger equation*, Ann. Math., 161 (2005), pp. 157–222.

[50] ——, *Profiles and quantization of the blow-up mass for critical nonlinear Schrödinger equation*, Commun. Math. Phys., 253 (2005), pp. 675–704.

[51] ——, *On a sharp lower bound on the blow-up rate for the L^2 critical nonlinear Schrödinger equation*, J. Amer. Math. Soc., 19 (2006), pp. 37–90.

[52] ——, *On one blow up point solutions to the critical nonlinear Schrödinger equation*, J. Hyperbolic Diff. Equat., 2 (2006), pp. 919–962.

[53] F. Merle and Y. Tsutsumi, *L^2 concentration of blowup solutions for the nonlinear Schrödinger equation with critical power nonlinearity*, J. Diff. Equat., 84 (1990), pp. 205–214.

[54] H. Nawa and M. Tsutsumi, *On blow-up for the pseudo-conformally invariant nonlinear Schrödinger equation*, Funkcial. Ekvac., 32 (1989), pp. 417–428.

[55] N. Nawa, *Mass concentration phenomenon for the nonlinear Schrödinger equation with critical power nonlinearity*, Funkcial. Ekvac., 35 (1992), pp. 1–18.

[56] T. Passot, C. Sulem, and P. Sulem, *Linear versus nonlinear dissipation for critical NLS equation*, Physica D, 203 (2005), pp. 167–184.

[57] D. Peregrine, *Water waves, nonlinear Schrödinger equations and their solutions*, J. Austral. Math. Soc. Ser. B, 25 (1983), pp. 16–43.

[58] G. Perelman, *On the blow up phenomenon for the critical nonlinear Schrödinger equation in 1D*, Séminaire É. D. P., Exposé No. 3 (2001), pp. 1999–2000.

[59] S. Pohozaev, *Eigenfunctions of the equation* $\triangle u + \lambda f(u) = 0$, Soviet Math. Dokl., 6 (1965), pp. 1408–1411.

[60] A. Slunyaev, G. F. Clauss, M. Klein, and M. Onorato, *Simulations and experiments of short intense envelope solitons of surface water waves*, Physics of Fluids, 25 (2013).

[61] R. Strichartz, *A guide to Distribution Theory and Fourier Transforms*, Studies in Advanced Mathematics, 1994.

[62] C. Sulem and P. Sulem, *The Nonlinear Schrödinger Equation: Self-focusing and wave collapse*, Springer, 1999.

[63] V. Talanov, *Focusing of light in cubic media*, JETP Lett., 11 (1970), pp. 199–201.

[64] S. Trillo, J. T. Gongora, and A. Fratalocchi, *Wave instabilities in the presence of non vanishing background in nonlinear Schrödinger systems*, vol. 4, 2014.

[65] S. Vlasov, V. Petrishchev, and V. Talanov, *Averaged description of wave beams in linear and nonlinear media*, Radiophys. Quant. Electron., 14 (1971), pp. 1062–1070.

[66] M. Weinstein, *Nonlinear Schrödinger equations and sharp interpolation estimates*, Comm. Math. Phys., 87 (1983), pp. 567–576.

[67] ——, *The nonlinear Schrödinger equations- singularity formation, stability and dispersion*, Contemp. Math., 99 (1989), pp. 213–232.

[68] H. Yoshida, *Construction of higher order symplectic integrators*, Phys. Lett. A, 150 (1990), pp. 262–268.

[69] V. Zakharov, *Collapse of langmuir waves*, Sov. Phys. JETP-USSR, 35, No. 5 (1972), pp. 908–914.